Adaptation of Chemical Biology Approaches for Dissecting Disordered Protein Dynamics

by

Oleta T. Johnson

A dissertation submitted in partial fulfillment
of the requirements for the degree of
Doctor of Philosophy
(Chemical Biology)
in the University of Michigan
2018

Doctoral Committee:

Assistant Professor Amanda L. Garner, Chair
Professor Anna K. Mapp
Professor Nouri Neamati
Associate Professor Zaneta Nikolovska-Coleska

Oleta T. Johnson

otjohn@umich.edu

ORCID iD: 0000-0001-5170-3003

Acknowledgements

I cannot acknowledge my graduate work without acknowledging the journey that lead me here. In 2006, if someone had told me I would be a Chemical Biology Ph.D. student at University of Michigan, I would have laughed. I look back on moments throughout my life, now realizing I was being conditioned to doubt my ability and my intellect, something I fight every day to reprogram. It was my high school chemistry teacher, Dr. Veronica Price, who made science accessible to me. I must graciously acknowledge and thank you Dr. Price, as you were influential in my decision to apply to college as a biochemistry major.

I applied to one college, with the mind that if I did not get accepted, it was a sign that more schooling was not for me. While awaiting that decision, a man travelled from Tallahassee, FL to North Charleston, SC to offer me a full academic scholarship to Florida A & M University, not the school I had chosen to decide my fate. After much trepidation, I accepted the offer. It was one of the best decisions I've ever made. I must thank Arian Baker, who was my advisor, and my friend. She pushed, prodded, and pressured me into doing laboratory research, and without that pressure, I would have never considered graduate research. Thank you to Prof. Bereket Mochona and Prof. Edith Onyeozili, for your scientific mentorship and support. Prof. James Boyer and Vice-President Maurice Edington, you gave me endless advice when I decided to apply to graduate school, a choice that many around me vocally opposed. Thank you for explaining how graduate school worked, what things to consider when choosing a graduate program, and for letting

me sit in each of your offices and cry about small setbacks when they felt debilitating to me. To Prof. Jesse Edwards, I must give a special acknowledgement. He was one of my biggest supporters and was instrumental in preparing me to apply to graduate school. In fact, he is the singular reason I applied to the University of Michigan. Dr. Edwards, you undeniably changed my trajectory and I am forever grateful for the exceptional support you poured into me.

I must thank Assistant Prof. Amanda Garner for allowing me to work as a student in her lab. Working on such interesting projects have molded my scientific outlook. I often reflect on my early days in the lab with the benefit of hindsight and cringe at the simple mistakes and missteps I made in my naiveté. I can't imagine what those times must have felt like for you; thus, I have immense gratitude for your acceptance of me. You provided a freedom that allowed me to develop exponentially as a scientist. Thank you to my committee members for your constant support and feedback. I feel honored to have been able to sharpen my scientific skills with guidance from scientists who are so immensely knowledgeable and for whom I have immeasurable respect. I give additional thanks to Prof. Anna Mapp, who in addition to her role as a committee member, has been a true mentor and advocate. Thank you Anna, for always reminding me of my value as a scientist and a human.

To my lab mates, we have lived an experience that is only ours. Working in a new lab is an experience with a unique set of challenges. There was an unlimited amount I didn't know or understand about how to be both an independent scientist and colleague who functions with of both scientific rigor and human compassion. I've learned an abundance about myself, and have done so in a way that I don't believe I could have

done with a different group of people and personalities. Thank you for your thoughtful scientific discussions and constant patience. I must especially thank Dr. Tanpreet Kaur and Jorge Sandoval for their friendship, advice, and support (and food—a lot of delicious food).

The most impactful experience I've had in graduate school has been the opportunity to do a research sabbatical in the Forman-Kay Lab as a part of the Chemistry-Biology Interface Training Program. I am eternally grateful to Prof. Julie Forman-Kay for accepting me as a visiting student, and for an abundance of guidance and mentorship. While in Julie's lab, my work with Dr. Alaji Bah set a new standard of mentorship for me. Alaji, you taught me basic quantum theory, tricks on working with difficult proteins, and you always found a reason to give me good life advice. I often recount times where you gave me what I describe as "the most positive, negative feedback" I've ever received; in the face of disappointing data, you showed me that it was not a failure, only an unanticipated shift of focus. I gained a level of confidence from working with you that I can never repay. I sincerely hope that I can one day be a fraction of the teacher that you were to me. Thank you to all of the staff, postdocs, and students in the labs of Prof. Julie Forman-Kay and Prof. Lewis Kay who made me feel at home and valued. In particular I must acknowledge Ranjith Muhandiram, who provided support with all of the protein NMR experiments I carried out while there. To Dr. Robert Culik, Dr. Jacob Brady, and Dr. Rui Huang, you were not only fantastic colleagues, but also fantastic friends. Thank you to the members of the Mapp Lab and the Nikolovska-Coleska Lab. I appreciate you all graciously allowing me to occupy your spaces, pick your brains, and commune with you in science and more.

To the friends I made during my time at Michigan, thank you for making this place feel like home. Through broken glassware, broken instruments, broken spirits, broken hearts, a broken finger, and just being broke; you have been there for me at some of my most vulnerable moments, supporting me and pushing me forward when I felt defeated. Thank you for “just being cool man”. I hope I’ve been half the friend to each of you that you have been to me. I feel blessed that there are too many of you to name individually. You all enveloped me in positivity and affirmation. You believed in me when I didn’t believe in myself. You fought for me and with me when I felt tired of fighting. I am here, in large part, as a result of the love you have poured into me. I hope I have done the same for you.

To the woman who will soon be Dr. Katherine Rush, thank you for the many nights of red wine, Scandal, puzzles, etc. You constantly remind me that the world is our eggplant. Your brilliance and your strength is tangible in a way that people aspire to experience. I’m so glad to have begun and finished this degree in solidarity with you. To Ciara Sivels, Aerial Murphy, and Autumn Bullard, all of whom will have their doctorate degrees by the end of the year, thank you for existing in this space with me. I can’t think of how to accurately describe the experience of being a black woman pursuing a graduate degree in a competitive STEM field; luckily, with you I don’t have to do that. I hate that we too often bond through the psychological and emotional trauma we’ve experienced over the past 5 years, but seeing first-hand the strength and grace with which you navigate this space has been deeply moving. I cannot imagine surviving this experience without you. To Dr. Sada McQuay, your unwavering love and support means so much to me. You have been a better friend to me than I often deserved. Thank you for everything.

To Dr. Paige Brockington, on May 29th, 1991, God created us to walk together through this life and I am eternally grateful. Many will, thankfully, never understand what it feels like to watch people they grew up with and around be murdered in a church, to hear of murders committed down the street from their high school, and still have to go into work and produce like any other day. To acknowledge the experience of emotional trauma often feels like a shameful thing in academic spaces, and it's something that often made me feel like I could not succeed in this space. Thank you for going first, proving it possible, and pulling me up behind you. You are truly my better half. I love you twin.

Last, but certainly not least, I must thank my parents, Tanya and Nathaniel Johnson. You have worked unfathomably hard, and made countless sacrifices to give me opportunities that you never had. Mommy, thank you for being my prayer warrior. Thank you for the texts that made me laugh and motivated me to keep going when I felt discouraged. Daddy, as I am writing this, I've just finished a phone conversation with you about Stevie Wonder. With that in mind, thank you for being the "Joy Inside My Tears". You are the most brilliant, resilient, hard-working, and compassionate human I know, and I am honored to call you my father and my best friend. In everything I do, I aim to make you both proud because you both deserve more than the opportunities you were handed. There were so many times with you I missed. There were so many times you both told me to just focus on school and my work. I hope this makes up for it.

Table of Contents

List of Tables

List of Figures

Abstract

Proteins containing intrinsic disorder often undergo dynamic conformational change in response to ligand binding or post-translational modification. Chemical dissection of these dynamic protein perturbations presents an approach for manipulating the resultant functional outcomes. Translational repressor protein 4E-BP1 is an example of an intrinsically disordered protein (IDP) that both folds into a short α-helix upon binding to its protein ligand, eIF4E, and a four-stranded β-sheet upon hyperphosphorylation.

Post-translational modifications (PTMs) are an important mode of regulation for IDPs and intrinsically disordered regions (IDRs); however, the enzymatic generation of uniformly modified proteins *in vitro* remains challenging. Studying PTMs in IDPs is further complicated by their instability and markedly dynamic nature. Chemical methods of site-specific PTM incorporation have been developed in attempt to circumvent this problem. Here, we evaluate a chemical mutagenesis-based approach for generating pCys as a phosphomimetic in the 4E-BPs, a family of proteins that acts to repress cap-dependent translation, and whose function is regulated by a hierarchy of phosphorylation events. Using NMR and CD spectroscopy, we have characterized pCys in two unique contexts within 4E-BPs: induction and destabilization of secondary structure. Understanding the applicability of pCys in these unique contexts is important for expanding its use to answer biological questions in complex protein systems.

Additionally, biophysical methods for analysis of binding-induced structural changes are low throughput, require large amounts of sample, or are extremely sensitive to signal

interference by the ligand itself. Herein, we describe the discovery and development of a conditionally fluorescent 4E-BP1 peptide that reports structural changes of its helix in high-throughput format. This reporter peptide is based on conditional quenching of fluorescein by thioamides. In this case, fluorescence signal increases as the peptide becomes more ordered. Conversely, destabilization of the α-helix results in decreased fluorescence signal. The low concentration and low volume of peptide required make this approach amenable for high-throughput screening to discover ligands that alter peptide secondary structure.

Chapter 1 : Introduction to Protein Disorder and its Role in Cap-Dependent Translation

1.1 An Introduction to Intrinsically Disordered Proteins

Figure 1.1 "The Protein Trinity Represents the Three Classes of Protein Structure"

For decades, the relationship between protein structure and function was held to be straightforward: the primary amino acid sequence of a protein dictates the formation of stable structures, that in turn, determine protein function.[1] Upending that long-held paradigm are the more recent estimates that approximately 66% of eukaryotic proteins contain segments of 30 res or more that are predicted to be structurally disordered, termed intrinsically disordered regions (IDRs). In fact, there are proteins completely lacking stable structures.[2] What we now know is that proteins tend to occupy three structural classes, termed the "protein trinity": ordered, molten globule, and random coil

(Figure 1.1).[3] Intrinsically disordered proteins (IDPs) primarily exhibit the properties of a random coil, although they usually contain residual secondary structural elements.[4] In other words, an IDP can be thought of as an ensemble of protein populations that occupy structural states over a continuum of conformational space. Given that the majority of the human proteome consists of IDRs or IDPs,[4] one question that arises is why this protein class was only recently uncovered. The answer to this is found by examination of the way proteins were historically discovered and isolated *in vitro*. Traditionally, new proteins were identified through functional screens of cell lysate, creating a bias for proteins that were both soluble and displayed enzymatic activity.[3] Because of this, the abundance and function of IDPs have were largely unexplored until the 1990's.[4]

In contrast to well-ordered proteins, IDPs do not adopt a single, stable 3D structure. Instead, they sample many conformations over time[2]. The resulting high flexibility of these proteins is encoded in their primary amino acid sequences. For example, IDP amino acid sequences are typically considered "low complexity",[5,6] containing multiple repeats of the same or similar amino acids that hinder the formation of a hydrophobic core.[3] They are specifically deficient in structure promoting amino acids, such as C, W, I, Y, F, L, H, V, and N.[2] Conversely, IDPs are enriched in amino acids A, G, R, T, S, K, Q, E, and P,[2] residues that are either disrupting to secondary structure, or commonly targeted for enzymatic post-translational modification, a central mechanism of IDP regulation.

While IDPs do not rely directly on stable structural motifs to inform their function, they often contain short, functional sequence repeats, that are conserved for regulatory

purposes,[2-4] A common example of this are PEST sequences, which are short stretches enriched with Pro, Glu, Ser, and Thr residues. These PEST sequences appear to regulate protein turnover, as these sequences motifs are usually phosphorylated, priming the protein for ubiquitination and protein degradation.[7,8] Another example of such sequences are protein recognition sequences that fold into secondary structures upon binding to their partner[4]. While it is not clear what the evolutionary origin of these sequence motifs are, is had been proposed that they may have arisen via repeat expansion.[3]

Although the highly dynamic nature of IDPs, presents a unique challenge for their study, biophysical and bioinformatic techniques have proven extremely useful for understanding their functions. Computational programs have arisen as powerful tools for identification of IDPs. A number of bioinformatic programs like PONDR, FoldIndex, and GlobPlot have been developed to predict protein disorder from primary amino acid sequence (Table 1.1).[1,3] Additionally, a number of biophysical techniques have been adapted to elucidate the dynamic nature of IDPs in solution, including: nuclear magnetic resonance (NMR) spectroscopy, circular dichroism (CD) spectroscopy, hydrodynamic measurements, fluorescence energy transfer (FRET) and small angle x-ray scattering (SAXS).[3,4] Occasionally, IDPs also form conditionally rigid secondary structures that can be observed in x-ray crystallography experiments.

Program	Description	Website
PONDR	Uses sequence attributes like fractional amino acid composition, hydropathy, and sequence complexity to evaluate sequence disorder over windows of 9 to 21 amino acids.	www.pondr.com
ANCHOR	Predicts disordered regions that fold upon ligand binding, without information of partner proteins[9]	http://prdos.hgc.jp/cgi-bin/top.cgi
PrDOS	Uses a predictor that considers sequence alignment of homologs[10]	http://anchor.enzim.hu/
Espritz	Uses two binary qualifiers: one for short disordered regions and one for long disordered fragments[11]	http://protein.bio.unipd.it/espritz/
D^2P^2	A database of disordered protein predictions[12]	http://d2p2.pro/
FoldIndex	Analyzes the ratio of local net charge relative to hydropathy[13]	https://fold.weizmann.ac.il/fldbin/findex
DisEMBL	Predicts disordered loops, and dynamics regions missing from the PDB	http://dis.embl.de
GlobPlot	Considers the relative propensity of an amino acid to be in an ordered or disordered state	http://globplot.embl.de
DISOPRED	Uses multiple sequence attributes to train algorthm against the entire polypetide sequence[14]	http://bioinf.cs.ucl.ac.uk/psipred/?disopred=1
DISPROT	A database of disordered protein regions	http://www.disprot.org

Table 1.1 "Bioinformatic Resources for Analysis of Protein Disorder"

1.2 Functions of Intrinsic Disorder in Cellular Processes

IDPs are particularly prevalent in cellular signaling pathways, where they mediate signal transduction through networks of protein-protein interactions (PPIs).[3] Intrinsic disorder creates a larger surface area for ligand binding, where multiple well-ordered proteins would be required to make the same contacts.[3] A thermodynamic consequence of this is the commonly observed, non-homogenous distribution of binding free energy, where multiple weakly binding motifs work synergistically to drive PPI formation (Figure 1.2).[4] It is often the case that, an IDP's PPI(s) are mediated through a single, indispensable hot spot peptide region. While the hot spot modulates PPI formation, other regions function to enhance overall binding affinity.[3,4] In both of the aforementioned cases, synergistic binding also contributes to the specificity of IDPs for the ligand.[3] Another benefit of multiple interacting motifs is that they allow for pathway crosstalk. Weak binding sites are highly dynamic, allowing for the IDP to interact with modifying enzymes or other binding partners. This property is of particular importance in signal

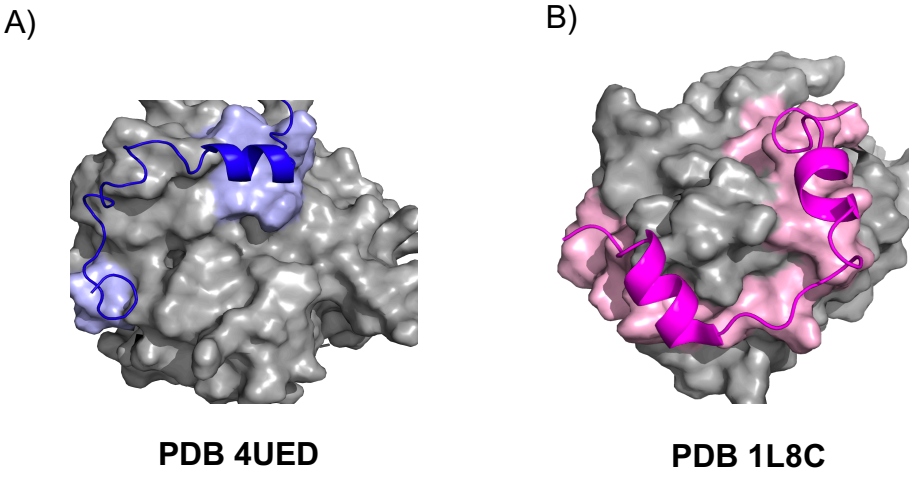

Figure 1.2 "Examples of IDPs that Exhibit Non-Homogenous Distribution of Binding Free Energy" A) 4E-BP1 utilizes two synergistic sites for eiF4E binding B) HIF1 utilizes multiple synergistic sites for CBP binding

transduction, as it allows for rapid dissociation after binding, enabling expeditious signal termination.[4]

Cellular Process	**Disordered Protein**	**Brief Description of Function**
Transcription	NCBD (CBP)	Binds coactivators for gene transcription[3]
Apoptosis	PUMA	Binds to sequester anti-apoptotic proteins & stimulate apoptosis[4]
Cell Cycle	p53	Regulation at G1/S checkpoint[4]
Circadian clock regulation	FQR	Regulates circadian clock of Neurospora spp. in a phosphorylation dependent manner[4]
Liquid-liquid phase separation	DYRK3	Recruits mTOR to stress granules for pathway inhibition[4]
Alternative splicing	Snu17p	Regulates pre-mRNA slicing and nuclear retention as a part of the RES complex[4]
Protein translation	4E-BP	Regulates initiation of cap-dependent translation[19]

Table 1.2 "Cellular Processes Mediated via Protein Disorder"

In addition to being critical for binding to partner proteins, hot spot regions often exhibit binding mediated structural polymorphism. Most commonly, IDPs fold into an α-helical structure at the binding interface, with the overall dynamics of an IDP being dependent on the identity of the ligand(s) bound at a given time; the thermodynamic favorability of protein binding offsets the decrease in entropy that results from folding. IDPs are also tightly regulated by post-translational modifications (PTMs), some of which include methylation, acetylation, and phosphorylation. In fact, phosphorylation is a

critically important regulatory modification in signal transduction. Of interest, regions of protein disorder comprise the majority of documented phosphorylation sites.[4] Phosphorylation regulation of IDPs, serve a variety of molecular functions, acting as a molecular clock, a molecular rheostat, or modulating structure and conformation.[4,15-18] Given the advantages of protein disorder for cell signaling, it is found to play an important role in a number of cellular functions (Table 1.2). These include the cell cycle, programed cell death, transcription, and translation.

mRNA transcript	Cellular Function
ornithine decarboxylase (ODC)	polyamine synthesis[20]
c-Myc	transcription[21]
VEGF	angiogenesis[22-24]
Bcl-2	apoptosis[25]
Survivin	apoptosis[26]
ATP5D	mitochodrial ATP synthesis[27]

Table 1.3 "mRNA Transcripts Regulated in a Cap-Dependent Manner"

1.3 Regulation of Cap-Dependent Translation Determines Cell Growth and Development

One cellular process that is heavily regulated by an IDP is cap-dependent translation. Within the flow of genetic information in eukaryotes, a subset of mRNA transcripts are regulated in a manner that is dependent upon molecular recognition of a

methylated guanine base that caps the 5' prime end of the mRNA transcript (Table 1.3). Expression of proteins that are critical for normal cell growth and development are specifically regulated in a dap-dependent manner.

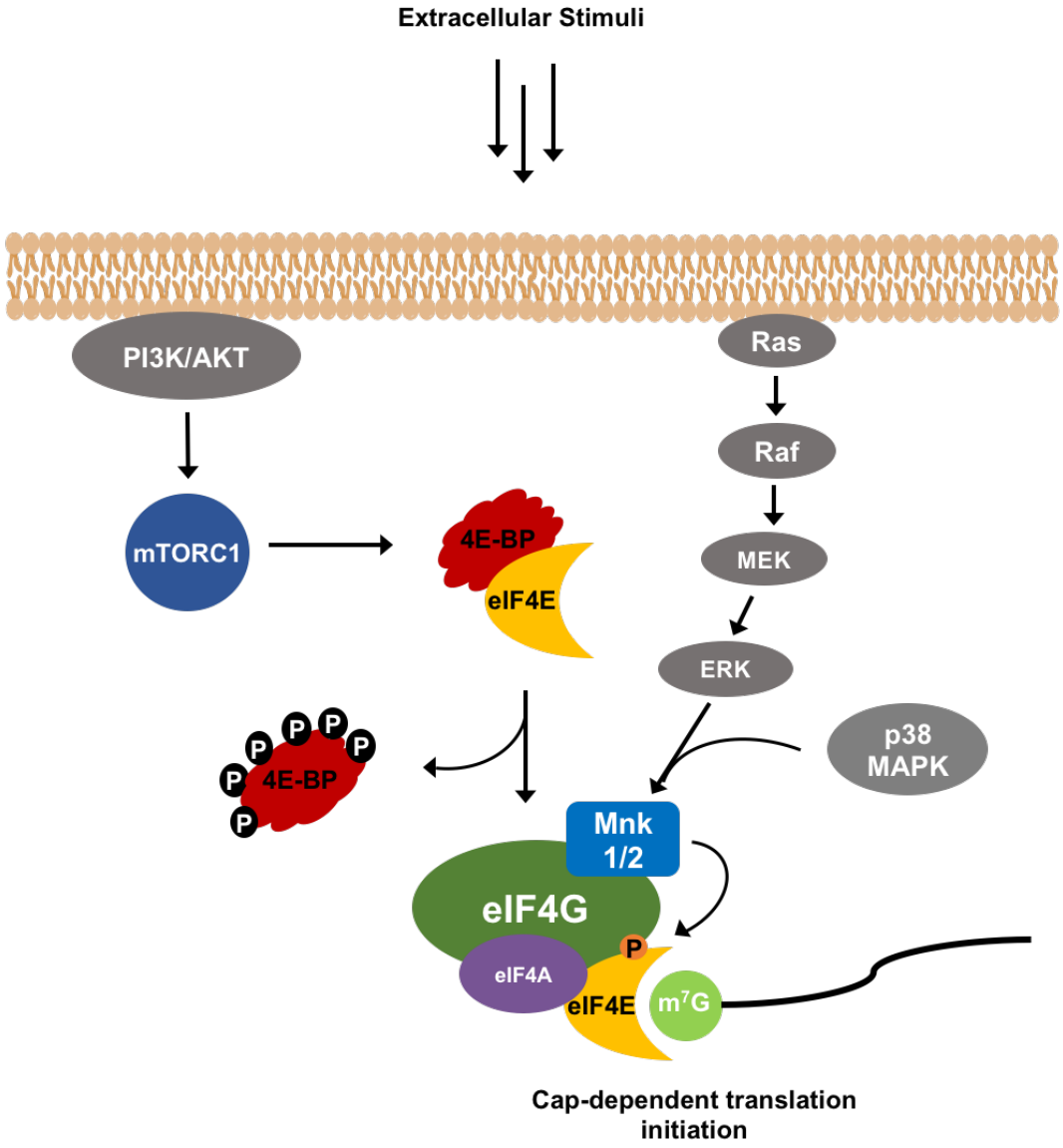

Figure 1.3 "Cap-Dependent Translation is Regulated by the Convergence of Multiple Signaling Pathways onto the 4E-BP/eIF4E axis"

Cap-dependent translation is most tightly controlled at the initiation step, which requires formation of the eukaryotic initiation factor (eIF) 4F complex. The eIF4F complex

is comprised of scaffolding protein eIF4G, RNA helicase eIF4A, and the cap-binding protein eIF4E. Recruitment of eIF4E to the eIF4F complex by eIF4G is the rate-limiting step for cap-dependent translation initiation, and is regulated by a family of intrinsically disordered 4E-binding proteins (4E-BPs) (Figure 1.3). By sequestering eIF4E away from the eIF4F complex, the 4E-BPs negatively regulate cell growth,[28-30] and proliferation.[31] More specifically, the 4E-BPs prevent progression of cells from G1 to S phase.[26] They also promote apoptosis by regulating translation of antiapoptotic proteins.[29] Many signaling pathways converge onto the eIF4E-4E-BP axis (Figure 1.3),[21,26,27,32-35] and as a result, dysregulation of cap-dependent translation, is correlated to a number of biological processes and disease states (Table 1.4). Thus, understanding 4E-BP disorder and dynamics as a mechanism for its function unlocks the potential for discovery and development of biologically active chemical probes that selectively reprogram the cap-dependent translational machinery. Directly targeting 4E-BP conformational dynamics could be a means by which possible chemoresistance, conferred through compensatory upstream signaling pathways, can be circumvented.

Cellular Process/Disease State		**Correlation to Cap-Dependent Translation Initiation**
Aging		Cap-dependent translation of proteins required for mitochondrial process induction[36]
Diabetes		Higher HDL is correlated to lower 4E-BP expression[37,38]
Obesity		Lower 4E-BP1/2 expression results in lower body fat and increased insulin resistance[27,39]
Viral Infection	Adenovirus	Possible increased in cap-dependent translation for early infection[32,]
		Increase in p4E-BP1[32,40]
	Rhabdovirus	Decrease in p4E-BP1[41]
	Herpesvirus	Increase in cap-dependent translation via ICP6 stabilization of eIF4E-eIF4G interaction[42,43]
	Papillomavirus	E6 dependent increase in cap-dependent translation[44]
Neurological Disease	Autism Spectrum Disorder	Increased cap-dependent translation via decrease 4E-BP2 activity[27,45]

	Alzheimer's Disease	Increased 4E-BP2 activity is correlated to neuronal death[46,47]
Cancer	Breast	Increased p4E-BP1 is associated with tumorogenesis[25,48]
	Ovarian	Increased p4E-BP1 is associated with tumorogenesis and poor prognosis[49]
	Melanoma	Increased p4E-BP1 is associated with tumorogenesis[50]
	Prostate	Increased p4E-BP is associated with tumorogenesis[51]
	Pancreatic	Increased 4E-BP1 expression; desensitization to mTORC1 phosphorylation[52]
		Lower 4E-BP1 expression in PDAC[53]
	Esophageal	Lower 4E-BP1 expression[54]
	Lung	Increased p4E-BP1 is associated with tumorogenesis and poor prognosis in NSCLC[55]

Table 1.4. "Disease States Correlated to Aberrant Cap-Dependent Translation"

1.4 4E-BP Molecular Function and Regulation

Early studies aimed at identifying new insulin responsive proteins in rat adipocytes[56-58] lead to the discovery and identification of Phosphorylated Heat and Acid Stable protein regulated by Insulin (PHAS-I).[59] Subsequent work provided a link between PHAS-I and cap-dependent translation via insulin-dependent eIF4E binding, leading to the protein being renamed 4E-binding protein 1 (4E-BP1).[60,61] There have been a total of three 4E-BP isoforms identified in humans, termed 4E-BP1, 4E-BP2, and 4E-BP3. 4E-BP molecular action involves binding eIF4E via a hotspot region that contains an eIF4E binding motif YXXXXFϕ. This motif is shared by eIF4G, which directly competes for eIF4E binding. The hotspot peptide alone has an eIF4E binding affinity of 50 nM, only 10-fold weaker than the 5 nM binding affinity of the full-length protein[19].

4E-BP function is regulated on a number of levels, from gene expression to post-translational control. The genes encoding 4E-BPs are transcriptionally regulated by ATF4 and SMAD4,[30,62] which increase 4E-BP expression, as well as EGR1,[54] which decreases expression,[63] and c-Myc. 4E-BP1 and 4E-BP2 are the most well characterized, differing largely in their tissue localization. Both isoforms are ubiquitously expressed;[63,64] however, 4E-BP1 is enriched in skeletal muscle and adipose tissue,[64] while 4E-BP2 is enriched in brain and neuronal tissue.[65] Little is known about the molecular or biological function of 4E-BP3; thus, there will not be further discussion of it here. Cellular concentration of 4E-BPs are also regulated through protein degradation. The normal half-life for 4E-BP1 is reported at about 16 h. Phosphorylation within 4E-BP PEST sequences appears to

decrease stability in cells.[7,8] 4E-BP1 has also been reported to be polyubiquitinated when unbound to eIF4E, targeting it for proteasomal degradation.[66,67]

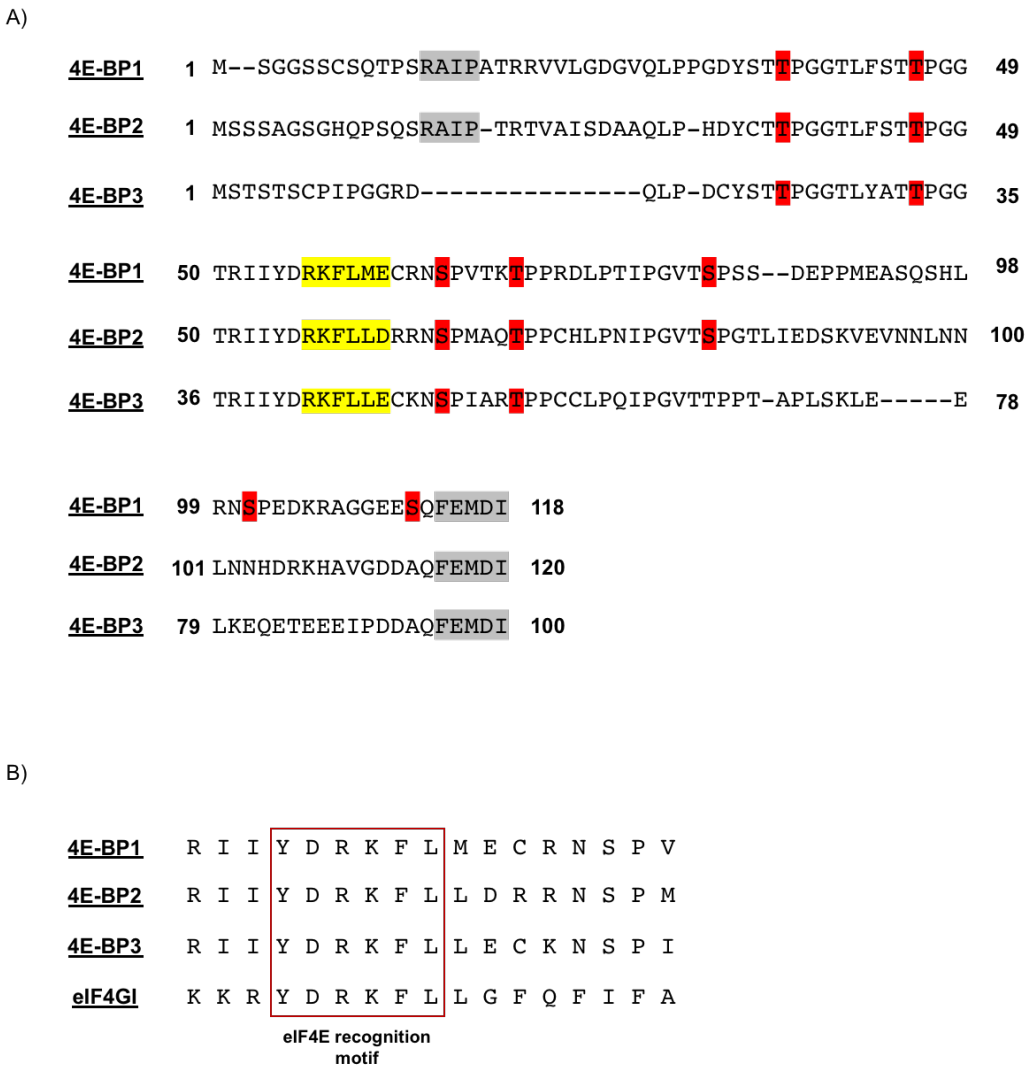

Figure 1.4 "Multiple Sequence Alignment of 4E-BP and eIF4E" A) Multiple Sequence Alignment of human 4E-BP isoforms; gray indicates a mTORC1 recognitions sequence, red indicates a canonical phosphorylation site and yellow indicates the binding induced α-helical region B) Comparison of the hot spot peptide regions of 4E-BP and eIF4G

Folding of a short region of 4E-BP into a short, amphipathic α-helix, a consequence of target binding, is regulatory feature that contributes to its eIF4E binding activity (Figure 1.5A). This is common in IDP mediated PPIs, with other notable examples of IDPs or

IDRs undergoing this phenomenon including the pKID IDR that folds upon the KIX surface[4] and p53 ordering upon MDM2 binding.[3] The 4E-BP helix is in the hotspot binding

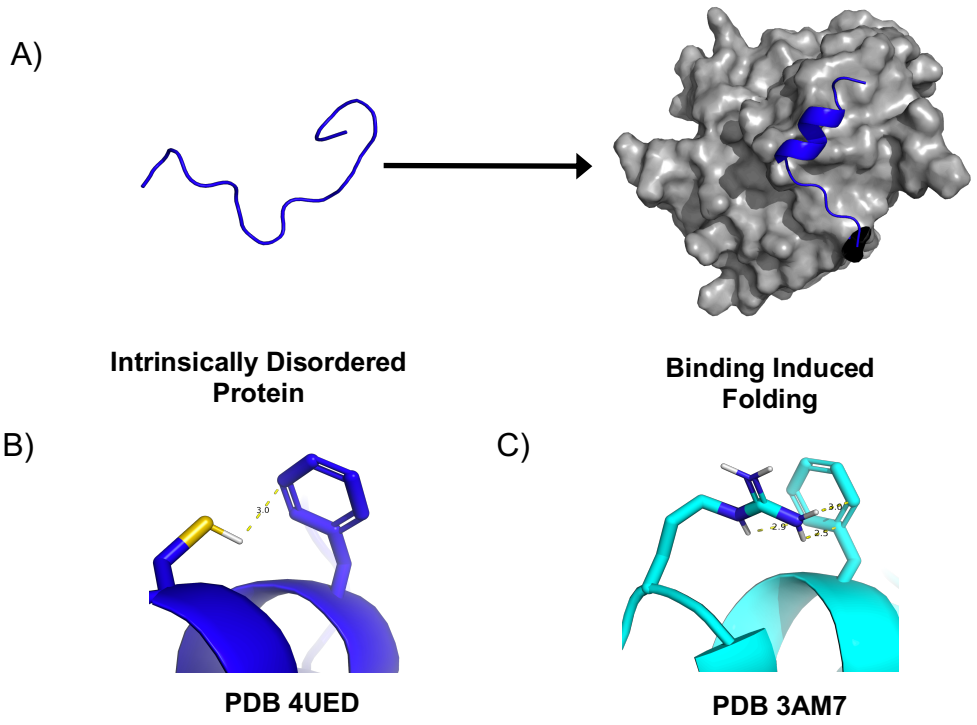

Figure 1.5 "4E-BP α-helix formation in mediated by eIF4E binding" A) A cartoon representation of 4E-BP helix formation on the eIF4E surface. B) a thiol-pi interaction and C) a cation-pi interaction appear to stabilize helices of 4E-BP1 and 4E-BP2, respectively.

region for eIF4E; however, 4E-BP forms a bipartite binding interface, with residues Ile78-Thr82 forming a weak antiparallel β-interaction with eIF4E (Figure 1.2A),[68,69] accounting for the higher eIF4E binding affinity of full-length protein relative to the hotspot peptide.[69,70] While favorable hydrophobic interactions at the PPI interface make up some of the entropic cost of protein ordering, a thiol—pi interaction between Phe58 and Cys62 of 4E-BP1 (Figure 1.5B) and a cation—pi interaction between Phe58 and Arg62 of 4E-BP2 (Figure 1.5C), likely stabilizes the folded structure on the eIF4E surface.[71]

Post-translational modification presents another powerful means of 4E-BP regulation. There are 6 canonical proline-directed 4E-BP phosphorylation sites, at Thr37, Thr46, Ser65, Thr70, Ser85, and Ser101, with an additional phosphorylation site reported

at Ser112 of 4E-BP1.[16,29,31,72-75] This is common mode of regulation for IDPs, which are often modulated sequentially or in specific combinations to effect function in signal transduction pathways.[4] Phosphorylation at Thr37, Thr46, Ser65, and Thr70 directly effect eIF4E binding in a mammalian target of rapamycin (mTOR) complex 1 (mTORC1)-dependent manner.[32,60,61,65,72,76] Activity of mTORC1 is stimulated in response to amino acids, growth factors and hormones to promote cell growth and proliferation.[77,78] Substrate recognition by mTORC1 is mediated by its Raptor protein component, which recognizes an N-terminal RAIP motif or a C-terminal TOS sequence of 4E-BP.[62,79-81]

A hierarchal mechanism of 4E-BP phosphorylation has been proposed, where phosphorylation of Thr37 and Thr46 is thought to prime the protein for subsequent phosphorylation events.[74] These two phosphoevents decrease the binding affinity of 4E-BP by almost 90-fold.[16] Structural studies indicate that this is likely due to a unique phosphorylation-induced folding phenomenon, where phosphorylation of these two sites, which are both located within a TTPGGT sequence repeat, results in partial protein folding into a four-stranded antiparallel β-sheet, and sequesters the eIF4E binding hot spot into the fold.[16] Despite the large decrease in 4E-BP binding affinity, data from both cell-based and *in vivo* studies, show that this phosphostate still preferentially binds to eIF4E over eIF4G. In fact, it is phosphorylation of Ser65 that appears to promote preferential binding by eIF4G and initiation of cap-dependent translation,[75,82] although there is conflicting data for this in brain tissue of a ischemia reperfusion stress model.[47]

Biophysical studies make a case for pSer65 as the critical phosphoevent abolishing eIF4E binding, as it is contained within the hot spot peptide region. While Ser65 does not directly contribute to the 4E-BP-eIF4E interaction,[69] phosphorylation at this site

is evidenced to destabilize helix formation upon eIF4E binding.[17,18] This is a precedented occurrence, as phosphorylation of Ser or Thr residues C-terminal to an α-helix is well documented to be destabilizing to the secondary structural element.[18,83] Destabilization of the 4E-BP helix by pSer65 is proposed to be due to an electrostatic repulsion mechanism, as α-helices form an electric dipole, where the C-terminal orientation of the backbone carbonyl oxygen atoms, create a net negative charge at the C-terminus of the helix. Thus, a negatively charged phosphate group, would disrupt the helix dipole. Intriguingly, pSer65 alone has been shown to be insufficient for loss of 4E-BP binding to eIF4E,[75,82,84] suggesting that this PTM downstream of pThr37 and pThr46, can be most accurately described as a threshold response to changes in cellular concentrations of growth promoting hormones and nutrients.

Even with the abundance of studies on hyperphosphorylated 4E-BP, particularly as a potential cancer biomarker, little is known about the role of phosphorylation of Ser83, Ser101, or Ser112. The Ser83 phosphorylation site appears to function outside the context of the accepted hierarchy.[85] In fact, asynchronous cells show very little pSer83 in its hyperphosphorylated population; however, nocodazole treated cells show CDK1-dependent enrichment in pSer83 specifically during mitosis.[85] In addition, pSer83 seems to play a specific, yet currently unelucidated role in cellular transformation that is not directly tied to the 4E-BP-eIF4E PPI.[85] There is also evidence that Ser101 is either constitutively phosphorylated or, in contrast with the accepted hierarchy, is directly required for phosphorylation of Ser65.[80] Phosphorylation of Ser112 in 4E-BP1 is the least understood of all phosphoevents. This site is purportedly modified by ataxia telangiectasia mutated (ATM) kinase in an insulin-dependent manner,[86,87] linking 4E-BP1 to DNA

damage response. At the present time, there is little known on the specific molecular function of pSer112, and there is ambiguity surrounding its possible effect on eIF4E binding[80,86].

1.5 The 4E-BP-eIF4E Axis is a Promising Target for Chemical Modulation of Cap-Dependent Translation

With the abundance of evidence demonstrating the correlation between initiation of cap-dependent translation and disease,[21,22,25,26,30,39,45,49,88-94] this process is a promising target for chemical intervention.[89,90,95-99] Particularly in cancer and neurological disease, there is a clear link between increased cap-dependent translation, disease progression and patient prognosis.[26,34,45,48-50,53,54] While activity of a number of eIF4F components have been shown to be sensitive to chemical modulation, for example eIF4A helicase[95] and eIF4E cap-binding,[100,101] I will focus on effectors of the 4E-BP/eIF4E PPI, including perturbation of the eIF4E-E-eIF4G PPI. Along these lines, the molecules mentioned here fall into two classes: upstream kinase-targeted compounds (Figure 1.6) and eIF4E PPI targeted compounds (Figure 1.7).

As mentioned above, 4E-BP ability to sequester eIF4E away from the translational machinery and inhibit cap-dependent translation is tightly controlled by mTORC1-dependent phosphorylation. Therefore, it is advantageous to target mTOR kinase activity as a way of increasing the cellular concentration of hypophosphorylated 4E-BP available to bind eIF4E. Indeed, this has been an effective approach. The natural product rapamycin is an allosteric mTOR inhibitor.[76,98] While rapamycin and its analogues, termed

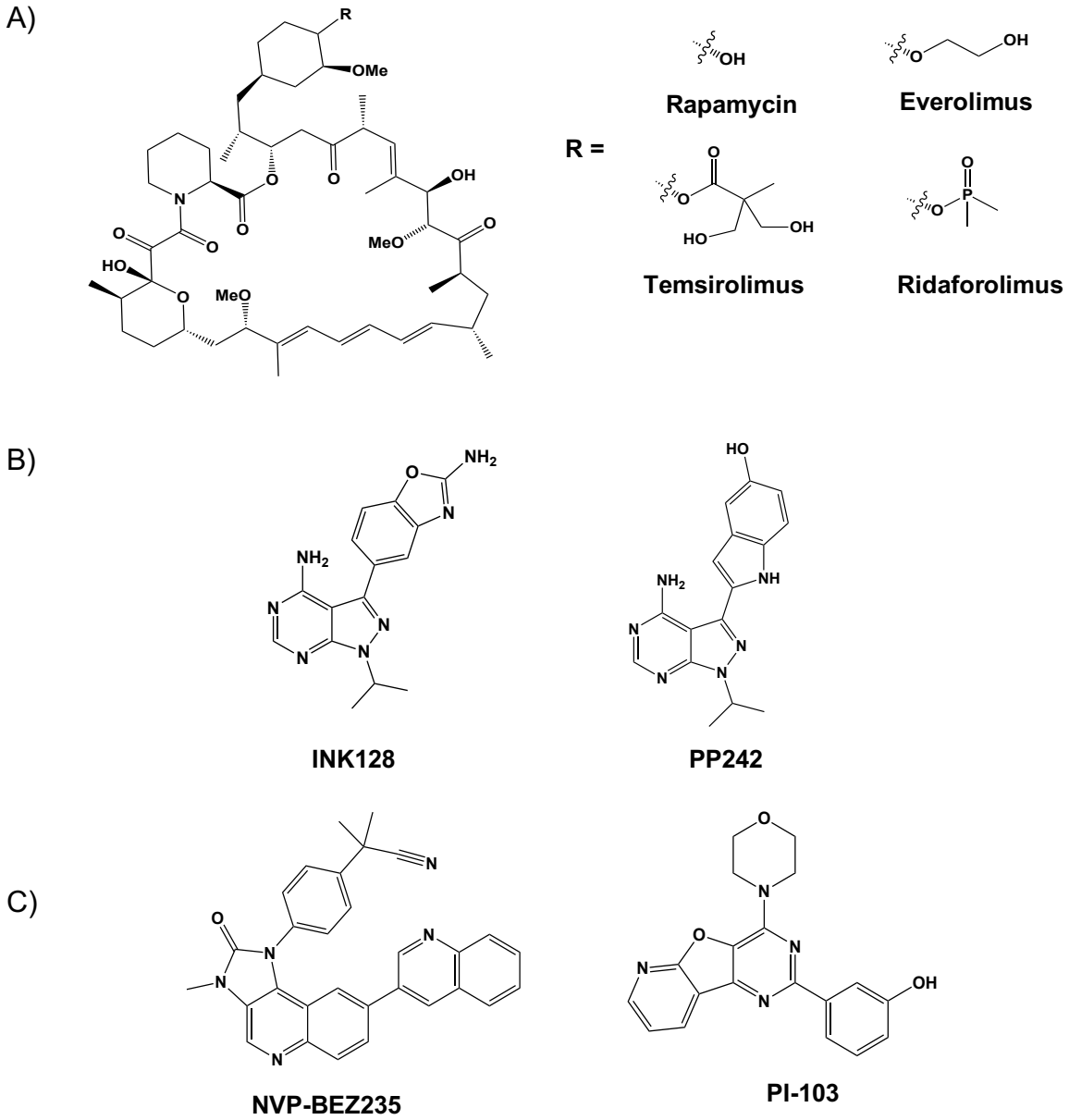

Figure 1.6 "Examples of mTORC1 inhibitors" A) Rapalogs B) mTORC1 active site inhibitors C) mTOR/PI3K dual specifity inhibitors

rapalogs, have found success in targeting cap-dependent translation in cancer and metabolic disease, they have displayed limited efficacy due in part to incomplete inhibition of 4E-BP relative to another mTORC1 substrate, S6K.[102]

In hopes of overcoming the apparent substrate selective inhibition profile of rapalogs, active site inhibitors of mTORC1 (mTORi) (Figure 1.6B), and dual specificity mTOR/PI3K inhibitors (Figure 1.6C) were developed. These inhibitors have shown favorable results in cancer models, as they both show more effective inhibition of 4E-BP phosphorylation, and also inhibit mTOR complex 2 (mTORC2), which can activate an AKT-dependent negative feedback loop that infers resistance to allosteric mTORC1 inhibition.[51,95,103] While showing great improvement over rapalogs, there is still evidence for incomplete p4E-BP inhibition, as in the case of PP242.[104] This can be attributed to a number of factors known to cause resistance to kinase inhibitors, including active site mutations[105] and activation of compensatory kinases.[106,107]

Another approach, which is complementary to kinase inhibition, is direct modulation of eIF4E interaction with eIF4G and/or 4E-BP. In this vein, peptide-based inhibitors such as caged peptides have been explored.[101] As is the case for 4E-BP, the hotspot region of eIF4G is disordered, until ligand binding induces formation of an amphipathic helix. This has prompted the development of stapled peptides based on bothe eIF4G and 4E-BP peptide sequences.[108,109] Hydrocarbon peptide stapling presents the opportunity to stabilize the bound conformation of a highly dynamic peptide, limiting the conformations that are sampled upon ligand binding, and improving the overall binding affinity by lowering the on rate,[110-112] although this is not always the case. The peptide stapling strategy involves synthesis of peptide containing an intramolecular

hydrocarbon linkage, usually replacing amino acids that are relatively dispensable for target binding, with i, i+4 spacing, mimicking the spacing of the backbone hydrogen bonding network that defines α-helicity. In addition to improvements in binding affinity relative to linear peptide sequences, stapled peptides have been found to increase cell permeability and proteolytic stability.[108,109] While this has proven to hold true in a number of cases, peptide stapling can have a negligible effect on some systems,[4,112] and have even been reported to upset PPI networks, as in the case of p53.[4] Stapled peptides have been designed to mimic both eIF4G[113,114] and 4E-BP[114], show modest improvements in eIF4E binding affinities. These data are encouraging for design of future iterations of conformationally restricted eIF4E binding peptides.

A)

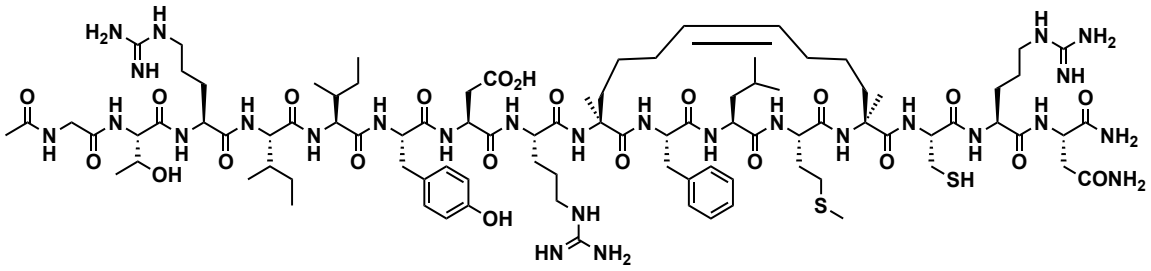

B)

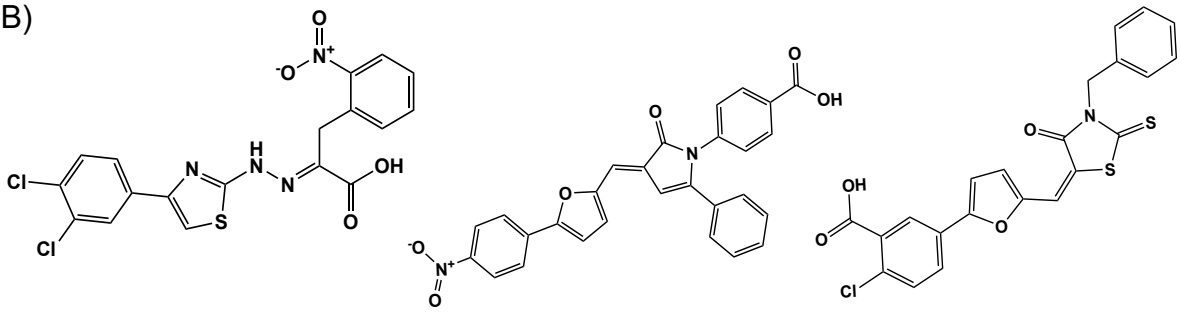

4EGI-1 **4E1RCat** **4E2RCat**

Figure 1.7 "Examples of eIF4E PPI Inhibitors" A) A 4E-BP-based stapled peptide B) Small molecules discovered via high-throughput screens

Small molecule modulators of eIF4E PPIs have also been explored. First, was the discovery of 4EGI-1,[99] from a fluorescence polarization based high-throughput screen. This compound was initially reported to inhibit eIF4G interaction, while at the same time promoting 4E-BP association. The discovery of 4EGI-1 undoubtedly set a precedent for small molecule perturbation of eIF4E PPIs; however, subsequent work revealed it to have an allosteric mode of action,[68,115] displaying off-target inhibition of cap-independent protein translation.[116] Two other small molecules identified through FRET based screening,[117] 4E1RCat[96] and 4E2Cat,[118] were later reported as inhibitors of both eIF4G and 4E-BP binding to eIF4G, with low micromolar affinity in *in vitro* assays. These compounds also exhibit minimal effect on cap-independent translation, although more work must be done to validate the long-term effects of inhibition of cap-dependent translation on cap-independent processes.[53]

1.6 Application of Chemistry-Based Strategies for Probing 4E-BP Conformational Dynamics

With the above work in mind, there are two major contexts in which to examine chemical perturbation of 4E-BP activity: through modulation of its amphipathic helix and through chemical dissection of phosphorylation-dependent 4E-BP structural dynamics. Studies of 4E-BP peptide stapling have demonstrated α-helix stabilization as a promising approach for modulating cap-dependent translation. Building upon this work, it would be advantageous to identify compounds that can induce helicity of the 4E-BP helix, while still allowing access to eIF4E binding. In this way, the cellular concentration of 4E-BP could be hijacked to inhibit cap-dependent translation, independent of 4E-BP phosphorylation state. While there is precedent of chemical compounds that function through secondary

structure stabilization,[119] there was previously no broadly applicable, high-throughput method to selectively screen for this class of compound. As a part of the work described here, I have developed a fluorescent peptide probe capable of doing this in the context of the 4E-BP helix, with the potential for application to a number of relevant systems. Additionally, with my collaborators at University of Toronto and the Hospital for Sick Children, evaluated a chemical mutagenesis approach to generation of pCys as a pSer/pThr phosphomimetic. This work, originally envisioned for application to elucidate the molecular roles of pSer83, pSer101, and pSer112, shed light on the chemical requirements of a potential 4E-BP phosphomimetic, as well as a number of considerations for development of chemical methods of PTM mimicry in complex biological systems.

1.7 References

1 He, B. *et al.* Predicting intrinsic disorder in proteins: an overview. *Cell Res* **19**, 929-949, doi:10.1038/cr.2009.87 (2009).

2 Peng, Z., Xue, B., Kurgan, L. & Uversky, V. N. Resilience of death: intrinsic disorder in proteins involved in the programmed cell death. *Cell Death Differ* **20**, 1257-1267, doi:10.1038/cdd.2013.65 (2013).

3 Dyson, H. J. & Wright, P. E. Intrinsically unstructured proteins and their functions. *Nat Rev Mol Cell Biol* **6**, 197-208, doi:10.1038/nrm1589 (2005).

4 Wright, P. E. & Dyson, H. J. Intrinsically disordered proteins in cellular signalling and regulation. *Nat Rev Mol Cell Biol* **16**, 18-29, doi:10.1038/nrm3920 (2015).

5 Wootton, J. C. F., S. Statistics of Local Complexity in Amino Acid Sequences and Sequence Databases. *Computers Chem* **17**, 149-163 (1993).

6 Marcotte, E. M. P., M.; Teates, T.O.;Eisenberg. A Census of Protein Repeats. *J. Mol. Biol.* **293**, 151-160 (1998).

7 Rechsteiner, M. R., Scott W. PEST sequesnces and regulation by proteolysis. *TIBS* **21**, 267-271 (1996).

8 Garcia-Alai, M. M. *et al.* Molecular basis for phosphorylation-dependent, PEST-mediated protein turnover. *Structure* **14**, 309-319, doi:10.1016/j.str.2005.11.012 (2006).

9 Dosztanyi, Z., Meszaros, B. & Simon, I. ANCHOR: web server for predicting protein binding regions in disordered proteins. *Bioinformatics* **25**, 2745-2746, doi:10.1093/bioinformatics/btp518 (2009).

10 Ishida, T. & Kinoshita, K. PrDOS: prediction of disordered protein regions from amino acid sequence. *Nucleic Acids Res* **35**, W460-464, doi:10.1093/nar/gkm363 (2007).

11 Walsh, I., Martin, A. J., Di Domenico, T. & Tosatto, S. C. ESpritz: accurate and fast prediction of protein disorder. *Bioinformatics* **28**, 503-509, doi:10.1093/bioinformatics/btr682 (2012).

12 Oates, M. E. *et al.* D(2)P(2): database of disordered protein predictions. *Nucleic Acids Res* **41**, D508-516, doi:10.1093/nar/gks1226 (2013).

13 Prilusky, J. *et al.* FoldIndex: a simple tool to predict whether a given protein sequence is intrinsically unfolded. *Bioinformatics* **21**, 3435-3438, doi:10.1093/bioinformatics/bti537 (2005).

14 Jones, D. T. & Cozzetto, D. DISOPRED3: precise disordered region predictions with annotated protein-binding activity. *Bioinformatics* **31**, 857-863, doi:10.1093/bioinformatics/btu744 (2015).

15 Despres, C. *et al.* Identification of the Tau phosphorylation pattern that drives its aggregation. *Proc Natl Acad Sci U S A* **114**, 9080-9085, doi:10.1073/pnas.1708448114 (2017).

16 Bah, A. *et al.* Folding of an intrinsically disordered protein by phosphorylation as a regulatory switch. *Nature* **519**, 106-109, doi:10.1038/nature13999 (2015).

17 Tait, S. *et al.* Local control of a disorder-order transition in 4E-BP1 underpins regulation of translation via eIF4E. *Proc Natl Acad Sci U S A* **107**, 17627-17632, doi:10.1073/pnas.1008242107 (2010).

18 Andrew, D. C. W., J.; Jones, G.R.; Doig, A.J. Effect of phosphorylation on alpha-helix stability as a function of position. *Biochemistry* **41**, 1897-1905 (2002).

19 Marcotrigiano, J. G., Anne-Claude; Sonenberg, Nahum; Burley, Stephen K. Cap-Dependent Translation in Eukaryotes Is Regulated by a Molecular Mimic of eIF4G. *Molecular Cell* **3**, 707-716 (1999).

20 Shantz, L. M. P., Anthony E. Overproduction of Ornithine Decarboxylase Caused by Relief of Translational Repression Is Associated with Neoplastic Transformation. *Cancer Research* **54**, 2313-2316 (1994).

21 Armengol, G. *et al.* 4E-binding protein 1: a key molecular "funnel factor" in human cancer with clinical implications. *Cancer Res* **67**, 7551-7555, doi:10.1158/0008-5472.CAN-07-0881 (2007).

22 Braunstein, S. *et al.* A hypoxia-controlled cap-dependent to cap-independent translation switch in breast cancer. *Mol Cell* **28**, 501-512, doi:10.1016/j.molcel.2007.10.019 (2007).

23 Silvera, D., Formenti, S. C. & Schneider, R. J. Translational control in cancer. *Nat Rev Cancer* **10**, 254-266, doi:10.1038/nrc2824 (2010).

24 Wouters, B. G. & Koritzinsky, M. Hypoxia signalling through mTOR and the unfolded protein response in cancer. *Nat Rev Cancer* **8**, 851-864, doi:10.1038/nrc2501 (2008).

25 Avdulov, S. *et al.* Activation of translation complex eIF4F is essential for the genesis and maintenance of the malignant phenotype in human mammary epithelial cells. *Cancer Cell* **5**, 553-563, doi:10.1016/j.ccr.2004.05.024 (2004).

26 Clemens, M. J. E., Androulla; Constantinou, Constantina. Control of Protein Synthesis in Malignant Transformation - the Role of eIF4E Binding Proteins in the Regulation of the Apoptosis. *Current Cancer Therapy Reviews* **3**, 151-163 (2007).

27 Morita, M. *et al.* mTORC1 controls mitochondrial activity and biogenesis through 4E-BP-dependent translational regulation. *Cell Metab* **18**, 698-711, doi:10.1016/j.cmet.2013.10.001 (2013).

28 Rousseau, D. G., AC; Pause, A; Sonenberg N. The eIF4E-binding proteins 1 and 2 are negative regulators of cell growth. *Oncogene* **13**, 2415-2420 (1996).

29 Li, S. *et al.* Translational Control of Cell Fate: Availability of Phosphorylation Sites on Translational Repressor 4E-BP1 Governs Its Proapoptotic Potency. *Molecular and Cellular Biology* **22**, 2853-2861, doi:10.1128/mcb.22.8.2853-2861.2002 (2002).

30 Azar, R., Alard, A., Susini, C., Bousquet, C. & Pyronnet, S. 4E-BP1 is a target of Smad4 essential for TGFbeta-mediated inhibition of cell proliferation. *EMBO J* **28**, 3514-3522, doi:10.1038/emboj.2009.291 (2009).

31 Dowling, R. J. *et al.* mTORC1-mediated cell proliferation, but not cell growth, controlled by the 4E-BPs. *Science* **328**, 1172-1176, doi:10.1126/science.1187532 (2010).

32 Gingras, A. C. K., Scott G.; O'Leary, Maura A.; Sonenberg, Nahum; Hay, Nissim. 4E-BP1, a repressor of mRNA translation, is phosphorylated and inactivated by the Akt(PKB) signaling pathway. *Genes Dev* **12**, 502-513 (1997).

33 Takata, M. *et al.* Requirement for Akt (Protein Kinase B) in Insulin-induced Activation of Glycogen Synthase and Phosphorylation of 4E-BP1 (PHAS-1). *Journal of Biological Chemistry* **274**, 20611-20618, doi:10.1074/jbc.274.29.20611 (1999).

34 She, Q. B. *et al.* 4E-BP1 is a key effector of the oncogenic activation of the AKT and ERK signaling pathways that integrates their function in tumors. *Cancer Cell* **18**, 39-51, doi:10.1016/j.ccr.2010.05.023 (2010).

35 Polunovsky, V. A. *et al.* Translational control of the antiapoptotic function of Ras. *J Biol Chem* **275**, 24776-24780, doi:10.1074/jbc.M001938200 (2000).

36 Zid, B. M. *et al.* 4E-BP extends lifespan upon dietary restriction by enhancing mitochondrial activity in Drosophila. *Cell* **139**, 149-160, doi:10.1016/j.cell.2009.07.034 (2009).

37 Petremand, J. *et al.* Involvement of 4E-BP1 in the protection induced by HDLs on pancreatic beta-cells. *Mol Endocrinol* **23**, 1572-1586, doi:10.1210/me.2008-0448 (2009).

38 Bhandari, B. K. F., Denis; Duraisamy, Senthil; Stewart, Jennifer L.; Gingras, Anne-Claude; Abboud, Hanna E.; Choudhury, Goutam Ghosh; Sonenberg, Nahum; Kasinath,

Balakuntalam S. Insulin regulation of protein translation repressor 4E-BP1, an eIF4E-binding protein, in renal epithelial cells. *Kidney International* **59**, 866-875 (2001).

39 Yu, X. X. *et al.* Reduced adiposity and improved insulin sensitivity in obese mice with antisense suppression of 4E-BP2 expression. *Am J Physiol Endocrinol Metab* **294**, E530-539, doi:10.1152/ajpendo.00350.2007 (2008).

40 O'Shea, C. K., K.; Choi, S.; Bagus, B.; Soria, C.; Shen, J.; McCormick, F.; Stokoe, D. Adenoviral proteins mimic mutrient/growth signals to activate the mTOR pathway for viral replication. *The EMBO Journal* **24**, 1211-1221, doi:10.1038/ (2005).

41 Connor, J. H. & Lyles, D. S. Vesicular Stomatitis Virus Infection Alters the eIF4F Translation Initiation Complex and Causes Dephosphorylation of the eIF4E Binding Protein 4E-BP1. *Journal of Virology* **76**, 10177-10187, doi:10.1128/jvi.76.20.10177-10187.2002 (2002).

42 Chuluunbaatar, U. *et al.* Constitutive mTORC1 activation by a herpesvirus Akt surrogate stimulates mRNA translation and viral replication. *Genes Dev* **24**, 2627-2639, doi:10.1101/gad.1978310 (2010).

43 Walsh, D. & Mohr, I. Assembly of an active translation initiation factor complex by a viral protein. *Genes Dev* **20**, 461-472, doi:10.1101/gad.1375006 (2006).

44 Spangle, J. M. & Munger, K. The human papillomavirus type 16 E6 oncoprotein activates mTORC1 signaling and increases protein synthesis. *J Virol* **84**, 9398-9407, doi:10.1128/JVI.00974-10 (2010).

45 Gkogkas, C. G. *et al.* Autism-related deficits via dysregulated eIF4E-dependent translational control. *Nature* **493**, 371-377, doi:10.1038/nature11628 (2013).

46 Ayuso, M. I., Martinez-Alonso, E., Cid, C., Alonso de Lecinana, M. & Alcazar, A. The translational repressor eIF4E-binding protein 2 (4E-BP2) correlates with selective delayed neuronal death after ischemia. *J Cereb Blood Flow Metab* **33**, 1173-1181, doi:10.1038/jcbfm.2013.60 (2013).

47 Ayuso, M. I., Hernandez-Jimenez, M., Martin, M. E., Salinas, M. & Alcazar, A. New hierarchical phosphorylation pathway of the translational repressor eIF4E-binding protein 1 (4E-BP1) in ischemia-reperfusion stress. *J Biol Chem* **285**, 34355-34363, doi:10.1074/jbc.M110.135103 (2010).

48 Rojo, F. *et al.* 4E-binding protein 1, a cell signaling hallmark in breast cancer that correlates with pathologic grade and prognosis. *Clin Cancer Res* **13**, 81-89, doi:10.1158/1078-0432.CCR-06-1560 (2007).

49 Castellvi, J. *et al.* Phosphorylated 4E binding protein 1: a hallmark of cell signaling that correlates with survival in ovarian cancer. *Cancer* **107**, 1801-1811, doi:10.1002/cncr.22195 (2006).

50 O'Reilly, K. E. *et al.* Phosphorylated 4E-BP1 is associated with poor survival in melanoma. *Clin Cancer Res* **15**, 2872-2878, doi:10.1158/1078-0432.CCR-08-2336 (2009).

51 Hsieh, A. C. *et al.* The translational landscape of mTOR signalling steers cancer initiation and metastasis. *Nature* **485**, 55-61, doi:10.1038/nature10912 (2012).

52 Chakravarthy, R. *et al.* Role of the eIF4E binding protein 4E-BP1 in regulation of the sensitivity of human pancreatic cancer cells to TRAIL and celastrol-induced apoptosis. *Biol Cell* **105**, 414-429, doi:10.1111/boc.201300021 (2013).

53 Martineau, Y. *et al.* Pancreatic tumours escape from translational control through 4E-BP1 loss. *Oncogene* **33**, 1367-1374, doi:10.1038/onc.2013.100 (2014).

54 Hsu, H. S. *et al.* The 4E-BP1/eIF4E ratio is a determinant for rapamycin response in esophageal cancer cells. *J Thorac Cardiovasc Surg* **149**, 378-385, doi:10.1016/j.jtcvs.2014.09.047 (2015).

55 Lee, H. W. L., Eun Hee; Lee, Ji Hyun; Kim, Jeong-Eun; Kim, Seok-Hyun; Kim, Tae Gyu; Hwang, Sang Won; Kang, Kyung Woo. Prognostic significance of phosphorylated 4E-binding protein 1 in non-small cell lung cancer. *Int J Clin Pathol* **8**, 3955-3962 (2015).

56 Belsham, G. J. B., Roger W.; Denton, R. M. Reversibility of the insulin-stimulated phosphorylation of ATP citrate lyase and a cytoplasmic protein of subunit Mr 22000 in adipose tissue. *Biochem J.* **204**, 345-352 (1982).

57 Blackshear, P. J. N., Raphael A.; Avruch, Joseph. Preliminary characterization of a heat-stable protein from rat adipose tissue whose phosphorylation is stimulated by insulin. *Biochem J.* **204**, 814-824 (1982).

58 Blackshear, P. J. N., Raphael A.; Avruch, Joseph. Insulin and growth factors stimulate the phosphorylation of a Mr-22000 protein in 3T3-L1 adipocytes. *Biochem J.* **214**, 11-19 (1983).

59 Hu, C. P., Suhong; Kong, Xianming; Velleca, Mark; Lawrence Jr., John C. Molcular cloning and tissue distribution of PHAS-I, an intracelluar target for insuling and growth factors. *PNAS* **91**, 3730-3734 (1994).

60 Lin, T.-A. K., Xianming; Haystead, Timothy A.; Pause, Arnim; Belsham, Graham; Sonenberg, Nahum; Lawrence Jr., John C. PHAS-I as a Link Between Mitogen-Activated Protein Kinase and Tranlation Initiation. *Science* **266**, 653-656 (1994).

61 Haghighat, A. M., Sylvie; Pause, Arnim; Sonenberg, Nahum. Repression of cap-dependent translation by 4E-binding protein 1: competition with p220 for binding to eukaryotic initiation factor 4E. *The EMBO Journal* **14**, 5701-5709 (1995).

62 Lee, V. H., Healy, T., Fonseca, B. D., Hayashi, A. & Proud, C. G. Analysis of the regulatory motifs in eukaryotic initiation factor 4E-binding protein 1. *FEBS J* **275**, 2185-2199, doi:10.1111/j.1742-4658.2008.06372.x (2008).

63 Martineau, Y., Azar, R., Bousquet, C. & Pyronnet, S. Anti-oncogenic potential of the eIF4E-binding proteins. *Oncogene* **32**, 671-677, doi:10.1038/onc.2012.116 (2013).

64 Tsukiyama-Kohara, K. V., Silvia M.; Gingras, Anne-Claude; Glover, Thomas W.; Hanish, Samir M.; Heng, Henry; Sonenberg, Nahum. Tissue Distrubution, Genomic Structure, and Chromosome Mapping of Mouse and Human Eukaryotic Initiation Factor 4E-Binding Proteins 1 and 2. *Genomics* **38**, 353-363 (1996).

65 Pause, A. B., Graham J.; Gingras, Anne-Claude; Donzé, Olivier; Lin, Tai-An; Lawrence Jr., John C.; Sonenberg, Nahum. Insulin-dependent stimulation of protein syntheisis by phosphorylatin of a regulator of 5'-cap function. *Nature* **371**, 762-767 (1994).

66 Elia, A., Constantinou, C. & Clemens, M. J. Effects of protein phosphorylation on ubiquitination and stability of the translational inhibitor protein 4E-BP1. *Oncogene* **27**, 811-822, doi:10.1038/sj.onc.1210678 (2008).

67 Yanagiya, A. *et al.* Translational homeostasis via the mRNA cap-binding protein, eIF4E. *Mol Cell* **46**, 847-858, doi:10.1016/j.molcel.2012.04.004 (2012).

68 Sekiyama, N. *et al.* Molecular mechanism of the dual activity of 4EGI-1: Dissociating eIF4G from eIF4E but stabilizing the binding of unphosphorylated 4E-BP1. *Proceedings of the National Academy of Sciences* **112**, E4036-E4045, doi:10.1073/pnas.1512118112 (2015).

69 Peter, D. *et al.* Molecular architecture of 4E-BP translational inhibitors bound to eIF4E. *Mol Cell* **57**, 1074-1087, doi:10.1016/j.molcel.2015.01.017 (2015).

70 Lukhele, S., Bah, A., Lin, H., Sonenberg, N. & Forman-Kay, J. D. Interaction of the eukaryotic initiation factor 4E with 4E-BP2 at a dynamic bipartite interface. *Structure* **21**, 2186-2196, doi:10.1016/j.str.2013.08.030 (2013).

71 Forbes, C. R. *et al.* Insights into Thiol-Aromatic Interactions: A Stereoelectronic Basis for S-H/pi Interactions. *J Am Chem Soc* **139**, 1842-1855, doi:10.1021/jacs.6b08415 (2017).

72 von Manteuffel, S. R. G., Anne-Claude; Ming, Xiu-Feng; Sonenberg, Nahum; Thomas, George. 4E-BP1 phosphorylation is mediated by the FRAP-p70s6k pathway and is independent of mitogen-activated protein kinase. *PNAS* **93**, 4076-4080 (1996).

73 Beretta, L. G., Anne-Claude; Svitkin, Yuri V.; Hall, Michael N.; Sonenberg, Nahum. Rapamycin blocks the phosphorylation of 4E-BP1 and inhibits cap-dependent initiation of translation. *The EMBO Journal* **15**, 658-664 (1996).

74 Gingras, A. C. G., Steven P.; Raught, Brian; Polakiewicz, Roberto D.; Abraham, Robert T.; Hoekstra, Merl F.; Aebersold, Ruedi; Sonenberg, Nahum. Regulation of 4E-BP1 phosphorylation: a novel two-step mechanism. *Genes Dev* **13**, 1422-1437 (1999).

75 Gingras, A. C. *et al.* Hierarchical phosphorylation of the translation inhibitor 4E-BP1. *Genes Dev* **15**, 2852-2864, doi:10.1101/gad.912401 (2001).

76 Beretta, L. G., Anne-Claude; Svitkin, Yuri V.; Hall, Michael N.; Sonenberg. Rapamycin blocks the phophorylation of 4E-BP1 and inhibits cap-dependent initiation of translation. *The EMBO Journal* **15**, 658-664 (1996).

77 Fleurent, M. G., Anne-Claude; Sonenberg, Nahum; Meloche, Sylvain. Angiotensin II Stimulates Phosphorylation of the Translational Repressor 4E-binding Protein 1 by a Mitogen-activated Protein Kinase-independent Mechanism. *The Journal of Biological Chemistry* **272**, 4006-4012 (1997).

78 Pyronnet, S. G., Anne-Claude; Bouisson, Michèle; Kowalski-Chauvel, Aline; Seva, Catherine; Vaysse, Nicole; Sonenberg, Nahum; Pradayrol, Lucien. Gastrin induces phophorylation of eIF4E binding protein 1 and translation initiation of ornithine decarboxylase mRNA. *Oncogene* **16**, 2219-2227 (1998).

79 Beugnet, A., Wang, X. & Proud, C. G. Target of rapamycin (TOR)-signaling and RAIP motifs play distinct roles in the mammalian TOR-dependent phosphorylation of initiation factor 4E-binding protein 1. *J Biol Chem* **278**, 40717-40722, doi:10.1074/jbc.M308573200 (2003).

80 Wang, X., Li, W., Parra, J. L., Beugnet, A. & Proud, C. G. The C Terminus of Initiation Factor 4E-Binding Protein 1 Contains Multiple Regulatory Features That Influence Its Function and Phosphorylation. *Molecular and Cellular Biology* **23**, 1546-1557, doi:10.1128/mcb.23.5.1546-1557.2003 (2003).

81 Choi, K. M., McMahon, L. P. & Lawrence, J. C., Jr. Two motifs in the translational repressor PHAS-I required for efficient phosphorylation by mammalian target of rapamycin and for recognition by raptor. *J Biol Chem* **278**, 19667-19673, doi:10.1074/jbc.M301142200 (2003).

82 Karim, M. M. *et al.* A quantitative molecular model for modulation of mammalian translation by the eIF4E-binding protein 1. *J Biol Chem* **276**, 20750-20757, doi:10.1074/jbc.M011068200 (2001).

83 Elbaum, M. B. & Zondlo, N. J. OGlcNAcylation and phosphorylation have similar structural effects in alpha-helices: post-translational modifications as inducible start and stop signals in alpha-helices, with greater structural effects on threonine modification. *Biochemistry* **53**, 2242-2260, doi:10.1021/bi500117c (2014).

84 Tomoo, K., Abiko, F., Miyagawa, H., Kitamura, K. & Ishida, T. Effect of N-terminal region of eIF4E and Ser65-phosphorylation of 4E-BP1 on interaction between eIF4E and 4E-BP1 fragment peptide. *J Biochem* **140**, 237-246, doi:10.1093/jb/mvj143 (2006).

85 Velasquez, C. *et al.* Mitotic protein kinase CDK1 phosphorylation of mRNA translation regulator 4E-BP1 Ser83 may contribute to cell transformation. *Proc Natl Acad Sci U S A* **113**, 8466-8471, doi:10.1073/pnas.1607768113 (2016).

86 Yang, D.-Q. K., M.B. Participation of ATM in insulin signailling through phosphorylation od eIF4-4E binding protein 1. *Nature Cell Biology* **2**, 893-898 (2000).

87 Matsuoka, S. B., B.A.; Smogorzewska, A.; McDonald III, E.R.; Hurov, K.E.; Luo, J.; Bakalarski, C.E.; Zhao, A.; Solimini, N.; Lerenthal, Y.; Shiloh, Y.; Gygi, S.P.; Elledge, S.J. . ATM and ATR Substrate Analysis Reveals Extensive Protein Networks Responsive to DNA Damage. *Science* **316**, 1160-1166 (2007).

88 Assouline, S. *et al.* Molecular targeting of the oncogene eIF4E in acute myeloid leukemia (AML): a proof-of-principle clinical trial with ribavirin. *Blood* **114**, 257-260, doi:10.1182/blood-2009-02-205153 (2009).

89 Assouline, S. *et al.* A phase I trial of ribavirin and low-dose cytarabine for the treatment of relapsed and refractory acute myeloid leukemia with elevated eIF4E. *Haematologica* **100**, e7-9, doi:10.3324/haematol.2014.111245 (2015).

90 Blagden, S. P. W., Anne E. The biological and therapeutic relevance of mRNA translation in cancer. *Nature Reviews Clinical Oncology* **8**, 281-290 (2011).

91 Buchkovich, N. J., Yu, Y., Zampieri, C. A. & Alwine, J. C. The TORrid affairs of viruses: effects of mammalian DNA viruses on the PI3K-Akt-mTOR signalling pathway. *Nat Rev Microbiol* **6**, 266-275, doi:10.1038/nrmicro1855 (2008).

92 George, A. *et al.* Hepatitis C virus NS5A binds to the mRNA cap-binding eukaryotic translation initiation 4F (eIF4F) complex and up-regulates host translation initiation machinery through eIF4E-binding protein 1 inactivation. *J Biol Chem* **287**, 5042-5058, doi:10.1074/jbc.M111.308916 (2012).

93 Santini, E. *et al.* Exaggerated translation causes synaptic and behavioural aberrations associated with autism. *Nature* **493**, 411-415, doi:10.1038/nature11782 (2013).

94 Polak, P. *et al.* Adipose-specific knockout of raptor results in lean mice with enhanced mitochondrial respiration. *Cell Metab* **8**, 399-410, doi:10.1016/j.cmet.2008.09.003 (2008).

95 Bhat, M. *et al.* Targeting the translation machinery in cancer. *Nature Reviews Drug Discovery* **14**, 261-278, doi:10.1038/nrd4505 (2015).

96 Cencic, R. *et al.* Reversing chemoresistance by small molecule inhibition of the translation initiation complex eIF4F. *Proc Natl Acad Sci U S A* **108**, 1046-1051, doi:10.1073/pnas.1011477108 (2011).

97 Fujimura, K., Sasaki, A. T. & Anderson, P. Selenite targets eIF4E-binding protein-1 to inhibit translation initiation and induce the assembly of non-canonical stress granules. *Nucleic Acids Res* **40**, 8099-8110, doi:10.1093/nar/gks566 (2012).

98 Li, J., Kim, S. G. & Blenis, J. Rapamycin: one drug, many effects. *Cell Metab* **19**, 373-379, doi:10.1016/j.cmet.2014.01.001 (2014).

99 Moerke, N. J. *et al.* Small-molecule inhibition of the interaction between the translation initiation factors eIF4E and eIF4G. *Cell* **128**, 257-267, doi:10.1016/j.cell.2006.11.046 (2007).

100 Brown, C. J., McNae, I., Fischer, P. M. & Walkinshaw, M. D. Crystallographic and mass spectrometric characterisation of eIF4E with N7-alkylated cap derivatives. *J Mol Biol* **372**, 7-15, doi:10.1016/j.jmb.2007.06.033 (2007).

101 Sadovski, O. *et al.* A collection of caged compounds for probing roles of local translation in neurobiology. *Bioorg Med Chem* **18**, 7746-7752, doi:10.1016/j.bmc.2010.04.005 (2010).

102 Choo, A. Y. Y., S.-O.; Kim, S.G.; Roux, P.P.; Blenis, J. Rapamycin differentially inhibits S6Ks and 4E-BP1 to mediate cell-type-specific repression of mRNA translation. *Proc Natl Acad Sci U S A* **105**, 17414-17419 (2008).

103 Hsieh, A. C. *et al.* Genetic dissection of the oncogenic mTOR pathway reveals druggable addiction to translational control via 4EBP-eIF4E. *Cancer Cell* **17**, 249-261, doi:10.1016/j.ccr.2010.01.021 (2010).

104 Ducker, G. S. *et al.* Incomplete inhibition of phosphorylation of 4E-BP1 as a mechanism of primary resistance to ATP-competitive mTOR inhibitors. *Oncogene* **33**, 1590-1600, doi:10.1038/onc.2013.92 (2014).

105 Balzano, D., Santaguida, S., Musacchio, A. & Villa, F. A general framework for inhibitor resistance in protein kinases. *Chem Biol* **18**, 966-975, doi:10.1016/j.chembiol.2011.04.013 (2011).

106 Liu, Y., Vertommen, D., Rider, M. H. & Lai, Y. C. Mammalian target of rapamycin-independent S6K1 and 4E-BP1 phosphorylation during contraction in rat skeletal muscle. *Cell Signal* **25**, 1877-1886, doi:10.1016/j.cellsig.2013.05.005 (2013).

107 Shuda, M. *et al.* CDK1 substitutes for mTOR kinase to activate mitotic cap-dependent protein translation. *Proc Natl Acad Sci U S A* **112**, 5875-5882, doi:10.1073/pnas.1505787112 (2015).

108 Walensky, L. D. K., A.L.; Escher, I.; Malia, T.J.; Barbuto, S.; Wright, R.D.; Wagner, G.; Verdine, G.L.; Korsmeyer, S.J. Activation of Apoptosis in Vivo by a Hydrocarbon-Stapled BH3 Helix. *Science* **305**, 1466-1470 (2004).

109 Walensky, L. D. & Bird, G. H. Hydrocarbon-stapled peptides: principles, practice, and progress. *J Med Chem* **57**, 6275-6288, doi:10.1021/jm4011675 (2014).

110 Zhou, H. X., Pang, X. & Lu, C. Rate constants and mechanisms of intrinsically disordered proteins binding to structured targets. *Phys Chem Chem Phys* **14**, 10466-10476, doi:10.1039/c2cp41196b (2012).

111 Mollica, L. *et al.* Binding Mechanisms of Intrinsically Disordered Proteins: Theory, Simulation, and Experiment. *Front Mol Biosci* **3**, 52, doi:10.3389/fmolb.2016.00052 (2016).

112 Saglam, A. S., Wang, D. W., Zwier, M. C. & Chong, L. T. Flexibility vs Preorganization: Direct Comparison of Binding Kinetics for a Disordered Peptide and Its Exact Preorganized Analogues. *J Phys Chem B* **121**, 10046-10054, doi:10.1021/acs.jpcb.7b08486 (2017).

113 Lama, D. *et al.* Rational optimization of conformational effects induced by hydrocarbon staples in peptides and their binding interfaces. *Sci Rep* **3**, 3451, doi:10.1038/srep03451 (2013).

114 Gallagher, E. E. S., J. M.; Menon, A.; Mishra, L. D.; Chmiel, A. F.; Garner, A. L. Probing the Importance of Folding Dynamics in the Design of Stapled Peptide Mimics of the Disordered Proteins 4E-BP1 and eIF4G. *in revision* (2018).

115 Papadopoulos, E. *et al.* Structure of the eukaryotic translation initiation factor eIF4E in complex with 4EGI-1 reveals an allosteric mechanism for dissociating eIF4G. *Proc Natl Acad Sci U S A* **111**, E3187-3195, doi:10.1073/pnas.1410250111 (2014).

116 Redondo, N., Garcia-Moreno, M., Sanz, M. A. & Carrasco, L. Translation of viral mRNAs that do not require eIF4E is blocked by the inhibitor 4EGI-1. *Virology* **444**, 171-180, doi:10.1016/j.virol.2013.06.008 (2013).

117 Cencic, R. Y., Y.; Pelletier, J. Homogenous time resolved fluorescence assay to identify modulators of cap sedendent translation initiation. *Comb Chem High Throughput Screen* **10**, 181-188 (2007).

118 Cencic, R. *et al.* Blocking eIF4E-eIF4G interaction as a strategy to impair coronavirus replication. *J Virol* **85**, 6381-6389, doi:10.1128/JVI.00078-11 (2011).

119 Perez-Miller, S. *et al.* Alda-1 is an agonist and chemical chaperone for the common human aldehyde dehydrogenase 2 variant. *Nature Structural & Molecular Biology* **17**, 159-164, doi:10.1038/nsmb.1737 (2010).

Chapter 2 – A Conditionally Fluorescent Peptide Reporter of Secondary Structure Modulation

*Note: This chapter contains an accepted manuscript: O.T. Johnson, T. Kaur, and Prof. A.L.Garner; *ChemBioChem* **(2018)** 10.1002/cbic.201800377

2.1 Introduction

Dynamic conformational change is a critically important mechanism of mediating and regulating protein function.[1] From regulating the active conformation of enzymes to mediate catalytic turnover, to inferring selectivity in interactions between protein binding partners, protein structure modulation yields information about its functional outcome(s).[1,2] Intrinsically disordered proteins (IDPs) and proteins containing intrinsically disordered regions (IDRs) are, by definition, highly dynamic, existing as conformational

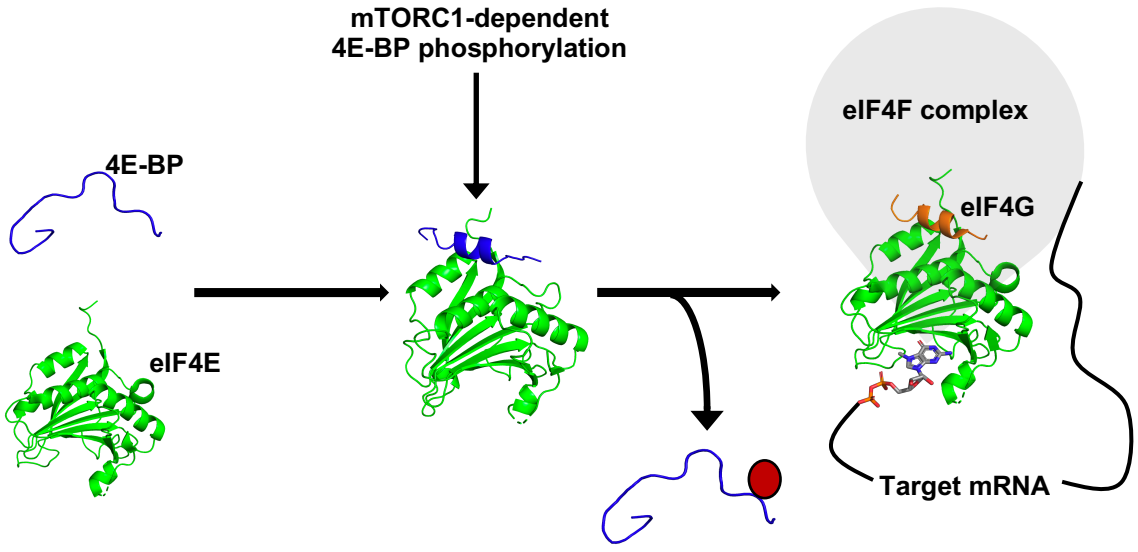

Figure 2.1 "α-Helix Formation Mediates 4E-BP binding to eIF4E"

ensembles as opposed to more ridged secondary and tertiary structures.[3] Their structural fluidity is directly related to their function as signaling hubs in protein interaction networks that regulate cellular growth and development.[1,2] Within these signaling cascades, binding-induced folding has been found to be an important aspect of the protein-protein interactions (PPIs) of many IDPs, affecting binding affinity and specificity.[1]

An example of such structural polymorphism in ligand binding can be found in a family of three intrinsically disordered translational repressor proteins known as the eIF4E-binding proteins (4E-BPs), which regulate a subset of mRNA transcripts that are integral for maintenance of cellular homeostasis, including Bcl-2, ODC, and c-Myc.[4-6] These proteins function by sequestering the mRNA cap-binding protein eIF4E from eIF4G, which shares a similar eIF4E-binding motif, to inhibit the initiation of cap-dependent translation (Figure 2.1).[7] The 4E-BPs form a short α-helix upon binding to eIF4E, where helix formation is a consequence of ligand binding.[1,2,7] Mechanistic target of rapamycin complex 1 (mTORC1)-dependent phosphorylation of 4E-BPs regulates their function[8] in part by destabilizing this helix,[9,10] suggesting that modulation of 4E-BP secondary structuring could be a promising strategy by which to impart functional control over the protein via chemical means. This rationale has been explored in the design of stapled peptides based on the peptide hot spot regions of 4E-BPs[11] as well as their biological competitor, eIF4G;[12] however, identifying 4E-BP helix modulators with specificity over the eIF4G helix presents a challenge.

Traditional biophysical methods for analyzing protein and peptide structure include circular dichroism (CD) and Nuclear Magnetic Resonance (NMR) spectroscopies as well as X-ray crystallography. While these are powerful techniques that yield detailed

information about protein structure, they are also low-throughput, require large amounts of sample, and data analysis can be onerous, particularly when studying IDPs.[1,2,14,15] Thus, there is a necessity for new approaches to identify modulators of conformational change in a broadly applicable format.

A)

B)

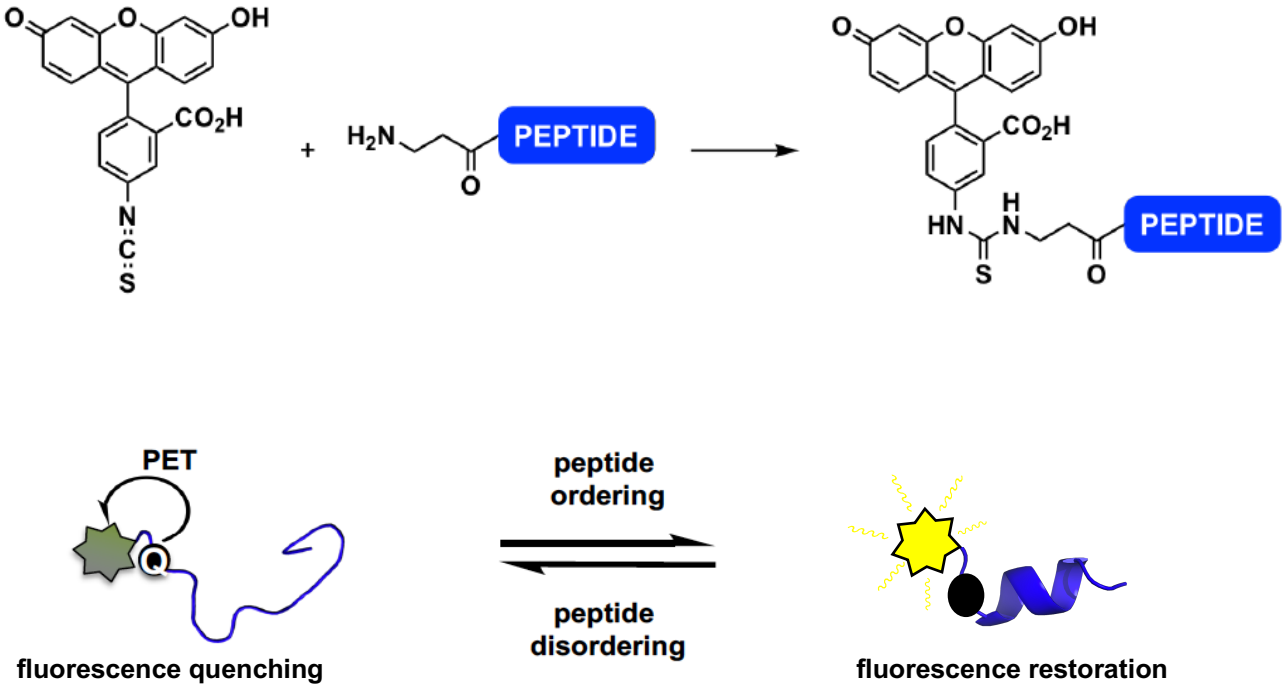

Figure 2.2 "Rationale for Fluorescent Peptide Reporter Assay"

Previous studies have demonstrated the utility of thioamides and their derivatives as minimally perturbing fluorescence quenchers in proteins through a photo-induced electron transfer (PET) mechanism.[16] In contrast to other processes that result in quenched fluorescence through energy transfer such as fluorescence resonance energy transfer (FRET), PET quenching does not require spectral overlap of the electron donor

and acceptor and occurs over very short distances (~3–5 Å).[17,18] Inspired by the use of conditional thioamide quenching for sensing protease activity[17] and conformational dynamics of macromolecules,[17,19,20] we adapted this approach to observe the disorder-to-order transition of a 4E-BP1 hot spot peptide. Herein, we describe the serendipitous discovery and development of a fluorescent peptide reporter that can detect modulation

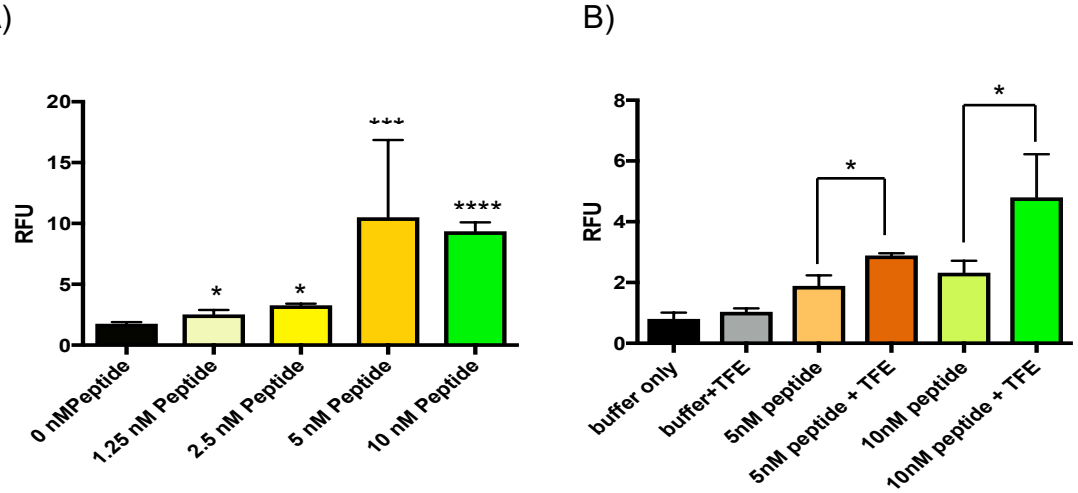

Figure 2.3 "Optimization of Fluorescent Peptide Concentration" A) Peptide relative fluorescence signal (RFU) (ex/em: 494/520 nm) was read to determine the minimum peptide concentration required to give significant fluorescence signal over assay buffer alone B) Fluorescence signal of 5 nM and 10 nM peptide were measured with and without the presence of 50% TFE, to determine which peptide concentration would give the best signal-to-background ratio.

of the 4E-BP1 helix using nanomolar peptide concentrations.

2.2 Thiourea from FITC conjugation can meditate PET fluorescence quenching

We initially synthesized a 15-amino acid peptide containing residues Thr50–Asn64 of the 4E-BP1 isoform for development of a fluorescence polarization assay. This hotspot peptide contained the eIF4E-binding motif conjugated to fluorescein isothiocyanate (FITC) at the N-terminus via a two β-alanine linker. Interestingly, rather than reporting polarization upon binding to eIF4E, the peptide demonstrated increased fluorescence (data not shown). Because the thiourea motif formed upon FITC coupling (Figure 2.2A)

has been shown to be quenching similar to thioamides, our hypothesis was that in a dynamic solution state, this moiety may be partially quenching the disordered 4E-BP1 peptide's fluorescence via PET. Any increase in peptide helicity (i.e. upon eIF4E binding) would subsequently reposition the thiourea out of the PET distance, thereby decreasing the effective concentration of quenched peptide and resulting in the observed increase in fluorescence signal (Figure 2.2B). Conversely, a decrease in fluorescence signal would be expected when the helix is destabilized due to an increase in the effective concentration of the quenched peptide.

To explore this hypothesis, fluorescence measurements of the FITC-4E-BP1 peptide and a FAM conjugated peptide were recorded in the presence and absence of 50% 2,2,2-trifluoroethanol (TFE), a solvent known to induce helicity in 4E-BP1 and other

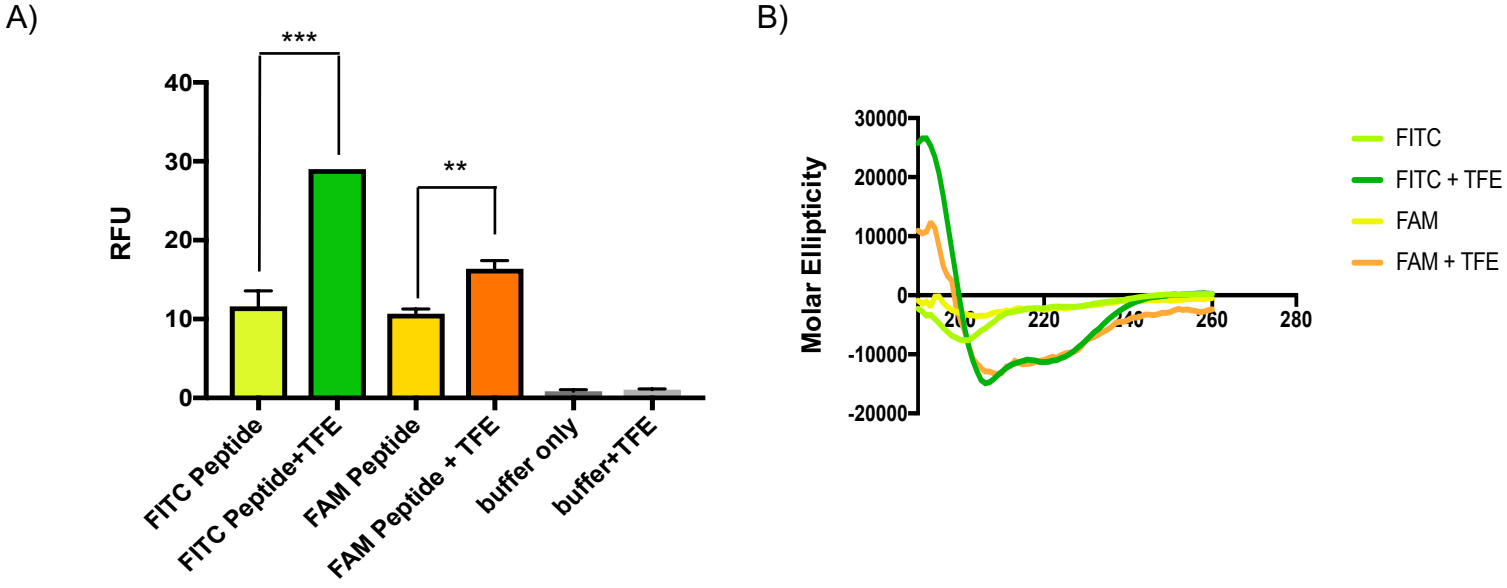

Figure 2.4 "Determination of Thiourea-Specific Fluorescence Quenching" A) RFU (ex/em: 494/520 nm) of 10 μL of 10 nM FITC- or FAM-conjugated 4E-BP1 peptides in Assay Buffer (50 mM sodium phosphate pH 7.4, 200 mM NaCl, 1 mM DTT, and 1 mM EDTA) in the absence or presence of 50% TFE. FAM-conjugated peptide fluorescence does not increase in TFE to the degree of the FITC-conjugated peptide.

peptides.[21] First, 10 μL solutions of peptide were prepared in assay buffer pH 7.4 at

concentrations from 1—10 nM and the signal, in relative fluorescence units (RFU) (ex/em: 494/520 nm) was read to determine the minimum concentration required to give significant fluorescence signal over assay buffer alone (Figure 2.3A). Accordingly, solutions of 5 nM and 10 nM peptide were prepared with and without the presence of 50% TFE to determine which peptide concentration would give the best signal-to-background ratio, treating solution containing peptide and buffer with 50% TFE as signal and peptide in buffer alone as background (Figure 2.3B). Based on this data, 10 nM peptide was used for all future fluorescence measurements.

As shown in Figure 2.4A, a 2.5-fold increase in fluorescence was observed upon the addition of TFE to a 10 nM solution of the FITC-4E-BP1 peptide, which was greater

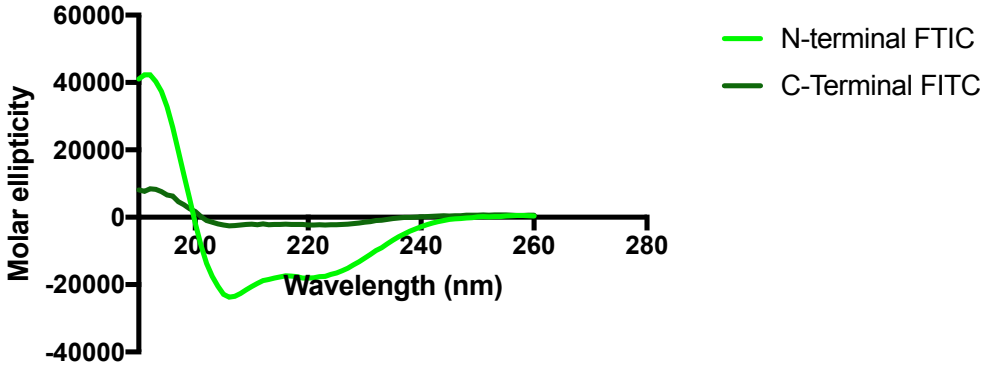

Figure 2.5 "C-terminal FITC conjugation diminishes peptide helical propensity"

than that observed for the FAM peptide. Importantly, using circular dichroism (CD) spectroscopy, we confirmed that TFE enhanced the FITC peptide's helical propensity from 7% to 33% in the absence and presence of TFE, respectively (Figure 2.4B), with a similar increase for the FAM peptide. Notably, a C-terminal FITC-4E-BP1 peptide was also prepared; however, it exhibited little helical propensity even in 50% TFE (Figure 2.5). This finding was unsurprising, as the available structural characterizations indicated that C-terminal modification of the 4E-BP1 helix likely disrupts the formation or stability of the

peptide helix by destabilization of the helix dipole. Together, these results offered preliminary substantiation for our hypothesis that the observed increase in fluorescence signal was linked to helix induction.

2.3 A Thiol-Aromatic Interaction Stabilizes the 4E-BP1 α-helix

As further proof for the mechanism of fluorescence enhancement, we probed a cysteine-aromatic interaction in the 4E-BP1 peptide (Cys62–Phe58; Figure 4A), which we hypothesized would stabilize helical conformation.[22] Consistent with our hypothesis, alkylation of the cysteine residue using iodoacetamide caused a 4.8-fold decrease in peptide fluorescence, which was not altered with 50% TFE (Figure 2.6B). Importantly, these results were corroborated by CD spectroscopy (Figure 2.6C). These data not only show the ability of our peptide reporter to detect helix disruption, but also serve as confirmation that the TFE-induced increase in fluorescence of the unmodified peptide is not due to non-specific solvent effects on fluorescein itself.

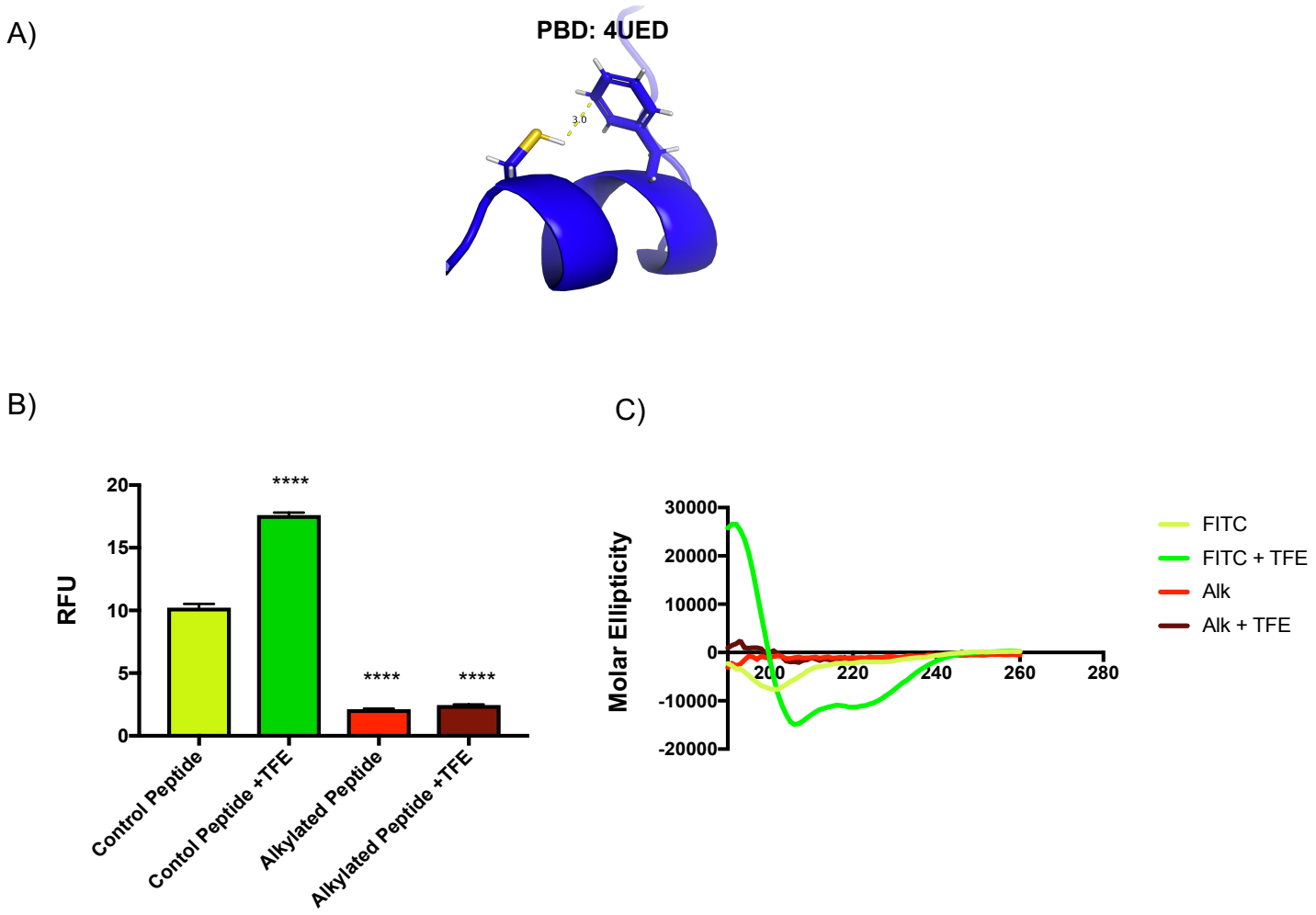

Figure 2.6 "A Thiol-Aromatic Interaction is Required for 4E-BP1 helix stabilization" A) Phe58 and Cys62 form a H-bond-like interaction in the 4E-BP1 helix. B RFU (ex/em: 494/520 nm) of 10 μL of 10 nM FITC-4E-BP1 peptides in Assay Buffer in the absence or presence of 50% TFE. Alkylation of Cys62 by iodoacetamide decreased peptide fluorescence relative to the unmodified FITC-4E-BP1 peptide. This decrease in RFU is unaffected by the presence of 50% TFE. C) Alkylation of Cys62 by iodoacetamide decreased peptide helicity relative to the unmodified FITC-4E-BP1 peptide. This decrease in helicity was unaffected by the presence TFE.

A)

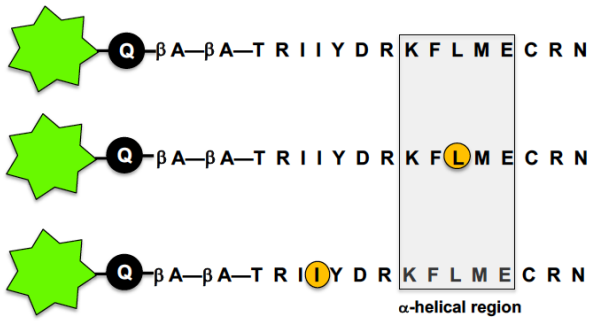

B)

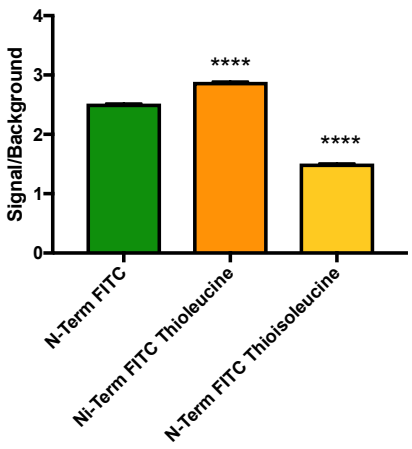

Figure 2.7 "Incorporation of Additional Thioamides does not Significantly Improve Signal-to-Background" A) Peptide sequences of thioamide-containing peptides (circled in orange). B) RFU (ex/em: 494/520 nm) of 10 μL of 10 nM FITC-4E-BP1 peptides in Assay Buffer in the absence or presence of 50% TFE. Signal to background ratios were determined by dividing the fluorescence signal of each peptide in 50% TFE by its fluorescence signal in assay buffer alone

2.4 Optimization for HTS format

To further characterize our reporter peptide and potentially improve the signal-to-background (S/B) of our assay, we explored the effect of incorporating additional

thioamides within the peptide sequence.[17,19,23] We chose to incorporate thioleucine in place of Leu59, which is contained within the helix, and thioisoleucine in place of Ile53, which is N-terminal to the helix (Figure 2.7A). Fmoc-protected thioamide amino acid precursors were synthesized as described[17,24] and used in solid-phase peptide synthesis. While additional thioamides did decrease the overall fluorescence of the peptides, the S/B was not significantly improved (Figure 2.7B). Thus, the native FITC-4E-BP1 peptide reporter was determined to be optimal as it does not require the synthesis of thioamide-containing amino acid precursors.

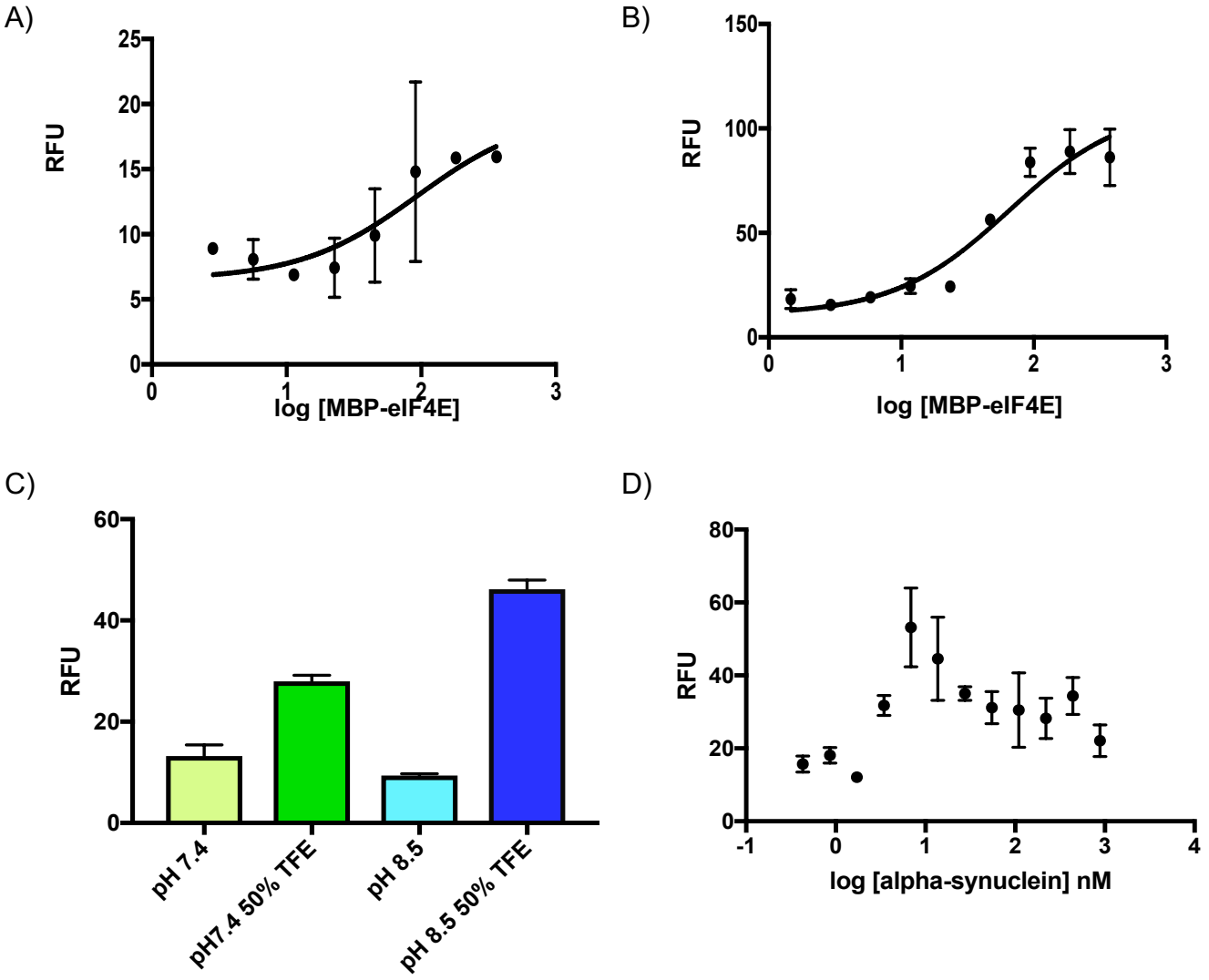

Figure 2.8 "Elevated pH Improves Signal-to-Background and Dose-Dependent Signal Response" RFU (ex/em: 494/520 nm) of peptide in assay buffer with TFE or protein titrations Final well volumes for fluorescence readings were 10 μL with a final peptide concentration of 10 nM.. All experiments were performed in triplicate. A) MBP-eIF4E (0–500 nM) titration at pH 7.4 exhibits low RFU signal and poor signal-to-background (1.9); B) MBP-eIF4E (0–500 nM) titration at pH 8.5 exhibits improvements in both RFU signal and signal-to-background; (4.8) C) S/B at pH 7.4 = 1.5; S/B at pH 8.5 = 4.5 in Assay Buffer with or without TFE; D) Addition of α-synuclein (0-900 nM) to the peptide in Assay Buffer at pH 8.5 does not give the dose-dependent response expected for a specific binding interaction, indicating that observed response for MBP-eIF4E titrations is likely due to specific binding, as opposed to a non-specific and/or aggregation induced phenomena.

To recapitulate our original observation, the FITC-labelled 4E-BP1 peptide was titrated with varying concentrations of MBP-eIF4E. As shown in Figure 2.8A, a dose-dependent increase in peptide fluorescence was observed. The calculated EC_{50} from this titration experiment was 93.5 ± 3.0 nM; however, the S/B from this experiment was low. We predicted that since fluorescein fluorescence is pH-dependent between pH 6.8–9.0,[25] raising the pH to 8.5 would improve S/B by increasing the maximum observable signal. Indeed, when the titration experiment was repeated at pH 8.5, a significant increase in S/B was observed (Figure 2.8B). Similar results were also found with TFE (Figure 2.8C). Moreover, no significant change in helicity trends was noted at elevated pH by CD spectroscopy outside of a small decrease in maximum TFE helicity, which can be attributed to the increase in intermolecular disulfide formation that is favored at above pH 8.1 (Table 2.1).

The measured EC_{50} value was 65.5 ± 1.4 nM, which is comparable to the reported K_d of 4E-BP1 peptide binding to eIF4E (50 nM by isothermal calorimetry).[7] We also

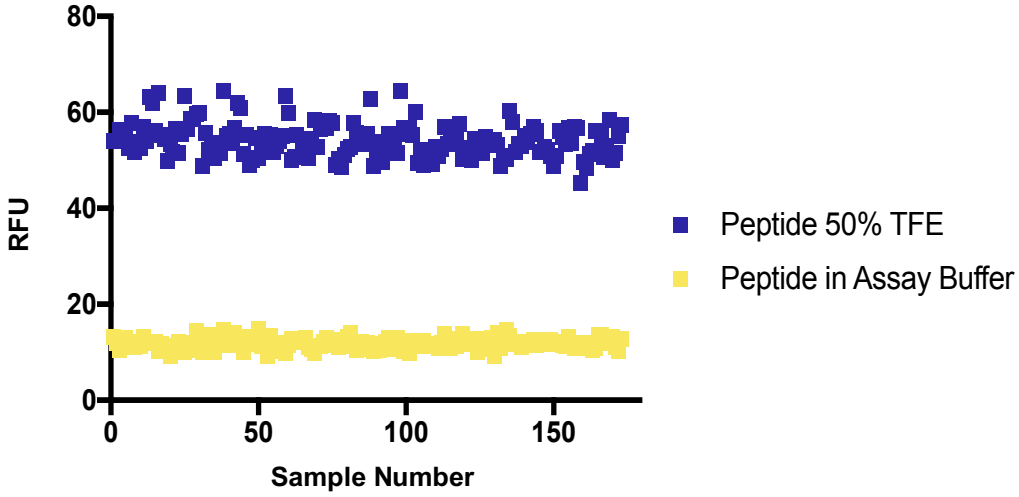

Figure 2.9 "Assay Z-Prime in 384-well Format" RFU (ex/em: 494/520 nm) of 10 μL of 10 nM FITC--E-BP1 peptide in Assay Buffer at pH 8.5 in the absence (negative controls) or presence (positive controls) of 50% TFE.

confirmed the specificity of the signal generation, and no fluorescence enhancement was observed when the peptide was titrated with α-synuclein, which is not known to bind to 4E-BP1 (Figure 2.8D). Intriguingly, the maximum fluorescence response for eIF4E titration was found to be much larger than the response with 50% TFE. This is likely due to additional hydrophobic contacts between the amino acid side-chains of eIF4E and the 4E-BP1 peptide N-terminus. While these interactions provide additional stabilization of the N-terminus, resulting in lower probability of fluorescence quenching, they are not directly involved in the 4E-BP1 helix.

Finally, we tested the robustness of the FITC-4E-BP1 reporter peptide for high-throughput screening (HTS) to discover novel inducers of the 4E-BP1 α-helix. To do so, we calculated Z-prime value, which statistically evaluates the dynamic range and standard deviation for high-throughput screening.[26] This yielded a Z-prime value of 0.7 in a 384-well plate experiment using automated liquid handling. Importantly, assays with Z-prime values of >0.5 are classified as excellent for HTS efforts. This shows the utility of such a probe for the discovery of secondary structure modulators.

2.5 Discussion

In conclusion, we have developed a fluorescent 4E-BP1 peptide that can report both induction and stabilization of its α-helix. Additionally, we have used our 4E-BP1 peptide to probe the thiol-aromatic interaction between Phe58 and Cys62 and its impact on 4E-BP1 helix stability. The prevalence of similar binding-induced folding transitions in biological signaling pathways indicates potential utility of a conditionally fluorescent peptide in systems including p27 linker ordering upon binding CDK4, p53 folding upon

MDM2 binding, and structuring of pKID coupled to binding of KIX.[1] Such peptides could be used for the discovery of novel modulators of structure and function.

Notably, not all IDPs form static secondary structures. Such "fuzzy complexes" retain varying levels of conformational restriction at the bound IDP's interaction site.[1, 27-28] It is likely that a reporter, such as the one we have described, would only be useful in a subset of these systems, dependent upon the relative conformational restriction occurring in the bound state of a given IDP, as well as optimization of thioamide placement. We look forward to application of our rationale in such systems to determine its applicability to studying a more diverse range of IDP PPIs. There is also the possibility to utilize such an approach for more complex systems. For example, native chemical ligation can be used for the incorporation of a fluorophore and quenching thioamide via protein semi-synthesis.[29-31]

Finally, what we describe is an equilibrium assay for a PPI in the nanomolar range; however, many IDPs interact with their ligands through multiple low affinity sites.[1-2] In application of our approach to such interactions, for example, those in the millimolar range, there will be two time-dependent processes affecting the equilibrium: the binding kinetics of the PPI and the timescale of PET quenching. PET quenching occurs on a nanosecond timescale, which presumably favors PPIs with a slower dissociation rate. Further exploration of PPI kinetics and the correlation to PET quenching studies are needed to determine the range in affinity interactions that can be reliably observed in our platform. With these considerations in mind, our described approach demonstrates great promise as a chemical biology tool for observation of protein structure perturbation in a high-throughput format.

2.6 Materials and Methods

General chemistry methods.

NMR spectra (^{1}H and ^{13}C) were recorded on a Bruker BioSpin GmbH NMR. Chemical shifts are reported in parts per million and referenced to TMS. Spectra were processed using MestReNova software. Mass spectrometry (HRMS) was performed using an Agilent 6520, Accurate-Mass QTOF LC/MS spectrometer using ESI ionization, with less than 5 ppm error for all HRMS analyses. RP-HPLC was performed using binary gradients of solvents A and B, where A is 0.1% HCO_2H in water and B is 0.1% HCO_2H in acetonitrile or 0.1% HCO_2H in methanol. Analytical RP-HPLC was performed using an Agilent 1260 Infinity HPLC equipped with a ZORBAX Eclipse SB-C18 column (4.6 × 150 mm; 5 μm) at a flow rate of 1 mL/min, with detection at 214 and 254 nm. Preparative RP-HPLC was performed using an Agilent 1260 Infinity HPLC equipped with a PrepHT SB-C18 column (21.2 × 150 mm; 5 μm) at a flow rate of 18.6 mL/min, with detection at 214 and 254 nm. In all cases, fractions were analyzed off-line using an Agilent Q-TOF HPLC-MS. Pure fractions were then pooled and lyophilized.

General assay methods. Peptide fluorescence measurements were carried out on a SpectraMax M Series Multimode Plate Reader using excitation/emission wavelengths of 490/520 nm with a 515 nm cutoff and 3 scans/well unless otherwise indicated. Fluorescence was read in Corning 3677 black round-bottom 384-well plates.

Data analysis.

All data was analyzed using GraphPad Prism version 7.0 for Mac OS X (GraphPad Software, www.graphpad.com). P-values for fluorescence data were determined using 2-way ANOVA and a 99% confidence interval. EC_{50} values for protein titrations of peptide were calculated using the "Sigmoidal Dose-Response" equation for data fitting. **** p-value < 0.0001; *** p-value = 0.001; **p-value = 0.02 ; *p-value = not statistically significant.

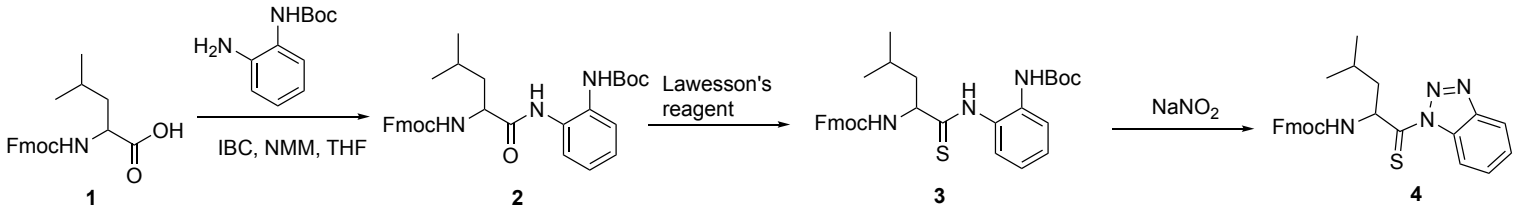

1 2 3 4

Scheme 2.1 "α-N-Fmoc-L-thioleucine-benzotriazolide synthesis"

Materials.

Fmoc-protected amino acids and Rink amide MBHA resin were purchased from P3 Biosystems and used as received. pHA-eIF4E (Plasmid #17343) was purchased from Addgene (GenBank ID NM_001968). pMCSG9 vector was provided by the Center for Structural Biology at University of Michigan.

Synthesis. The synthesis of α-*N*-Fmoc-L-thioleucine-benzotriazolide **(4)** was adapted from Shalaby *et al.*:[17,29]

α-*N*-Fmoc-*L*-leucine-(*N*-Boc)-2-aminoanilide (2): To a solution of Fmoc-Leu-OH (1.7675 g, 5 mmol) in dry tetrahydrofuran (50 mL) at -10 °C, was sequentially added *N*-methylmorpholine (NMM, 1.10 mL,10 mmol) and isobutyl chloroformate (0.65 mL, 5 mmol) with stirring. The reaction mixture was stirred for 15 min at this temperature and followed by slow addition of *N*-Boc-1,2-phenylenediamine (1.0483 g, 5 mmol). The

reaction mixture was warmed to 25 °C and stirred overnight. Upon reaction completion by thin layer chromatography, the solvent was evaporated *in vacuo* and extracted 3× with ethyl acetate (~50 mL). The combined organic layers were washed with 30 mL of brine and 20 mL of 5% $NaHCO_3$ and dried over anhydrous sodium sulfate. The mixture was again concentrated *in vacuo* and the crude product was purified via silica gel column chromatography (eluent: 10%-40% EtOAc/petroleum hexanes) to yield a white foam (75%). ^{1}H NMR (300 MHz, Chloroform-*d*) δ 8.66 (s, 1H), 7.76 (d, *J* = 7.4 Hz, 2H), 7.58 (d, *J* = 6.4 Hz, 3H), 7.38 (d, *J* = 6.5 Hz, 3H), 7.28 (s, 1H), 7.18 (t, *J* = 7.6 Hz, 1H), 7.08 (d, *J* = 15.1 Hz, 1H), 7.01 (s, 1H), 5.61 (d, *J* = 7.3 Hz, 1H), 5.30 (s, 1H), 4.40 (s, 3H), 4.18 (dt, *J* = 14.7, 6.7 Hz, 2H), 1.71 (d, *J* = 41.2 Hz, 3H), 1.49 (s, 10H), 1.07 – 0.92 (m, 6H). HRMS (ESI-TOF) *m/z* calculated for $C_{32}H_{37}N_3O_5$: $[M + H]^+$ 544.2811; observed: 544.2801.

α-*N*-Fmoc-*L*-thioleucine-(*N*-Boc)-2-aminoanilide (3): To a solution of **2** (1.86 g, 3.42 mmol) in THF (50 mL), Lawesson's Reagent (1.80 g, 4.45 mmol) was added and refluxed at 70 °C under an argon environment for 6 h. After completion of the reaction (monitored with TLC), the solvent was evaporated *in vacuo*. The crude reaction mixture was purified by silica gel column chromatography (eluent: 10%-40% EtOAc/petroleum hexanes) to

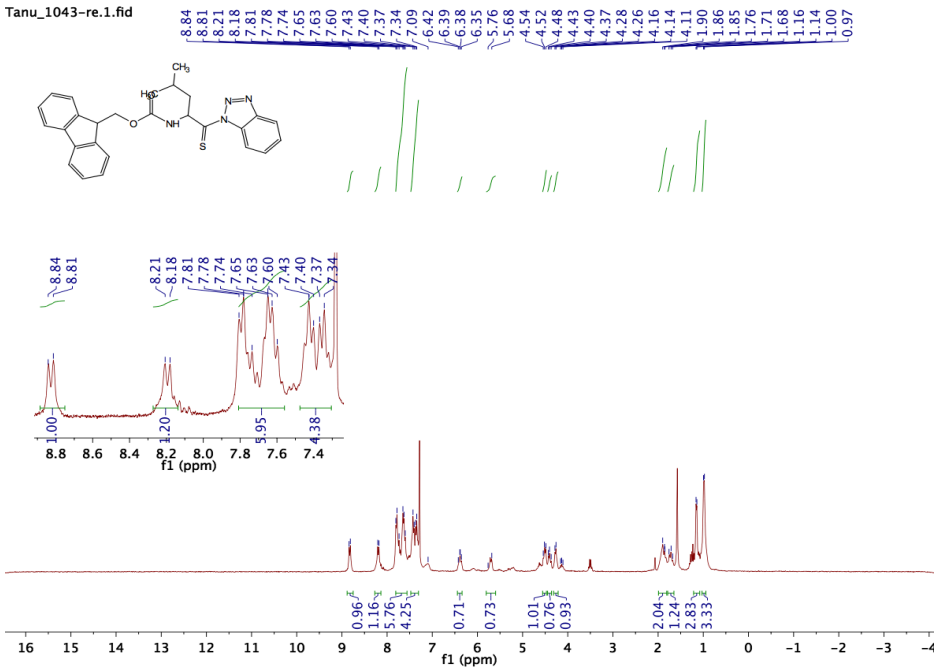

Figure 2.10 "^{1}NMR of α-N-Fmoc-L-thioleucine-benzotriazolide"

yield **3** (1.6 g, 84% yield). ^{1}H NMR (300 MHz, Chloroform-*d*) δ 9.69 (s, 1H), 7.78 (d, *J* = 7.8 Hz, 3H), 7.61 (t, *J* = 6.5 Hz, 3H), 7.40 (dt, *J* = 13.8, 6.7 Hz, 3H), 7.32 (d, *J* = 7.5 Hz, 2H), 7.23 – 7.16 (m, 1H), 5.63 (s, 1H), 4.75 – 4.67 (m, 1H), 4.54 (d, *J* = 7.8 Hz, 1H), 4.46 (d, *J* = 6.9 Hz, 1H), 4.25 (t, *J* = 7.1 Hz, 1H), 1.81 (d, *J* = 21.2 Hz, 4H), 1.48 (s, 10H), 1.03 (s, 5H). HRMS (ESI-TOF) *m/z* calculated for $C_{32}H_{37}N_3O_4S$: $[M + H]^+$ 560.2583; observed: 560.2570.

α-*N*-Fmoc-*L*-thioleucine-benzotriazolide (4): To an ice-cold solution of **3** (1.83 g, 3.27 mmol), 25% TFA in CH_2Cl_2 (40 mL) was added and stirred for 2 h. After completion of the reaction, the solvent was removed *in vacuo* and dried on a high vacuum overnight. The resulting orange solid was treated with 20 mL of 95% glacial acetic acid and cooled to 0 °C. Sodium nitrite (0.3384 g, 4.90 mmol) was added in small portions over 5 min. After 30 min, the reaction was quenched with 75 mL of ice-water. The resulting precipitate was collected, dried and purified via silica gel column chromatography (eluent: 10%-20%

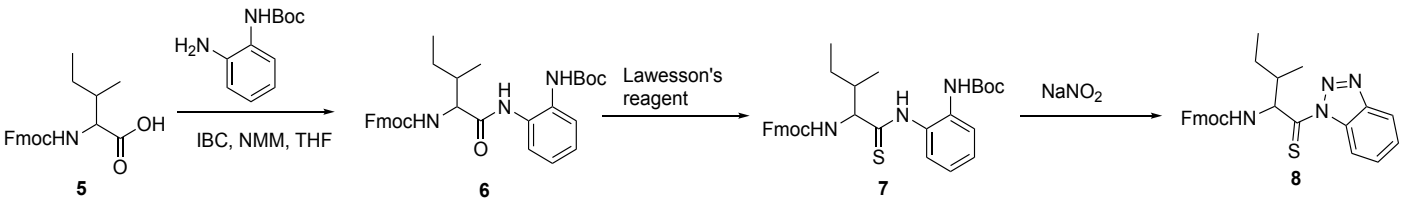

5 6 7 8

Scheme 2.2. "α-N-Fmoc-L-thioisoleucine-benzotriazolide synthesis"

EtOAc/petroleum hexanes) to yield **4** as a yellow solid (0.85 g, 55% yield). ^{1}H NMR (300 MHz, Chloroform-*d*) δ 8.83 (d, *J* = 8.4 Hz, 1H), 8.19 (d, *J* = 8.1 Hz, 1H), 7.81 – 7.56 (m, 6H), 7.38 (dd, *J* = 17.4, 7.5 Hz, 4H), 6.44 – 6.34 (m, 1H), 5.72 (d, *J* = 24.6 Hz, 1H), 4.56 – 4.47 (m, 1H), 4.45 – 4.36 (m, 1H), 4.27 (d, *J* = 7.0 Hz, 1H), 1.99 – 1.81 (m, 2H), 1.79 – 1.65 (m, 1H), 1.15 (d, *J* = 5.5 Hz, 3H), 0.99 (d, *J* = 6.1 Hz, 3H). HRMS (ESI-TOF) *m/z* calculated for $C_{27}H_{27}N_4O_2S$: $[M + H]^+$ 471.1855; observed: 471.1821.

The synthesis of α -*N*-Fmoc-L-thioisoleucine-benzotriazolide[17,29] (**8**) was adapted from Shalaby *et al.*:

α-*N*-Fmoc-*L*-isoleucine-(*N*-Boc)-2-aminoanilide (6): Same as for α-*N*-Fmoc-*L*-leucine-(*N*-Boc)-2-aminoanilide. White foam (85%). ^{1}H NMR (300 MHz, Chloroform-*d*) δ ^{1}H NMR (300 MHz, Chloroform-*d*) δ 8.57 (s, 1H), 7.76 (d, *J* = 7.4 Hz, 2H), 7.57 (d, *J* = 6.2 Hz, 2H), 7.49 (d, *J* = 7.8 Hz, 1H), 7.39 (s, 3H), 7.26 – 7.07 (m, 3H), 7.01 (s, 1H), 5.62 (d, *J* = 8.7 Hz, 1H), 4.54 – 4.35 (m, 2H), 4.23 (d, *J* = 6.2 Hz, 2H), 1.48 (s, 9H), 1.09 – 0.98 (m, 4H), 0.98 – 0.88 (m, 4H). HRMS (ESI-TOF) *m/z* calculated for $C_{32}H_{37}N_3O_5$: $[M + H]^+$ 544.2811; observed: 544.2831.

α-*N*-Fmoc-*L*-thioisoleucine-(*N*-Boc)-2-aminoanilide (7): Same as for α-*N*-Fmoc-*L*-thioleucine-(*N*-Boc)-2-aminoanilide. Yellowish foam (75%). ^{1}H NMR (300 MHz, Chloroform-*d*) δ 7.78 (d, *J* = 7.3 Hz, 3H), 7.59 (d, *J* = 6.3 Hz, 3H), 7.46 – 7.30 (m, 4H),

7.20 (d, *J* = 7.6 Hz, 1H), 4.44 (d, *J* = 3.5 Hz, 2H), 4.26 (d, *J* = 6.6 Hz, 1H), 1.48 (s, 9H), 1.11 – 0.90 (m, 6H). HRMS (ESI-TOF) *m/z* calculated for $C_{32}H_{37}N_3O_4S$: $[M + H]^+$ 560.2583; observed: 560.2575.

α-*N*-Fmoc-*L*-thioisoleucine-benzotriazolide (8). Same as for α-*N*-Fmoc-*L*-thioleucine-benzotriazolide. Yellow solid (50%). ^{1}H NMR (300 MHz, Chloroform-*d*) δ 8.85 (d, *J* = 8.3 Hz, 1H), 8.21 (d, *J* = 7.9 Hz, 1H), 7.88 – 7.54 (m, 7H), 7.47 – 7.30 (m, 4H), 6.32 – 6.18 (m, 1H), 5.81 (d, *J* = 9.9 Hz, 1H), 4.35 (dt, *J* = 55.0, 6.7 Hz, 4H), 2.14 (s, 1H), 1.92 – 1.60 (m, 2H), 1.13 – 0.75 (m, 7H). HRMS (ESI-TOF) *m/z* calculated for $C_{27}H_{26}N_4O_2S$: $[M + Na]^+$ 493.1674; observed: 493.1640.

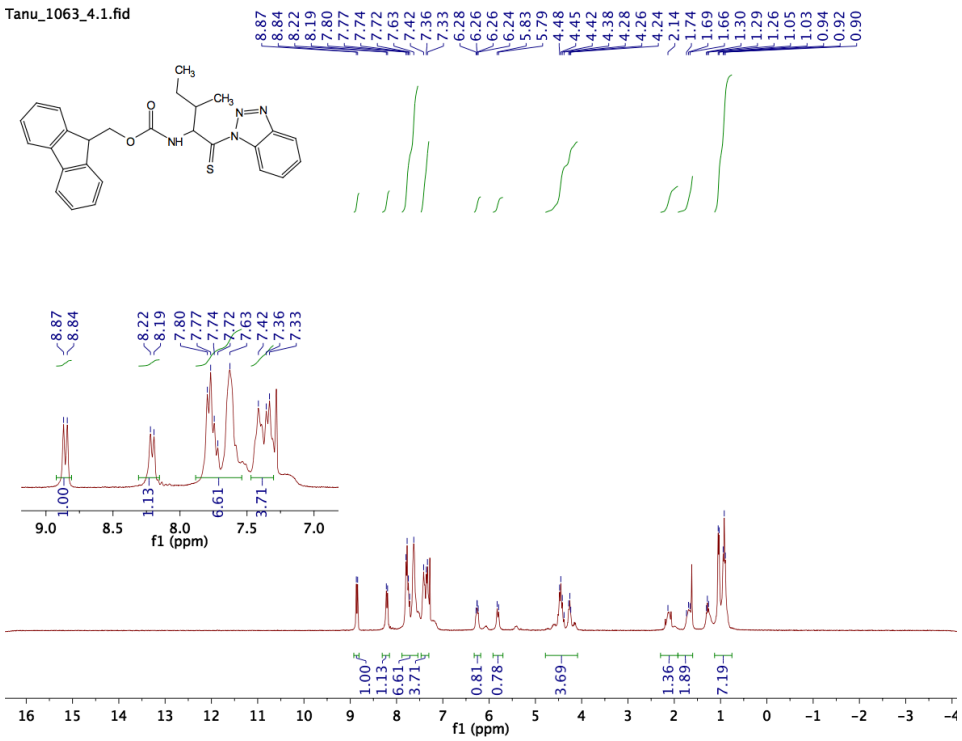

Figure 2.11 "^{1}NMR of α-N-Fmoc-L-thioisoleucine-benzotriazolide"

Peptide Synthesis.

FITC-4E-BP1 peptide sequences without additional thioamides were synthesized on a Liberty Blue peptide synthesizer on 0.1-mmol scale using Rink Amide resin. All amino acid coupling reactions were performed using 5 excess equivalents of Fmoc-AA-OH with 1:1:1 of AA:DIC:Oxyma in DMF for 4 min at 90°C for all amino acids. Fmoc deprotections was performed for 1 min at 90°C in 20% piperidine in DMF. FITC was coupled to the unprotected N-terminus using a previously reported method.[30]

FITC-4E-BP1 peptide sequences containing additional thioamides were synthesized manually in a 20-mL fritted syringe using MBHA Rink resin. After the initial deprotection in 20% piperidine in DMF, the peptide was synthesized using standard SPPS procedures with HBTU/DIPEA activation. For coupling of thioamide-containing amino acid precursors, 3.5 equiv of the amino acid was dissolved in a minimal volume (~2 mL) of dry DCM with 10 equiv of DIPEA[17,24]. Thioamide amino acid couplings were carried out for 2 h and repeated for a total of 3 couplings before checking thioamide addition to the peptide by a TFA test cleavage and mass spectrometry. After confirmation of thioamide incorporation, Fmoc was removed using 2% DBU in DMF to reduce side products[24]. FITC was coupled to the unprotected N-terminus using a previously reported method.[30] All peptides were cleaved from the resin by agitation in a 90:0.4:0.4:0.2 by volume solution of TFA:thioanisole:TIPS:H_2O for 4 h at 25 °C. The cleaved peptide in TFA solution was then precipitated in ice-cold diethyl ether, and the precipitate was centrifuged, dissolved, and purified via RP-HPLC.

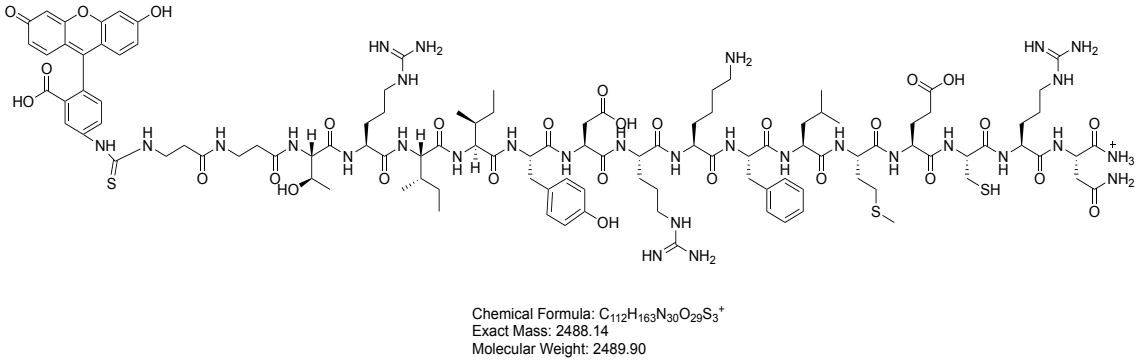

Chemical Formula: $C_{112}H_{163}N_{30}O_{29}S_3^+$
Exact Mass: 2488.14
Molecular Weight: 2489.90

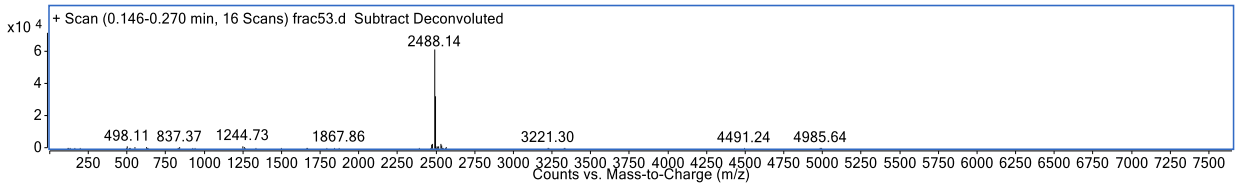

Figure 2.12 "N-terminal FITC conjugated 4E-BP1 peptide Q-TOF-MS"

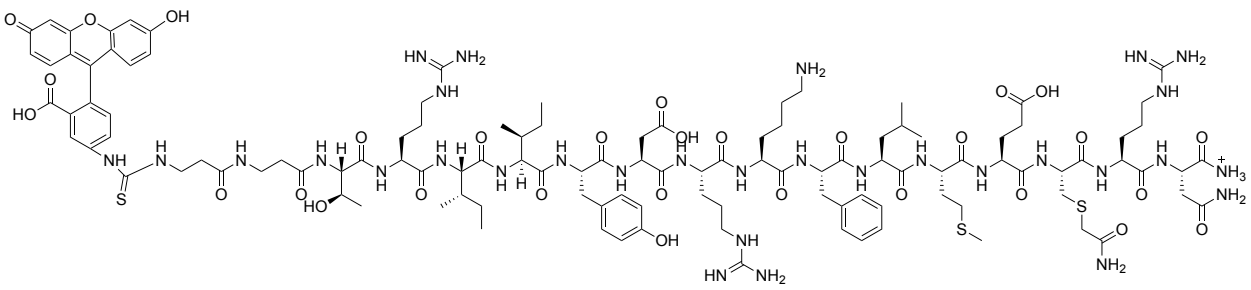

Chemical Formula: $C_{114}H_{166}N_{31}O_{30}S_3^+$
Exact Mass: 2545.16
Molecular Weight: 2546.95

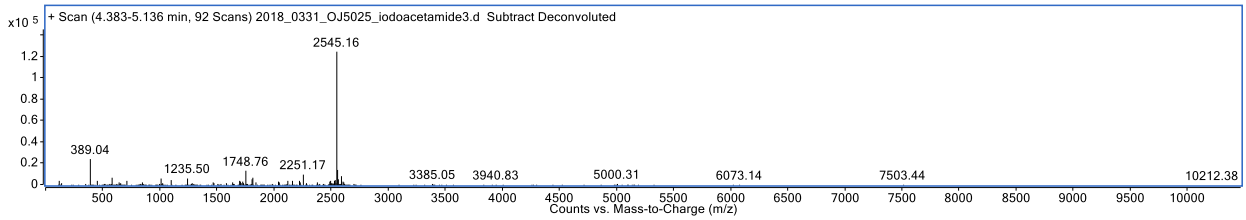

Figure 2.13 “C-terminal FITC conjugated 4E-BP1 peptide Q-TOF-MS”

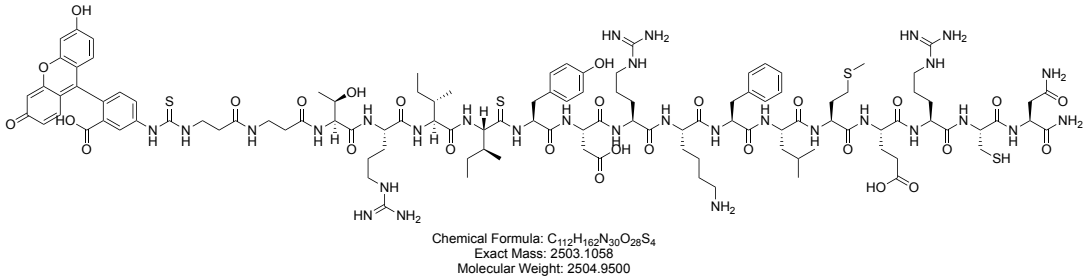

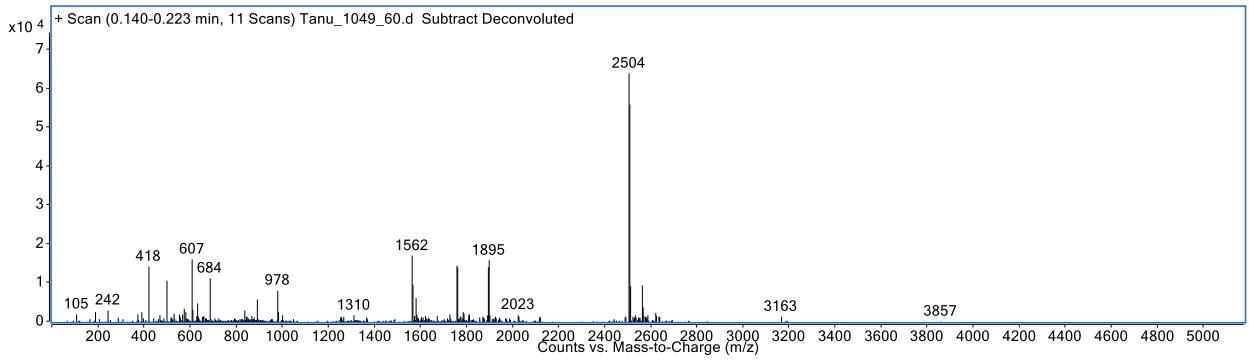

Figure 2.14 "N-terminal thioisoleucine 4E-BP1 peptide Q-TOF-MS"

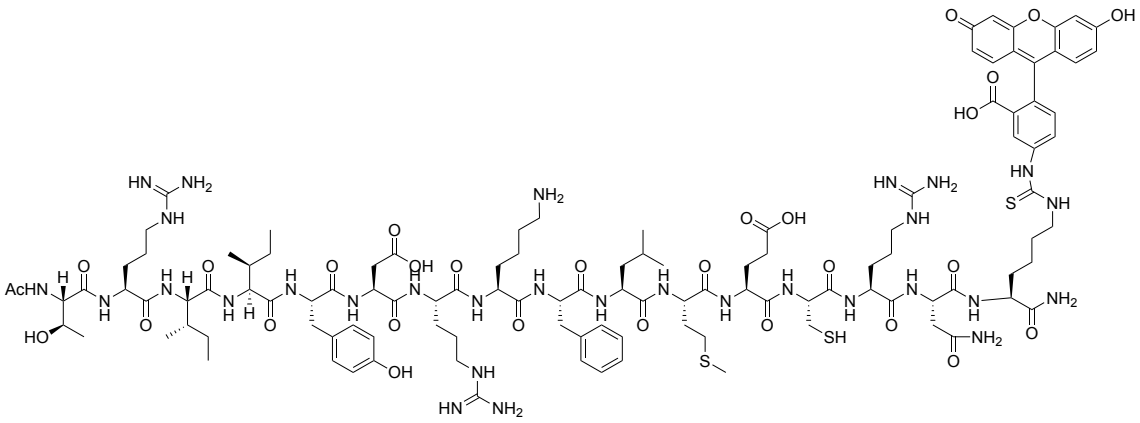

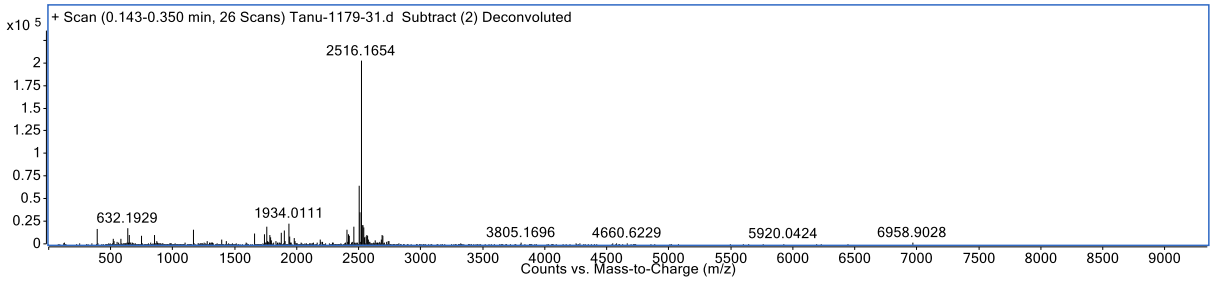

Figure 2.15 "N-terminal FITC conjugated 4E-BP1 peptide alkylated at cysteine Q-TOF-MS"

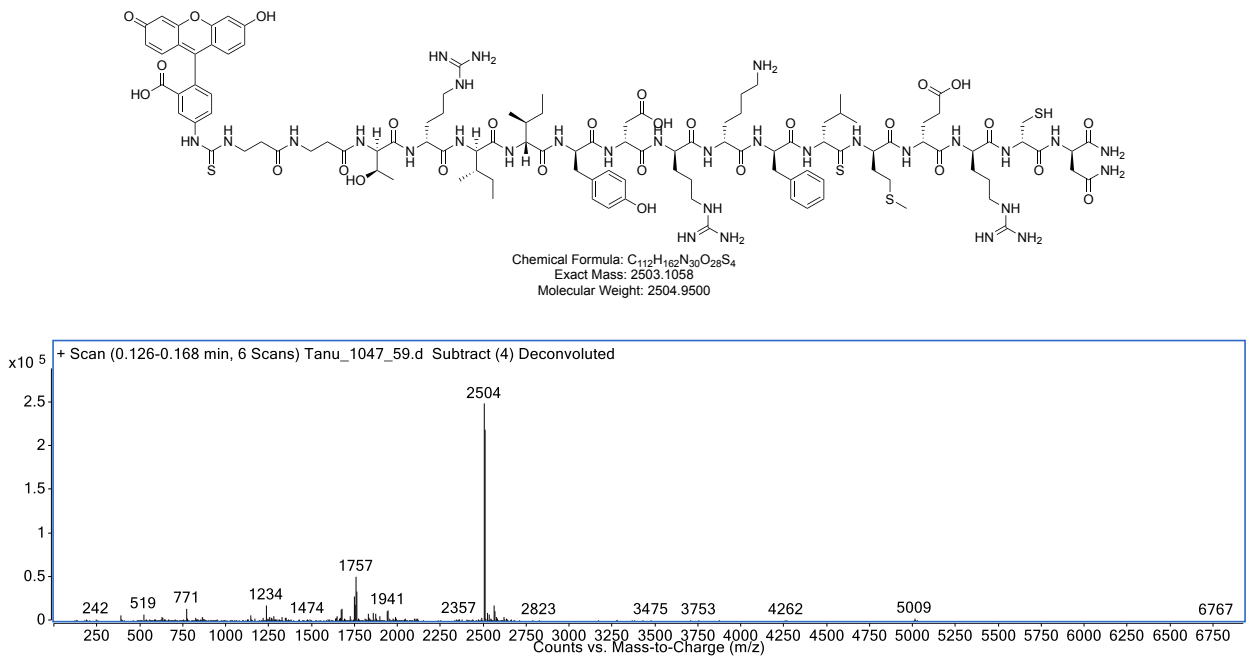

Figure 2.16 “N-terminal thioleucine 4E-BP1 peptide Q-TOF-MS“

Protein Expression and Purification.[14,15]

Human eIF4E cDNA was cloned into a pMCSG9 from pHA-eIF4E via LIC cloning for expression of an MBP-tagged eIF4E protein. MBP-eIF4E plasmid was transformed into Rosetta cells using a standard transformation protocol. Single colonies were picked to inoculate 6 × 6 mL overnight cultures in LB media containing 50 mg/mL ampicillin (amp) that were incubated shaking at 37 °C. Overnight cultures were used to inoculated 1 L of LB media containing 50 mg/mL amp, and that culture was grown to an OD_{600} of 0.6. At this stage, the culture was induced with 1 mM IPTG and incubated shaking at 16 °C for 16 h. Cells were pelleted by centrifugation at 6000× g for 15 min at 25 °C, re-suspended in lysis buffer (50 mM Tris pH 7.5, 500 mM NaCl, 1 mM PMSF, 1 mM EDTA, 2 mM DTT), and lysed by sonication. Lysate was then clarified by centrifugation at 16,000× g for 20 min at 4 °C. Clarified lysate was incubated 15 min on Ni-NTA resin in a Bio-Rad column, then the flow-through was collected. The Ni-NTA resin was washed 3 × with 10 column volumes of wash buffer (50 mM Tris pH 7.5, 200 mM NaCl, 1 mM EDTA, 2 mM DTT), and eluted with the same buffer containing a gradient of 0–500 nM imidazole. The protein was dialyzed 3 × against 2 L of storage buffer (50 mM Sodium Phosphate pH 7.4, 200 mM NaCl, 1 mM EDTA, 2 mM DTT, 15% glycerol), distributed into 15-mL aliquots, and flash frozen until use. Before using protein for experiments, aliquots were thawed on ice, concentrated to 5 mL, purified by size-exclusion chromatography (SEC) to remove aggregates, and concentrated as needed, with concentration monitored by A_{280}. Purified protein was stored at 4 °C for up to 5 days after SEC, after which it was discarded.

Circular Dichroism (CD) Spectroscopy.

Peptides, which were dissolved as 1 mM stocks in 50 mM Sodium Phosphate pH 7.4 or 8.5 and 30% acetonitrile, were diluted to 100–150 μM with additional phosphate buffer or phosphate buffer with TFE for a final TFE concentration of 50%. CD measurements were carried out on a JASCO J-1500 CD spectrophotometer. Baseline measurements were conducted using 50 mM Sodium Phosphate pH 7.4 or 8.5 and 3% acetonitrile. 50% TFE was added to the baseline solution for peptide measurements in TFE. The baseline was automatically subtracted by the Jasco software. CD spectra for the peptides were measured from 190–260 nm over 3 scans. Helicity was determined by molar ellipticity of each peptide at 222 nm using the equations below[31].

Equation 1:

$$\%_H = (([\theta]_{obs222} - [\theta]_C)/([\theta]_{\infty 222} - [\theta]_C)) * 100$$

Equation 2:

$$[\theta]_C = 2220 - 53T$$

Equation 3:

$$[\theta]_{\infty 222} = (-44000 + 250T)(1 - \frac{k}{N_p})$$

Where,

$\%_H$ = percent α-helix content

$[\theta]_{obs222}$= observed molar ellipticity at 222 nm

$[\theta]_C$= Random coil molar ellipticity

$[\theta]_{\infty 222}$= Infinite molar α-helix molar ellipticity

T = temperature in degrees Celsius

k = finite length correction

N_p = Number of peptide units

Peptide	% helicity	TFE	Buffer pH
N-Term FITC	7	-	7.4
N-Term FITC	33	+	7.4
C-Term FITC	-3	-	7.4
C-Term FITC	7	+	7.4
N-Term FITC Cys-alkylated	3	-	7.4
N-Term FITC Cys-alkylated	5	+	7.4
N-Term FITC	6	-	8.5
N-Term FITC	17	+	8.5
N-Term FITC Cys-alkylated	5	-	8.5
N-Term FITC Cys-alkylated	8	+	8.5

Table 2.1 "Peptide Helicity from CD Experiments"

Peptide Fluorescence Measurements.

Peptides, which were dissolved as 1 mM stocks in Assay Buffer (50 mM Sodium Phosphate pH 7.4 or 8.5, 200 mM NaCl, 1mM DTT, 1mM EDTA) and 30% DMF, were diluted to appropriate working concentrations for subsequent experiments. For fluorescence measurements, peptides were diluted to 20 nM working solutions with buffer A. For TFE experiments, the working solutions were further diluted to 10 nM using either buffer A or TFE. To each well, 10 μL of the 10 nM peptide working solution was added, and the fluorescence was read immediately using excitation/emission wavelengths of 490/520 nm with a 515 nm cutoff and 3 scans per well. For MBP-eIF4E and α-synuclein titrations, 10 μL of the working solution was titrated serially with 10 μL of the protein solutions for a final peptide concentration of 10 nM, and final protein concentrations of 0–500 nM and 0–900 nM for MBP-eIF4E and α-synuclein, respectively. All conditions were measured in triplicate.

2.7 References

1 Wright, P. E. & Dyson, H. J. Intrinsically disordered proteins in cellular signalling and regulation. *Nat Rev Mol Cell Biol* **16**, 18-29, doi:10.1038/nrm3920 (2015).

2 Dyson, H. J. & Wright, P. E. Intrinsically unstructured proteins and their functions. *Nat Rev Mol Cell Biol* **6**, 197-208, doi:10.1038/nrm1589 (2005).

3 He, B. *et al.* Predicting intrinsic disorder in proteins: an overview. *Cell Res* **19**, 929-949, doi:10.1038/cr.2009.87 (2009).

4 Martineau, Y., Azar, R., Bousquet, C. & Pyronnet, S. Anti-oncogenic potential of the eIF4E-binding proteins. *Oncogene* **32**, 671-677, doi:10.1038/onc.2012.116 (2013).

5 Averous, J. & Proud, C. G. When translation meets transformation: the mTOR story. *Oncogene* **25**, 6423-6435, doi:10.1038/sj.onc.1209887 (2006).

6 Qin, X., Jiang, B. & Zhang, Y. 4E-BP1, a multifactor regulated multifunctional protein. *Cell Cycle* **15**, 781-786, doi:10.1080/15384101.2016.1151581 (2016).

7 Marcotrigiano, J. G., Anne-Claude; Sonenberg, Nahum; Burley, Stephen K. Cap-Dependent Translation in Eukaryotes Is Regulated by a Molecular Mimic of eIF4G. *Molecular Cell* **3**, 707-716 (1999).

8 Gingras, A. C. *et al.* Hierarchical phosphorylation of the translation inhibitor 4E-BP1. *Genes Dev* **15**, 2852-2864, doi:10.1101/gad.912401 (2001).

9 Tait, S. *et al.* Local control of a disorder-order transition in 4E-BP1 underpins regulation of translation via eIF4E. *Proc Natl Acad Sci U S A* **107**, 17627-17632, doi:10.1073/pnas.1008242107 (2010).

10 Tomoo, K., Abiko, F., Miyagawa, H., Kitamura, K. & Ishida, T. Effect of N-terminal region of eIF4E and Ser65-phosphorylation of 4E-BP1 on interaction between eIF4E and 4E-BP1 fragment peptide. *J Biochem* **140**, 237-246, doi:10.1093/jb/mvj143 (2006).

11 Gallagher, E. E. S., J. M.; Menon, A.; Mishra, L. D.; Chmiel, A. F.; Garner, A. L. Probing the Importance of Folding Dynamics in the Design of Stapled Peptide Mimics of the Disordered Proteins 4E-BP1 and eIF4G. *in revision* (2018).

12 Lama, D. *et al.* Rational optimization of conformational effects induced by hydrocarbon staples in peptides and their binding interfaces. *Sci Rep* **3**, 3451, doi:10.1038/srep03451 (2013).

13 Peter, D. *et al.* Molecular architecture of 4E-BP translational inhibitors bound to eIF4E. *Mol Cell* **57**, 1074-1087, doi:10.1016/j.molcel.2015.01.017 (2015).

14 Lukhele, S., Bah, A., Lin, H., Sonenberg, N. & Forman-Kay, J. D. Interaction of the eukaryotic initiation factor 4E with 4E-BP2 at a dynamic bipartite interface. *Structure* **21**, 2186-2196, doi:10.1016/j.str.2013.08.030 (2013).

15 Bah, A. *et al.* Folding of an intrinsically disordered protein by phosphorylation as a regulatory switch. *Nature* **519**, 106-109, doi:10.1038/nature13999 (2015).

16 Goldberg, J. M., Wissner, R. F., Klein, A. M. & Petersson, E. J. Thioamide quenching of intrinsic protein fluorescence. *Chem Commun (Camb)* **48**, 1550-1552, doi:10.1039/c1cc14708k (2012).

17 Goldberg, J. M., Batjargal, S., Chen, B. S. & Petersson, E. J. Thioamide quenching of fluorescent probes through photoinduced electron transfer: mechanistic studies and applications. *J Am Chem Soc* **135**, 18651-18658, doi:10.1021/ja409709x (2013).

18 Chen, Y., Tsao, K. & Keillor, J. W. Fluorogenic protein labelling: a review of photophysical quench mechanisms and principles of fluorogen design. *Canadian Journal of Chemistry* **93**, 389-398, doi:10.1139/cjc-2014-0405 (2015).

19 Petersson, E. J., Goldberg, J. M. & Wissner, R. F. On the use of thioamides as fluorescence quenching probes for tracking protein folding and stability. *Phys Chem Chem Phys* **16**, 6827-6837, doi:10.1039/c3cp55525a (2014).

20 Doose, S., Neuweiler, H. & Sauer, M. Fluorescence quenching by photoinduced electron transfer: a reporter for conformational dynamics of macromolecules. *Chemphyschem* **10**, 1389-1398, doi:10.1002/cphc.200900238 (2009).

21 Hackl, E. V. Limited proteolysis of natively unfolded protein 4E-BP1 in the presence of trifluoroethanol. *Biopolymers* **101**, 591-602, doi:10.1002/bip.22422 (2014).

22 Forbes, C. R. *et al.* Insights into Thiol-Aromatic Interactions: A Stereoelectronic Basis for S-H/pi Interactions. *J Am Chem Soc* **139**, 1842-1855, doi:10.1021/jacs.6b08415 (2017).

23 Walters, C. R. *et al.* The effects of thioamide backbone substitution on protein stability: a study in alpha-helical, beta-sheet, and polyproline II helical contexts. *Chem Sci* **8**, 2868-2877, doi:10.1039/c6sc05580j (2017).

24 Petersson, E., Szantai-Kis, D., Walters, C., Barrett, T. & Hoang, E. Thieme Chemistry Journals Awardees – Where Are They Now? Improved Fmoc Deprotection Methods for the Synthesis of

Thioamide-Containing Peptides and Proteins. *Synlett* **28**, 1789-1794, doi:10.1055/s-0036-1589027 (2017).

25 Martin, M. M. L., Lars. The pH Dependence of Fluorescein Fluorescence. *Journal of Luminescence* **10**, 381-390 (1975).

26 Zhang, J. H., Chung, T. D. & Oldenburg, K. R. A Simple Statistical Parameter for Use in Evaluation and Validation of High Throughput Screening Assays. *J Biomol Screen* **4**, 67-73, doi:10.1177/108705719900400206 (1999).

27 Mollica, L. *et al.* Binding Mechanisms of Intrinsically Disordered Proteins: Theory, Simulation, and Experiment. *Front Mol Biosci* **3**, 52, doi:10.3389/fmolb.2016.00052 (2016).

28 Borgia, A. *et al.* Extreme disorder in an ultrahigh-affinity protein complex. *Nature* **555**, 61-66, doi:10.1038/nature25762 (2018).

29 Batjargal, S., Huang, Y., Wang, Y. J. & Petersson, E. J. Synthesis of thioester peptides for the incorporation of thioamides into proteins by native chemical ligation. *J Pept Sci* **20**, 87-91, doi:10.1002/psc.2589 (2014).

30 Wang, Y. J., Szantai-Kis, D. M. & Petersson, E. J. Semi-synthesis of thioamide containing proteins. *Org Biomol Chem* **13**, 5074-5081, doi:10.1039/c5ob00224a (2015).

31 Shalaby, M. A., Grote, C. W. & Rapoport, H. Thiopeptide Synthesis. α-Amino Thionoacid Derivatives of Nitrobenzotriazole as Thioacylating Agents. *The Journal of Organic Chemistry* **61**, 9045-9048, doi:10.1021/jo961245q (1996).

32 Kim, Y. W., Grossmann, T. N. & Verdine, G. L. Synthesis of all-hydrocarbon stapled alpha-helical peptides by ring-closing olefin metathesis. *Nat Protoc* **6**, 761-771, doi:10.1038/nprot.2011.324

33 Shepherd, N. E. H., H.N; Abbenante, G.; Fairlie, D.P. Single Turn Peptide Alpha Helices with Exceptional Stability in Water. *J Am Chem Soc* **127**, 2974-2983 (2005).

Chapter 3 – Biophysical Evaluation of Chemically Generated pCys as a Phosphomimetic for Studying Phosphorylation-Dependent Protein Conformational Dynamics

**Note: The work in this chapter was carried out as part of a collaboration with Asst. Prof. Alaji Bah and Prof. Julie Forman-Kay at University of Toronto and the Toronto Hospital for Sick Children. Protein NMR Experiments were carried out by A. Bah. All other work described was carried out by the author (O.T. Johnson).*

3.1 Introduction

Intrinsically disordered proteins (IDPs) and intrinsically disordered regions (IDRs) are protein components of the cellular machinery that are highly dynamic in conformation and play an integral role in many biological events. They often serve as signaling hubs in protein-interaction networks and modulate processes including the cell cycle, transcription, and translation.[1,2] Consequently, IDPs/IDRs are critical to understanding human pathology, as they are often dysregulated in cancer, metabolic, and neurological diseases.[2] IDRs and IDPs are often regulated at a post-translational level.[1,2] Post-translational modifications (PTMs), namely phosphorylation at serine (Ser) and threonine (Thr) residues, can modulate IDP function in a manner that is additive, combinatorial, or a sequential,[2] yielding intricate networks of post-expression protein regulation. Studying these phosphorylation events, both in isolation and combination, can yield a great deal of insight into IDPs and their role in disease; however, this can be a challenging undertaking.

In vitro phosphorylation of IDPs by kinases has provided information on both hierarchal and additive phosphorylation events where the appropriate kinase is known. In contrast, when there is ambiguity in the identity of the biologically relevant kinase, or the goal is to understand the individual function or contribution of a single phosphoevent to a larger, hierarchal context, *in vitro* kinase phosphorylation methods can become complicated and labor intensive. This issue has prompted the exploration and development of phosphomimetics. While site-directed mutagenesis to introduce aspartate (Asp) and glutamate (Glu) as mimics of serine and threonine phosphorylation, respectively, has been successful in many systems, the differences in charge, pKa, and geometry of these amino acids limit their suitability in many protein systems. Thus, developing tools to effectively and selectively study PTMs is of particular importance to studies aimed at elucidating IDP and IDR function and regulation.

For decades, chemists have undertaken the challenge of developing chemical tools to answer biological questions via site-specific expansion of amino acid side-chain diversity. Chemical techniques, including unnatural amino acid incorporation via amber codon suppression[3,4] and native chemical ligation (NCL),[5,6] have provided a powerful means of introducing non-canonical amino acids, including PTM mimics;[7-10] however, limited success of phosphomimetic incorporation,[11,12] poor protein yields, and incompatibility of the phosphomimetic with many required subsequent chemistries[13] limit the application of such approaches.

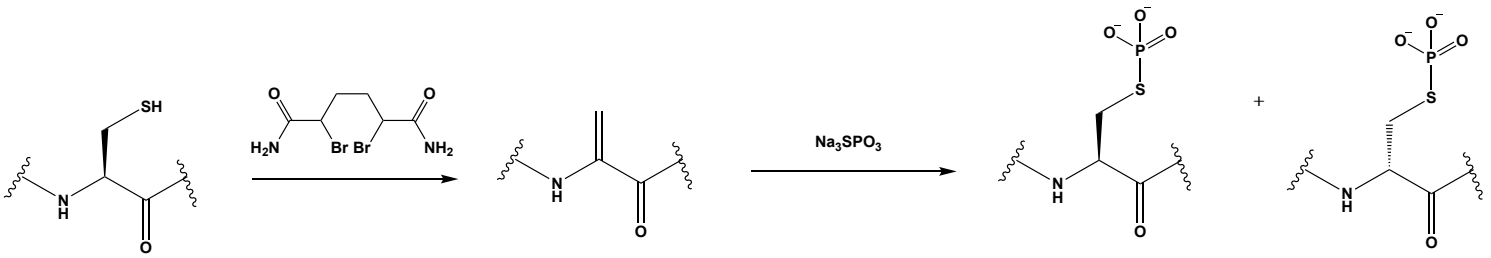

Scheme 3.1 ‘‘Chemical conversion of Cys to pCys using ‘tag-and-modify’ approach”

Chemical mutagenesis methodology that site-specifically targets a canonical amino acid can provide easy access to the post-translational expansion of amino acid side-chain diversity *in vitro*. Recently, the laboratory of Ben Davis has built upon the work of Koshland and others,[14-18] by using cysteine (Cys) residues as substrates for conversion to the reactive Michael-acceptor, dehydroalanine (Dha).[19,20] Cys occurs in low abundance in proteins, and when present, typically participates in disulfide bonds, limiting non-specific reactivity with native Cys residues in a given protein. This work, branded as a “tag-and-modify” approach combines site-directed mutagenesis of the desired pSer or pThr residue to Cys, and a bis-alkylation elimination reaction to obtain Dha (Scheme 3.1).[19,21] After generation of Dha, the protein is treated with sodium thiophosphate to

generate a pCys residue (Scheme 3.1). Thus, we were inspired to adapt this methodology in an attempt to study a multiply phosphorylated IDP.

4E-BPs are a family of three intrinsically disordered translational repressor proteins. Studies of the predominate isoforms, 4E-BP1 and 4E-BP2, have shown that the 4E-BPs act by outcompeting scaffolding protein eIF4G for binding the mRNA cap-binding protein eIF4E, thus sequestering it away from the eIF4F translational initiation complex and inhibiting cap-dependent translation. Control of 4E-BP function is regulated by mTORC1-dependent phosphorylation,[22,23] with the hyperphosphorylated state having a significantly lower eIF4E binding affinity relative to the hypophosphorylated state, causing the 4E-BPs to be out-competed by eIF4G, and cap-dependent translation to be

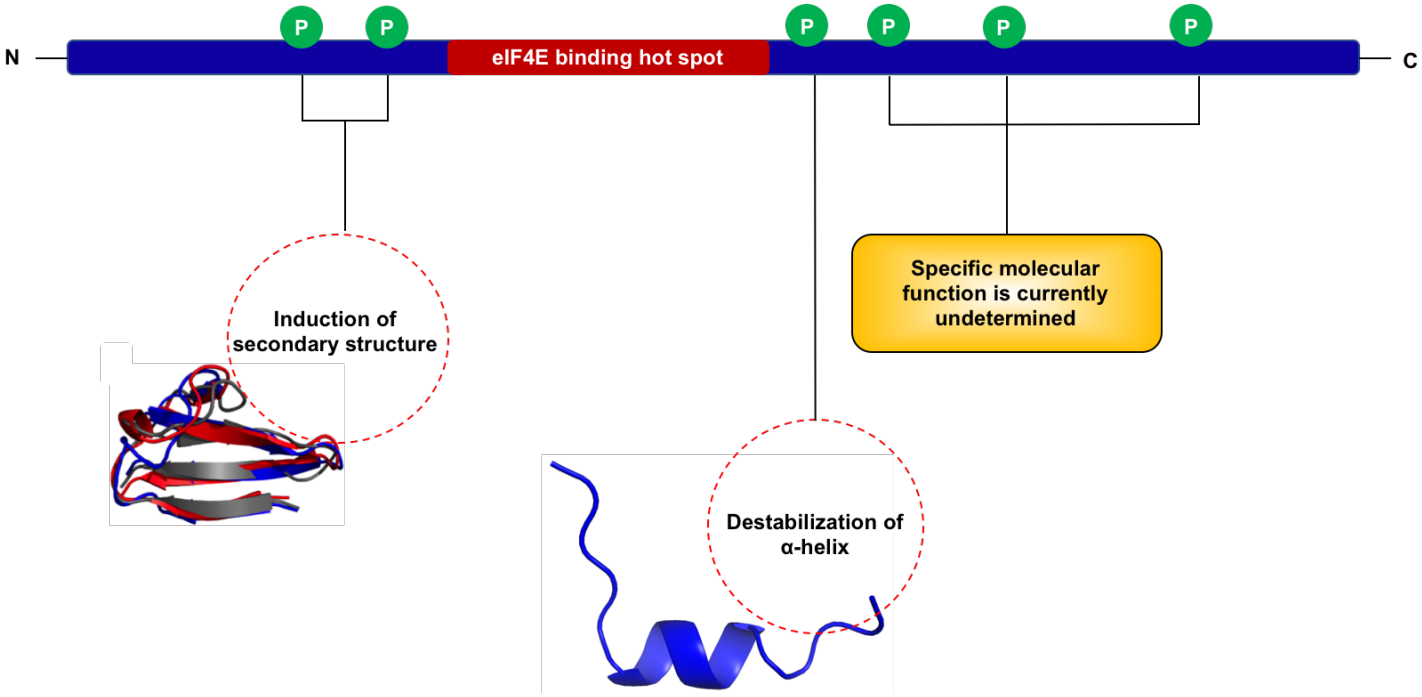

Figure 3.1 "Structural Outcomes of 4E-BP Phosphorylation"

initiated.[24-26] Much of the work regarding 4E-BP phosphorylation has focus on four of the six canonical p4E-BP sites, Thr37, Thr46, Ser65, Thr70. However, there is conflicting

data on the hierarchal phosphorylation of these sites.[27,28] There is also ambiguity on the possible function(s) of the C-terminal phosphosites Ser83 and Ser101.

Work by Bah and colleagues demonstrated that phosphorylation at Thr37 and Thr46 induces formation of two identical β-hairpins that are stabilized by hydrogen bonding interactions between the phosphate moiety and the amide backbone of nearby glycine residues in the 4E-BP2 TPGGT motifs, where these phosphosites are contained.[29] These hairpins order 4E-BP2 residues Thr19-Arg62 into a 4 stranded antiparallel β-sheet, a structure that sequesters the eIF4E binding "hot-spot" region when unbound to eIF4E, thereby reducing its binding affinity. Their findings also provide a structurally informed explanation for the observation that Asp or Glu mutations are ineffective phosphomimetics at these positions in 4E-BPs.[29,30] While the structural consequence of phosphorylation at Thr37 and Thr46 is critical for regulation of 4E-BP function, a subsequent phosphorylation event at Ser65 is what abrogates the PPI.[28,31] In fact this PTM, positioned immediately C-terminal to a short α-helix formed at the eIF4E binding interface, results in destabilization of the α-helix. This occurrence is at least in part driven by electrostatic repulsion.[31] Given the precise and opposing roles of the aforementioned phosphosphorylation events, we felt that 4E-BP1/2 to be an ideal system to test the applicability of pCys as a true phosphomimetic. Thus, in the context of these opposing structural outcomes in a highly dynamic IDP, we have evaluated pCys as a Ser/Thr phosphomimetic, using circular dichroism (CD) spectroscopy and nuclear magnetic resonance (NMR) spectroscopy to assess its structural outcomes.

3.2 The "tag-and-modify" approach is a proximity sensitive method for multiple Dha conversions on 4E-BPs

We expressed a $^{13}C^{15}N$-labelled 4E-BP1 T37C/T46C mutant, with the two Cys in the wildtype sequence were mutated to Ala, in an attempt to recapitulate the entire phosphorylation induced 4E-BP β-fold using pCys. Treatment of the protein with 2,5-dibromohexanediamide (DBHDA) yielded a population of protein that had undergone complete elimination to Dha and a population of protein that was doubly alkylated by the reagent as determined by mass spectrometry (Figures 3.2A and 3.2C). This is likely due to the close proximity of Cys37 and Cys46, as Dha modification of both Cys residues in the wild-type 4E-BP1 sequence was obtained in preliminary experiments (Figure 2B). Efforts to separate the two populations by various chromatographic methods were unsuccessful (data not shown), leading us to focus on an individual pCys37 modification, which was easier to obtain and isolate using chemical mutagenesis (Figure 3.3). While this single phosphorylation site is not able to induce the full 4E-BP β-fold, as singly phosphorylated Thr37 of 4E-BP does induce a single, observable hairpin and partial protein ordering.[29]

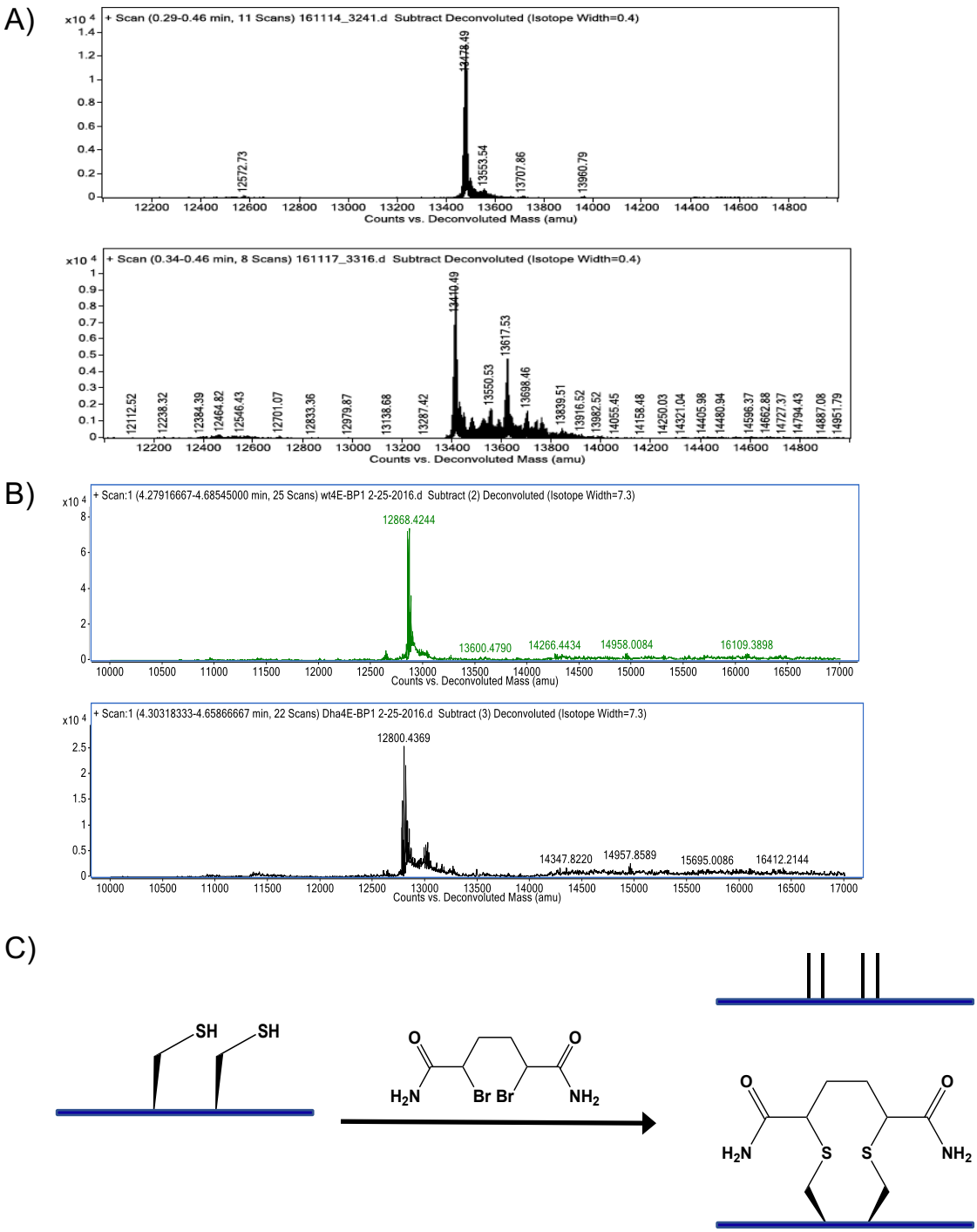

Figure 3.2 "Conversion of Cys to Dha in systems with multiple Cys is proximity dependent" A) $^{15}N^{13}C$-labelled T37C/T46C 4E-BP1 mutant showed about 65% conversion to the desired Dha product upon treatment with 150 eq. DBHDA. The remaining 35% appears to form an dialkylation product where 1 molecule of DBHDA alkylates both cysteines of a single 4E-BP1 molecule, thus forming a covalent linkage between them; B) In wt4E-BP1, two Cys residues (Cys7 and Cys62) in the native sequence are fully converted to Dha, without any apparent dialkylation product

A)

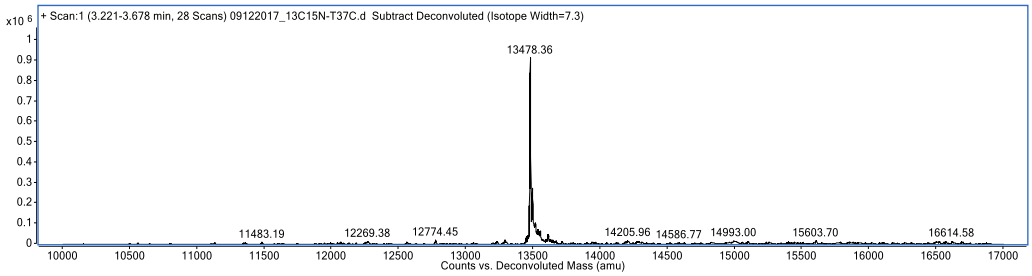

B)

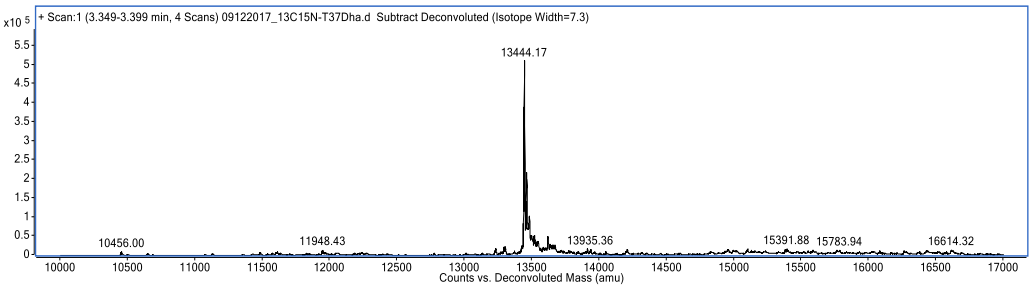

C)

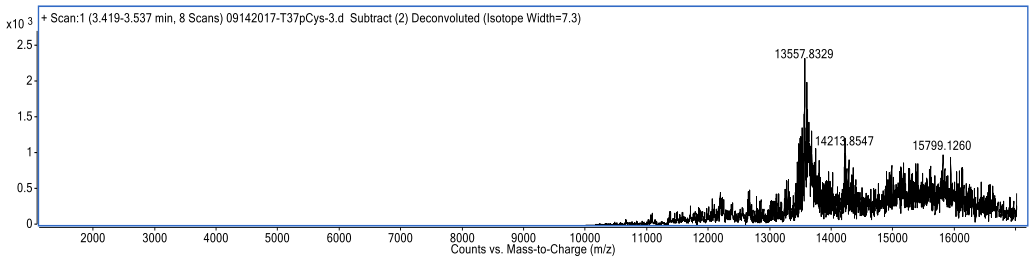

Figure 3.3 "Chemical conversion of the $^{15}N^{13}C$-labelled T37C 4E-BP1 mutant" A) to Dha; B) and subsequently pCys C), as monitored by QTOF mass-spectrometry

3.3 pCys37 is not sufficient for induction of β-hairpin structure in 4E-BPs.

After expression and purification of $^{13}C^{15}N$-labelled 4E-BP1, the pure protein was phosphorylated by the proline-directed kinase MAPK in vitro, and the reaction was monitored by mass spectrometry to ensure phosphorylation of at least the two sites required for hairpin formation, Thr37 and Thr46 (Figure 3.4). The six canonical 4E-BP1 phosphorylation sites and an additional Thr-Pro motif that can be recognized as a substrate by MAPK at the N-terminus of the protein sequence. Most of the protein appears to have been phosphorylated at 5 or 6 sites, indicating phosphorylation at bona fide sites, with a small population having apparent phosphorylation of the N-terminal Thr10, as well as another population of protein that is only phosphorylated at 4 sites. This protein was then purified to remove residual kinase, and used as a mixture of phosphostates. Having access to the p4E-BP2 data from Bah et al. for direct comparison of HSQC spectra,[29] we determined such a mixture was indeed sufficient to see hairpin formation and peak dispersion from protein ordering.

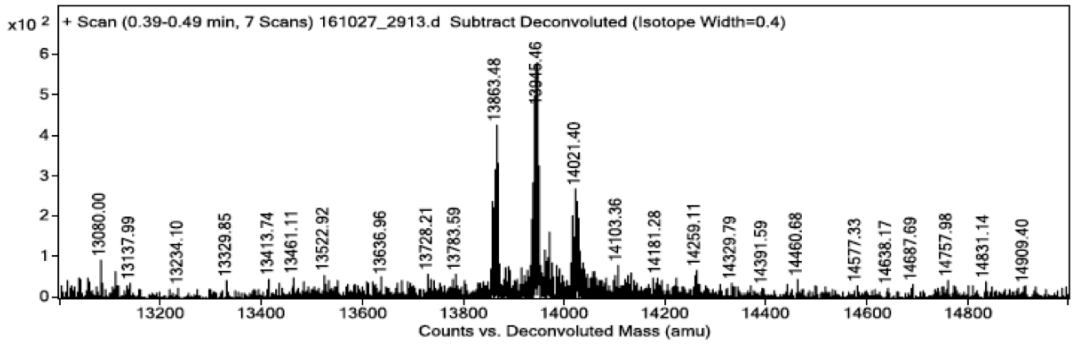

Figure 3.4 "Phosphorylation of 15N13C-labeled 4E-BP1 by the proline-directed kinase MAPK as monitored by QTOF mass spectrometry"

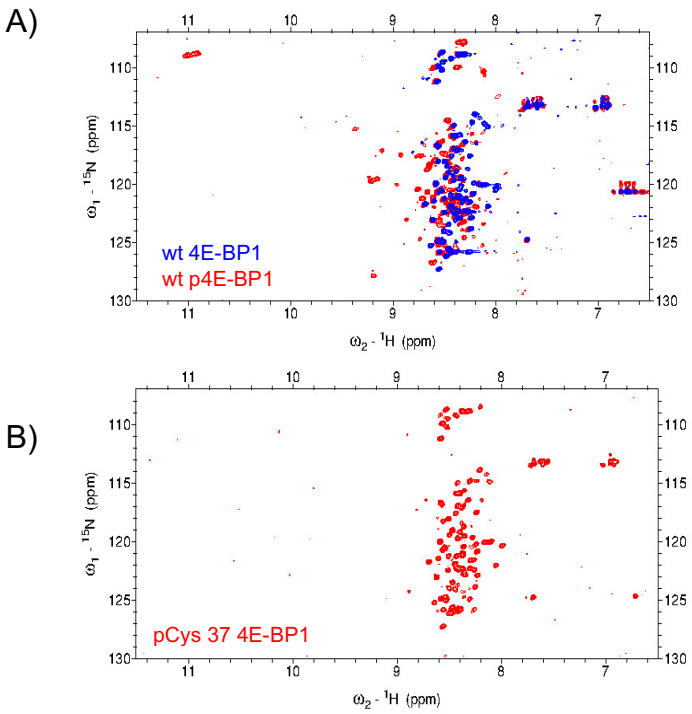

Figure 3.5 "HSQC NMR spectra of 4E-BP1" Protein NMR samples were all at concentrations of 100-300 μM in 30 mM Na_2HPO_4, 100 mM NaCl, 1 mM EDTA, 10% D2O v/v, pH 6.0. A) Phosphorylated wt-4E-BP1 (red) overlayed with unphosphorylated 4E-BP1 (blue); B) pCys37 4E-BP1. The absence of a downfield glycine chemical shift indicates lack of hairpin formation by pCys.

As expected, the wildtype 4E-BP1 does in fact undergo phosphorylation-induced secondary structuring, as demonstrated by the characteristic downfield Gly backbone proton chemical shifts for the two β hairpins at 11 ppm and the broader peak dispersion in the $^1H^{15}N$ HSQC NMR spectra (Figure 3.5A). At this point, we were optimistic that pCys could induce 4E-BP hairpin formation, as its incorportation in lieu of pThr180 of p38α kinase has been used to stimulate its enzymatic activity, an event that requires conformational restriction of the loop containing the phosphoylated residue, although this work was not followed up with structural studies.[32] After chemical modification and purification to obtain Thr37pCys 4E-BP1, we performed $^1H^{15}N$ HSQC NMR to characterize the effect of pCys37 on 4E-BP1 backbone chemical shifts. Intriguingly, our

data showed that pCys is not sufficient to induce hairpin formation in the context of 4E-BP1 (Figure 3.5B).

3.4 pCys as an apparent destabilizer of 4E-BP α-helicity

Phosphorylation of a Ser or Thr residue C-terminal to an α-helix is a PTM known to disrupt the helix dipole through electrostatic repulsion between the negatively charge phosphate moiety and the net negative charge at the C-terminal end of the α-helix dipole.[33,34] In the 4E-BPs, phosphorylation of Ser65 is indeed a helix destabilizing modification that critically weakens its affinity for eIF4E binding.[31] The ability of pCys to destabilize the 4E-BP helix relative to pThr or pSer was examined by CD spectroscopy, using 4E-BP-derived peptides containing residues Arg51-Val67 of 4E-BP1 or 4E-BP2, which contains the eIF4E-binding hot spot region. Peptides were prepared using standard solid phase peptide synthesis to generate the native peptide sequence, and peptides substituting the native Ser65 with pSer, pThr. It proved difficult to obtain full conversion to a pure pCys-containing peptide, due to observed chemical modification of Cys62, despite the -StBu protecting group (Figure 3.6). As a result of these complications, we decided to instead study pCys65 in the context of 4E-BP2 peptides. 4E-BP2 undergoes the same order-to-disorder transition in response to phosphorylation at Ser65, and contains an Arg residue in the place of the 4E-BP1 Cys62. While this did abrogate the need to consider non-specific Cys modification, 4E-BP2 peptides presented another chemical challenge; after some amount of the desired pCys product is formed, the thiophosphate nucleophile is postured to participate in two competing reactions:

nucleophilic addition to the remaining Dha, or nucleophilic substitution at the pCys phosphorous atom (Scheme 3.2).

A)

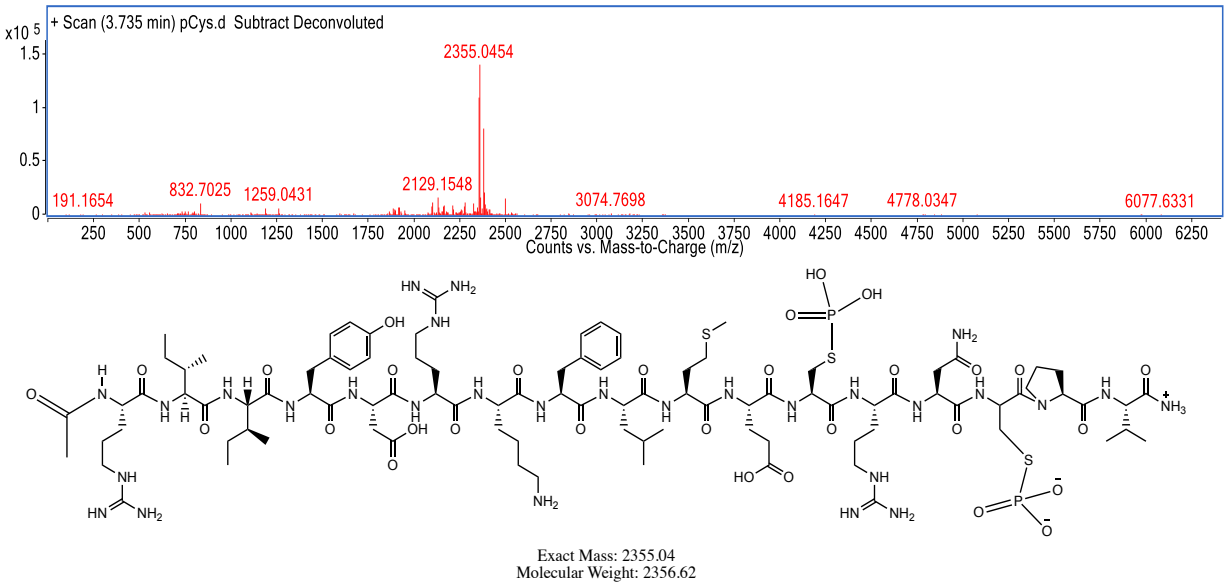

B)

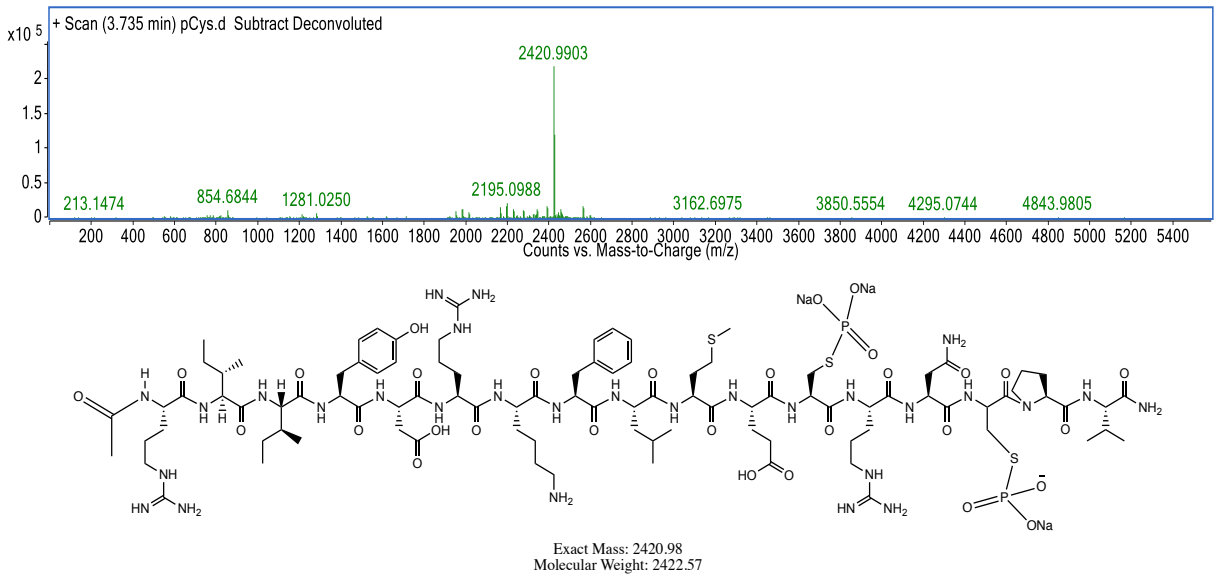

Figure 3.6 "Mass spectrometry data for attempts at pCys generation at Cys65Dha of a 4E-BP1 based peptide that was protected at Cys62 by an -StBu protecting group"

Interestingly, in the case of the 4E-BP2 based peptide, the latter reaction appears to be favored. Attempts at purification, proved difficult, largely due to the limited stability of pCys under chromatographic conditions (data not shown). We attempted to circumvent this by monitoring pCys conversion to the maximum relative ratio of pCys to Dha peptide before nucleophilic substitution becomes favored by mass spectrometry. This yielded an estimated 1:1 ratio of pCys to Dha substituted peptides.

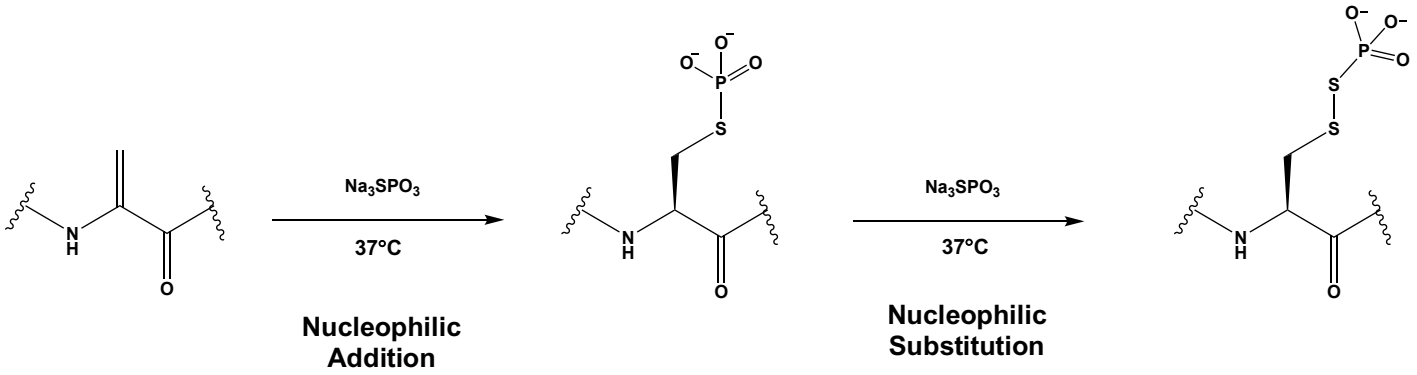

Scheme 3.2 "Nucleophilic Addition of Sodium Thiophosphate to pCys can Occur Before Complete pCys Conversion

2,2,2-Trifluoroethanol (TFE) is a solvent known to induce helicity in peptides and proteins by promoting favorability of the required backbone hydrogen bonding networks.[35,36] By doing CD experiments in 50% TFE, the destabilization of maximum peptide helicity was examined. CD data for 4E-BP2 peptides show the expected result of decreased maximum α-helicity of phosphopeptides relative to the native sequence in TFE. Notably, the pCys65 containing peptide appears to be between 68% and 90% less helical than the Ser65 peptide and between 33% and 50% less helical than the pSer65 peptide; however, the mixture of pCys-Dha, along with other apparent peptide impurities limit the ability to draw a simple conclusion on pCys specific helix destabilization. Because the estimated ratio of Dha to pCys peptide was 1:1, as determined by mass spectrometry,

this lead us to consider CD measurements using a solution of pSer peptide with Dha peptide at a 1:1 ratio for direct comparison.

Sample	Percent Helicity
Ser in TFE	19%
pSer in TFE	12%
pThr in TFE	11%
pCys in TFE (*pCys mix)	6% (*2%)
Dha in TFE	10%
pSer mix in TFE	10%

Table 3.1 "Percent Helicity of 4E-BP2 S65 Substituted Peptides by CD Spectroscopy"

pSer was chosen over other peptides for such a comparison, as we wished to assess the effectiveness of helix destabilization by pCys relative to pSer. If the mixed pCys sample gave CD spectra that was equal to, or less than the helicity of the pSer-Dha

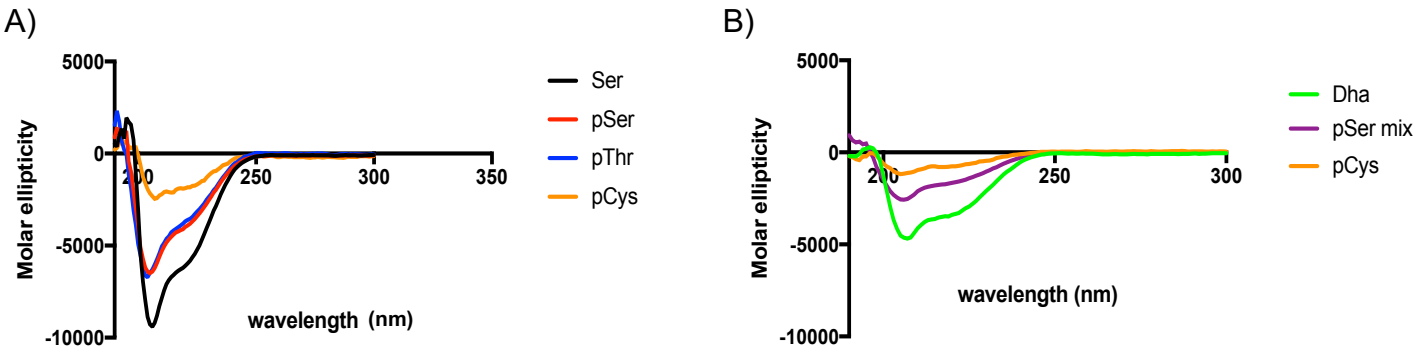

Figure 3.7 "CD spectra for 4E-BP2 based peptides" All peptide CD data was collected at 250 µM peptide concentrations in 50 mM Sodium Phosphate pH 7.4 and 15% acetonitrile, supplemented with 50% TFE. A) Comparison of phosphopeptides on helicity relative to the native sequence pCys molar ellipticity values were calculated from the difference of Dha and pCys-Dha mixture molar ellipticities; B) Comparison of pCys-Dha mixed solution helicity relative to both a pSer-Dha mixture, and Dha alone. No Dha subtraction was done for these spectra.

peptide mixture, we could more confidently propose that pCys itself is helix destabilizing. Conversely, if the CD spectra appeared more helical than pSer-Dha peptide mixture, further characterization would be necessary to make any conclusion. As shown in Figure 3.7B, the pCys-Dha peptide mixture is at least two-fold less helical than the pSer-Dha peptide mixture. This observation is likely due to the contribution of pCys or possibly other peptide impurity, as Dha peptide alone displays a higher maximum helicity than that of either mixture. While it is encouraging that pCys appears to be effective in the context of 4E-BP helix disruption, even relative to pSer, more work must be done to obtain definitive characterization of this modification.

3.5 Discussion

In conclusion, we have presented a structural biology evaluation of the "tag-and-modify" generation of pCys in the context of IDP structural modulation. While this approach does require system specific considerations, it does exhibit the potential for broad use by any group looking to study phosphorylation by means not completely dependent on kinase activity. The broader utility of the current "tag-and-modify" approach appears to be limited by the biological or structural context in which a given PTM occurs.

The inability of pCys to induce hairpin formation can be attributed to a number of differences in chemical environment. First, pCys lacks the γ-methyl group possessed by pThr, allowing for additional rotation around that bond. Yet, while studies from the Forman-Kay Lab corroborate the importance of the pThr γ-methyl for hairpin stability, a phosphorylated T37S,T46S 4E-BP2 mutant, shows that pSer can, in fact induce β-hairpin formation, albeit a less stable structure, as demonstrated by the upfield change in proton chemical shift of the hairpin Gly amide protons from 11 ppm in the case of pThr, to 10.5

ppm in the case of pSer of 4E-BP2.[29]

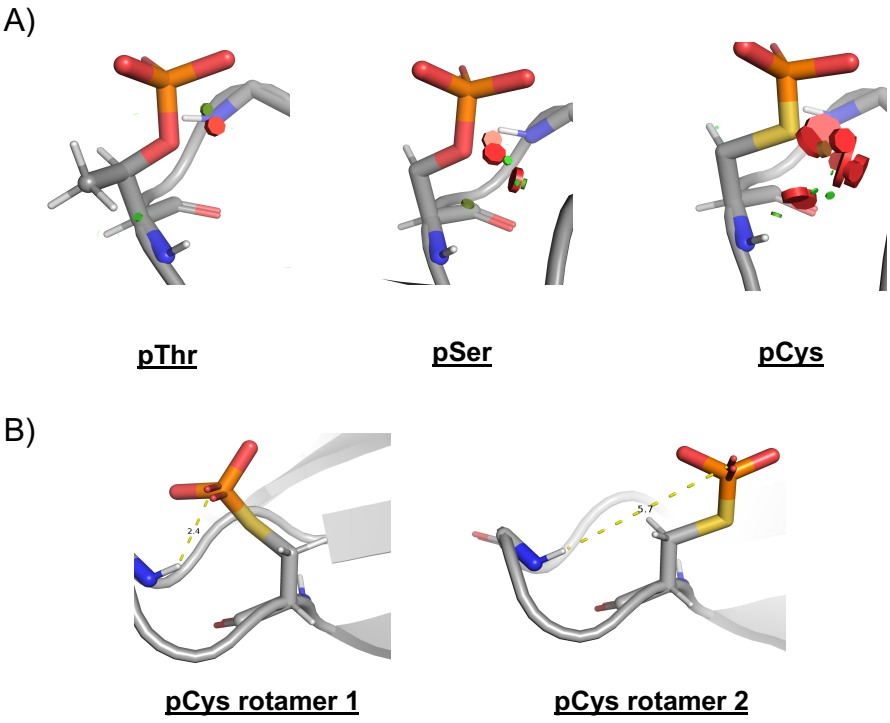

Figure 3.8 "Mutation of the phosphorylated residue to Ser or Cys in PyMol" A) In the conformation required for hairpin formation, pCys makes many unfavorable steric clashes compared to pThr and pSer, as visually depicted by red disks; B) The most sterically favorable rotamer (pCys rotamer 2) places that phosphate oxygens at an unfavorable distance for making the necessary contacts for hairpin formation

The larger Van der Waals radius of the sulfur atom is likely a major factor influencing the effectiveness pCys as a phosphomimetic. In addition to the resulting increased C-S and P-S bond lengths (~1.8 Å and 2.1 Å respectively) relative to C-O and P-O bond length (~1.5 Å and 1.6 Å respectively)[37] from the larger Van der Waals radius of sulfur compared to that of oxygen, there is also an increase in Van der Waals strain within the local structural environment of the 4E-BP hairpin (Figure 3.8A). The increase in strain is such that the most sterically favorable pCys rotamer is, in fact, predicted to adopt a conformation that is unable to make the necessary contacts for hairpin formation

(Figure 3.8B). Thus, those considering using pCys as a phosphomimetic will benefit greatly from a preliminary assessment of tolerance for the larger sulfur atom in a given protein's local environment.

In the case of helix destabilization, Cys has been described in some literature as somewhat destabilizing at the C-terminus of α-helices,[38,39] exhibiting an inherent helical propensity that is lower than those of both Ser and Thr,[39] although this observation likely depends on the local environment of a given helix.[40-43] Thus, it is reasonable to deduce that the more polarizable sulfur atom itself plays a role in destabilizing the 4E-BP helix, by increasing the entropic cost of helix formation. In addition, evaluation of this data must consider the method for converting Cys to pCys. This conversion is obtained through a Dha intermediate, which results in a loss of chirality. After the addition of sodium thiophosphate, the resultant pCys residue exists in an average ratio of 3:2 of L- and D-conformers respectively.[32,44] Precise stereochemistry is crucial to protein folding, and is of particular importance when considering the structural regulation of an IDP. The naturally occurring L- conformer is the conformer that is biologically relative, with the mixture of L- and D- pCys lowering the effective concentration of the relevant pCys conformer. There is also evidence that the local environment influences the efficiency of conversions of Cys to Dha, and Dha to pCys,[32] which may explain the difficulties in obtaining full conversion in at residue 65 of the 4E-BP peptides, as these difficulties were not observed when the chemistry was applied at the singular position 37 of 4E-BP1.

Development of an approach that generates a stereospecific phosphomimetic will vastly expand the applicability of chemical mutagenesis to biological contexts that have been historically difficult to study. There has already been work toward this by Bertran-

Vincente et al., although the yield and solvent requirements of their published method are not amenable to modification of most proteins.[45] Radical addition to Dha, as developed by the Davis Lab, is another method of chemical phosphomimetic generation. The radical chemistry would likely overcome many steric limitations, as a C-C bond is formed in lieu of a C-S bond, and also presents the potential to infer stereospecificity through hydrogen introduction at the α-carbon; however, this chemistry is extremely oxygen sensitive, with no currently published method for such modifications outside of a glovebox, limiting the scope of its practical application. Additionally, the iodophosphonates required for the radical addition of the phosphomimetic to Dha are not commercially available, further restricting application of this methodology. A future study aimed at defining the physical-chemical properties that directly influence pCys chemistry would be an impactful and exciting next step for continuing this work, and broadening the use of pCys in biophysical and biochemical studies.

3.6 Materials and Methods

General chemistry methods

NMR spectra for small molecules (^{1}H) were recorded on a Bruker BioSpin GmbH NMR. Chemical shifts are reported in parts per million and referenced to TMS. Spectra were processed using MestReNova software. Mass spectrometry (HRMS) was performed using an Agilent 6520, Accurate-Mass QTOF LC/MS spectrometer using ESI ionization, with less than 5 ppm error for all HRMS analyses. RP-HPLC was performed using binary gradients of solvents A and B, where A is 0.1% HCO_2H in water and B is 0.1% HCO_2H in acetonitrile or 0.1% HCO_2H in methanol. Preparative RP-HPLC was performed using an Agilent 1260 Infinity HPLC equipped with a PrepHT SB-C18 column (21.2 × 150 mm; 5

μm) at a flow rate of 18.6 mL/min, with detection at 214 and 254 nm. In all cases, fractions were analyzed off-line using an Agilent Q-TOF HPLC-MS. Pure fractions were then pooled and lyophilized.

2,5-dibromodiamide synthesis (DBDHA)

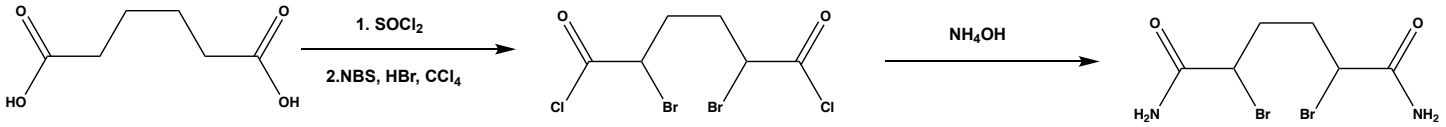

Scheme 3.3 "2,5-dibromohexaneamide synthesis"

Synthesis of 2,5-dibromohexaneamide from adipic acid was performed as previously described[32]. Briefly, adipic acid (10.00 g, 68.4 mmol, 1.0 equiv.) was suspended in thionyl chloride (30 mL, 414 mmol, 6.0 equiv.) and the mixture heated under reflux at 80°C under a steady stream of N_2. After all the adipic acid had dissolved, the reaction was refluxed for an additional 1.5 h, after which the mixture was returned to room temperature and diluted with carbon tetrachloride (40 mL). N-bromosuccinimide (24.27 g, 136 mmol, 2.0 equiv.) and conc. HBr (4 drops of a 42% solution in H_2O) were subsequently added and the reaction was further refluxed at 80°C for 2 h. The reaction solution was then lower to 0°C for 30 min before being filtered and washed with Et2O (40 mL). The filtrate concentrated in vacuo to give 2,5-dibromoadipoyl dichloride (1) as a dark red oil. The product was immediately used for the next reaction without characterization or purification. ^{1}H-NMR values were in agreement with literature values.

The crude acid chloride (1) was added dropwise to a stirred solution of NH_4OH (80mL of a 25% solution in water, 1180 mmol, 17.2 equiv.) over 25 min at 0 °C. The

reaction was then to stirred at 0 °C for 1 h, after which it was filtered to give an olive-green precipitate and a dark filtrate. The precipitate was triturated by suspending in 1:1 methanol:H2O (80 mL) and heating the mixture at 60°C for 30 min and filtered once more. The precipitate was further washed with methanol (80 mL) and dried under vacuum to give adequately pure 2,5-dibromoadipic acid diamide, as an off-white powder, and without the need for further purification.

^{1}H NMR (500 MHz, DMSO) δ ppm 7.68 (2 H, s, NH2), 7.30 (2 H, s, NH2), 4.29–4.36 (2 H, m, 2 x CHBr), 1.81–2.06 (4 H, m, CH_2CH_2).

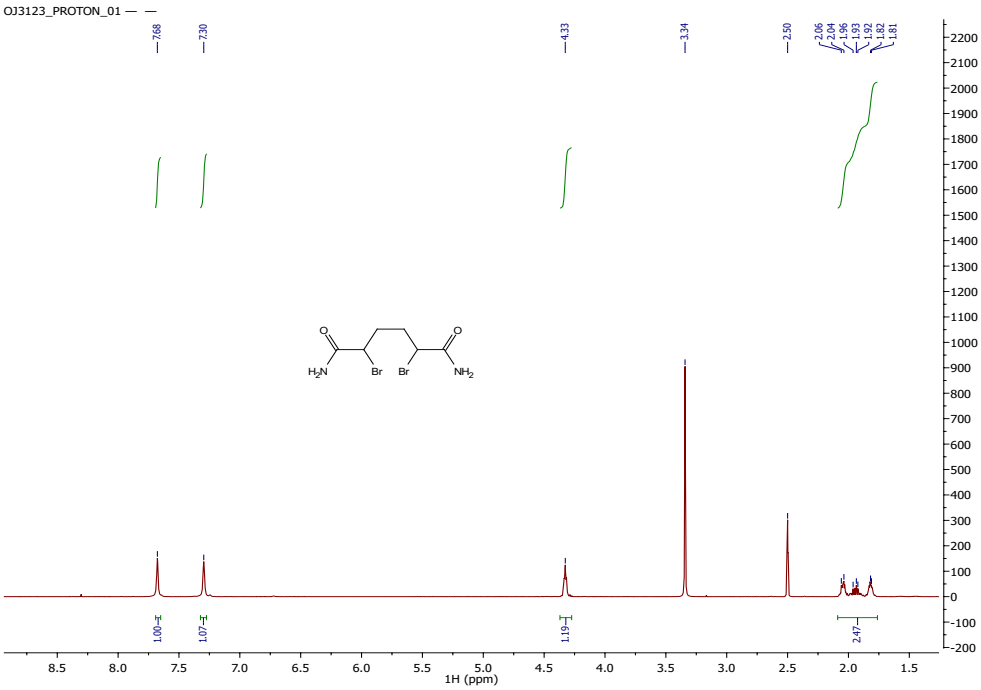

Figure 3.9 "^{1}NMR spectra of 2,5-dibromohexanediamide"

4E-BP1 Plasmids and Mutagenesis

Primer Label	Description	Sequence
P1	4E-BP1 LIC Forward	5’ - TACTTCCAATCCAATGCAATGTCCGG – 3’
P2	4E-BP1 LIC Reverse	5’ – TTATCCACTTCCAATGTTAAATGTCCATCTCAAAC – 3’
P3	C7A mutant Forward	5’- GGGCAGCAGCGCCAGCCAGACCCCAAGC – 3’
P4	C7A mutant Reverse	5'- GCTTGGGGTCTGGCTGGCGCTGCTGCCC -3
P5	C62A mutant Forward	5'- CCTGATGGAGGCTCGGAACTCACCTGTGACCAAAACACC -3'
P6	C62A mutant Reverse	5'- GGTGTTTTGGTCACAGGTGAGTTCCGAGCCTCCATCAGG -3'
P7	T37C mutant Forward	5’-CAGCTCCCGCCCGGGGACTACAGCACGTGCCCCGGCGGCACGCTC-3’
P8	T37C mutant Reverse	5’ – GAGCGTGCCGCCGGGGCACGTGCTGTAGTCCCCGGGCGGGAGCTG-3’
P9	T46C mutant Forward	5'- GGCACGCTCTTCAGCACCTGCCCGGGAG -3'
P10	T46C mutant Reverse	5'- CTCCCGGGCAGGTGCTGAAGAGCGTGCC -3'

Table 3.2 “4E-BP1 Primers”

Human 4E-BP1 plasmid was purchased from Kazusa DNA Research Institute in pFN21A HaloTag vector. All primers for cloning and mutagenesis were purchased from IDT. The 4E-BP1 insert was transferred from pFN21A to a pMCSG9 vector via LIC cloning for amplification of MBP-4E-BP1 plasmid in the DH5α E. coli strain[46]. Site-directed mutagenesis was performed using the QuikChange II Site-Directed Mutagenesis Kit (Agilent). All DNA sequencing was performed by the University of Michigan DNA Sequencing Core.

Protein Expression and Purification

Expression and purification of activated His-tagged MAPK was done according to a protocol and plasmid co-expressing Erk2 and MEK1 obtained by the Forman-Kay Lab

from Attila Remenyi at Eo¨tvo¨s Lora´nd University. For unlabeled and $^{13}C^{15}N$ labeled 4E-BP1 constructs in pMCSG9, plasmid was transformed into Rosetta cells using a standard transformation protocol. Single colonies were picked to inoculate 6 × 6 mL overnight cultures in either LB media or M9 minimal media containing 50 mg/mL ampicillin (amp) that were incubated shaking at 37 °C. Overnight cultures were used to inoculate 1 L of LB media containing 50 mg/mL amp, and that culture was grown to an OD_{600} of 0.8. At this stage, the culture was induced with 1 mM IPTG and incubated shaking at 37 °C for 4h. Cells were pelleted by centrifugation at 6000× g for 15 min at 25 °C, re-suspended in Lysis Buffer (6M Guanidium HCl, 50 mM Tris pH 7.5, 500 mM NaCl, 1 mM PMSF, 1 mM EDTA, 2 mM DTT), and lysed by sonication. Lysate was then clarified by centrifugation at 16,000× g for 20 min at 4 °C. Clarified lysate was incubated 15 min on Ni-NTA resin in a Bio-Rad column, then the flow-through was collected. The Ni-NTA resin was washed 3 × with 10 column volumes of Wash Buffer A (6M Guanidium HCl, 50 mM Tris pH 7.5, 200 mM NaCl, 1 mM EDTA, 2 mM DTT), followed by 3 × 10 column volumes washes with Wash Buffer B (50 mM Tris pH 7.5, 200 mM NaCl, 1 mM EDTA, 2 mM DTT), and eluted with Wash Buffer B without Guanidium HCl, and containing a gradient of 0–500 nM imidazole. The protein was then concentrated to 5 mL, purified by size-exclusion chromatography (SEC), using Storage Buffer (50 mM Sodium Phosphate pH 7.4, 100 mM NaCl, 1 mM EDTA, 1 mM DTT) to remove aggregates, and concentrated as needed, with concentration monitored by A_{280}. Purified protein was aliquoted, stored at -80°C, and aliquots were thawed at 4°C immediate prior to use.

Protein Construct	Description	Isotopic Labeling	Mass Expected (Da)	Mass Observed (Da)
wt-4E-BP1	wild-type sequence expressed in pFN29K vector and cleaved by TEV protease	N/A	12868	12868
4E-BP1 Cys7Dha, Cys62Dha	wild-type sequence expressed in pFN29K vector and cleaved by TEV protease, and reacted with DBHDA	N/A	12800	12800
wt-4E-BP1	wild-type sequence expressed in pMCSG9 vector and cleaved by TEV protease	$^{13}C^{15}N$	13557*	13542
wt-4E-BP1	wild-type sequence expressed in pMCSG9 vector and cleaved by TEV protease and phosphorylated by MAPK	$^{13}C^{15}N$	14022^	13863, 13945, 14021
4E-BP1 T37C/T46C	C7A, C62A, T37C, T46C 4E-BP1 mutant expressed in pMCSG9 vector and cleaved by TEV protease	$^{13}C^{15}N$	13496*	13478
4E-BP1 T37Dha/T46Dha	C7A, C62A, T37C, T46C 4E-BP1 mutant expressed in pMCSG9 vector, cleaved by TEV protease and reacted with DBHDA	$^{13}C^{15}N$	13410^	13410, 13617
4E-BP1 T37C	C7A, C62A, T37C 4E-BP1 mutant expressed in pMCSG9 vector and cleaved by TEV protease	$^{13}C^{15}N$	13494*	13478
4E-BP1 T37Dha	C7A, C62A, T37C 4E-BP1 mutant expressed in pMCSG9 vector, cleaved by TEV protease and reacted with DBHDA	$^{13}C^{15}N$	13444^	13444
4E-BP1 T37pCys	C7A, C62A, T37C 4E-BP1 mutant expressed in pMCSG9 vector, cleaved by TEV protease and	$^{13}C^{15}N$	13555^	13557

	reacted with DBHDA, followed by sodium thiophosphate			
*"Mass Expected" assumes 100% isotopic labeling where applicable, it is important to note that isotopic labelling of protein is rarely perfectly efficient.				
^"Mass Expected" based on "Mass Observed" in previous step				

Table 3.3 "4E-BP1 Protein Constructs"

4E-BP1 protein kinase phosphorylation

Wild-type 4E-BP1 was phosphorylated with MAPK using the dialysis technique described by Bah and colleagues[29]. In brief, the phosphorylation reaction was made up of 50 ml of 50 mM Tris pH 7.5 at 25 °C, 1 mM EGTA, 2 mM DTT, 20 mM $MgCl_2$ and 10 mM ATP containing a 5:1 ratio of 4E-BP1:MAPK by molar concentration. The reaction was transferred to a dialysis bag placed in 5L of phosphorylation buffer. Phosphorylation was allowed to proceed overnight with stirring and completion of phosphorylation being monitored by Q-TOF mass spectrometry.

4E-BP1 chemical phosphorylation

pCys 4E-BP1 protein was generated as previously described[20,32]. Briefly, TEV-cleaved and purified 4E-BP1 was incubated with 1mM fresh DTT for 30 min before buffer exchange into Reaction Buffer (6M Guanidinium-HCl, 50mM Sodium Phosphate pH 8.4, 100mM NaCl, 1mM EDTA). Once in Reaction Buffer, protein was incubated shaking with 150 equivalents of DBDHA at 37°C for 3h to convert Cys to Dha. Completion of reaction was determined by mass spectrometry. The protein was then buffer exchanged into Reaction Buffer with the pH adjusted to 7.4. Additions 5000 equivalents of sodium thiophosphate pH 8.0 in a solution of 700mg/mL in water were made to the Dha 4E-BP1

solution in 10 min increments, with completion of the pCys reaction being monitored by Q-TOF mass spectrometry.

pCys modification of 4E-BP peptide was generated in a similar manner to full-length protein. Peptide was dissolved in Reaction Buffer. Then incubated shaking with 150 equivalents of DBDHA at 37°C for 1h to convert Cys to Dha. Completion of reaction was determined by mass spectrometry. The reaction was centrifuged at 15,000 xg for one minute and the supernatant was transferred to a new tube. Precipitate was washed with Reaction Buffer, centrifuged again, and supernatants were pooled. Serial additions of 1 µL of a solution of 700mg/mL sodium thiophosphate in water, pH 8.0 in were made to the Dha 4E-BP1 peptide solution in 1 min increments, with completion of the pCys reaction being monitored by Q-TOF mass spectrometry.

4E-BP Peptide Synthesis

Peptide Label	**Sequence**	**Mass Expected (Da)**	**Mass Observed (Da)**
4E-BP1 Ser65Cys	**RIIYDRKFLMEC(StBu)RN CPV**	2285.16	2285.16
4E-BP1 Ser65Dha	**RIIYDRKFLMEC(StBu)RN A'PV**	2251.16	2251.16
4E-BP1 Ser65pCys	**RIIYDRKFLMECRNpCPV**	2275.07	2355.04, 2420.99 (Figure 5)

4E-BP2 native	**RIIYDRKFLLDRRNSPV**	2202.26	2202.27
4E-BP2 pSer65	**RIIYDRKFLLDRRNpSPV**	2279.21	2282.21
4E-BP2 pThr65	**RIIYDRKFLLDRRNpTPV**	2293.22	2298.26
4E-BP2 Ser65Cys	**RIIYDRKFLLDRRNCPV**	2218.24	2218.23
4E-BP2 Ser65Dha	**RIIYDRKFLLDRRNA'PV**	2184.25	2184.25
4E-BP2 Ser65pCys	**RIIYDRKFLLDRRNpCPV**	2295.18	2184.24, 2393.27*, 2330.17 (Figure 6)
*M+H_3PO_4, a common adduct in phosphorous containing compounds A' = Dha			

Table 3.4 "4E-BP1 Peptide Sequences"

4E-BP peptide sequences were synthesized on a Liberty Blue peptide synthesizer on 0.1-mmol scale using Rink Amide resin. All amino acid coupling reactions were performed using 5 excess equivalents of Fmoc-AA-OH with 1:1:1 of AA:DIC:Oxyma in DMF for 4 min at 90°C for all amino acids. Fmoc deprotections were performed for 1 min at 90°C in 20% piperidine in DMF. All peptides were cleaved from the resin by agitation in a 90:0.4:0.4:0.2 by volume solution of TFA:thioanisole:TIPS:H_2O for 4 h at 25 °C. The cleaved peptide in TFA solution was then precipitated in ice-cold diethyl ether, and the precipitate was centrifuged, dissolved, and purified via RP-HPLC.

R I I Y D R K F L L D R R N X P V

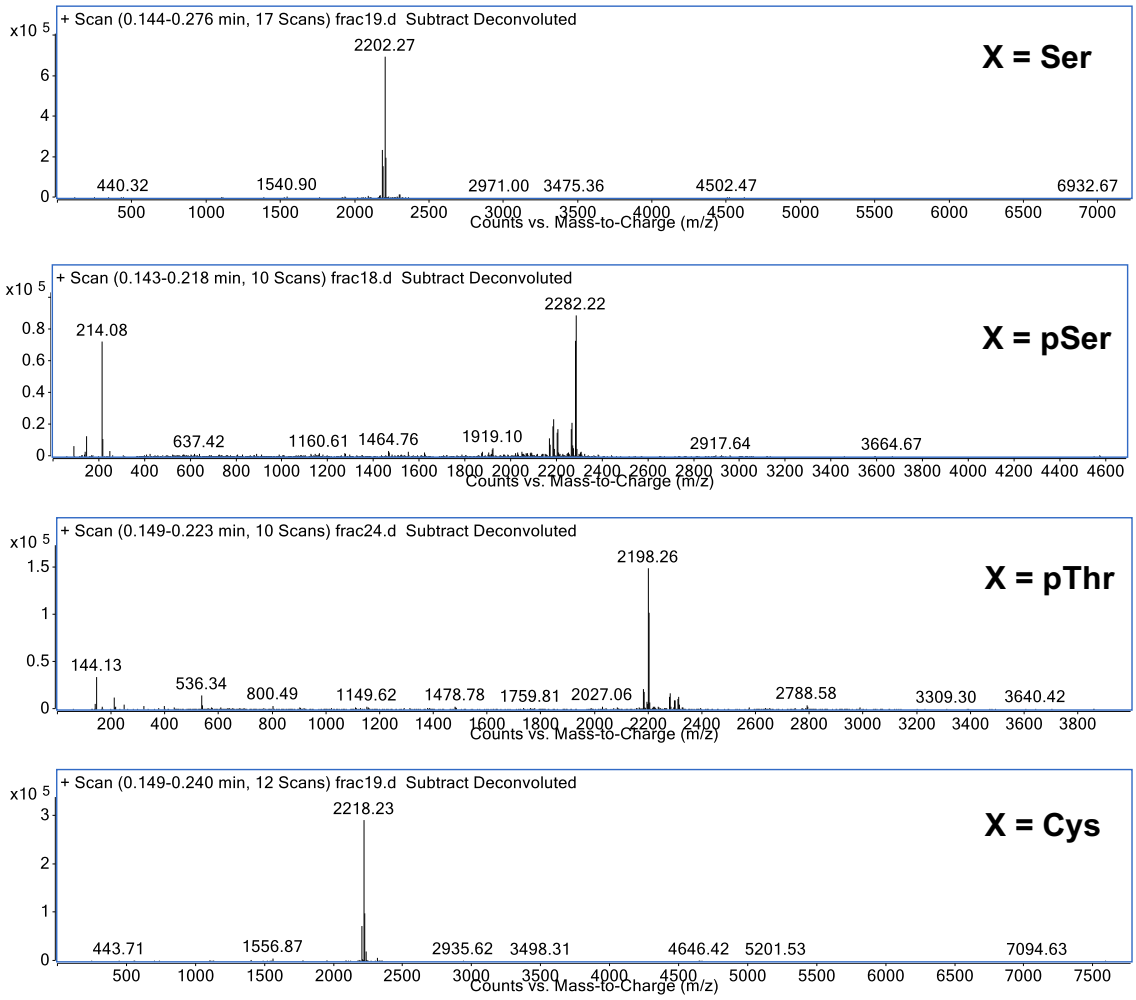

Figure 3.10 "Mass Spectrometry Data for Purified 4E-BP2 Peptides"

Protein NMR experiments

NMR experiments were conducted on Varian INOVA 500 and 600 MHz spectrometers, equipped with pulsed-field gradient units, and triple resonance probes, and a cryogenically cooled probe. NMR samples contained approximately 0.1mM $^{15}N^{13}C$-labelled protein in NMR Buffer (30 mM Na_2HPO_4, 100 mM NaCl, 1 mM EDTA, 10% D_2O

v/v, pH 6.0). HSQC experiments were performed at 5°C. NMR data sets were processed with the NMRPipe software package[47] and analyzed using SPARKY.[48]

CD Experiments

CD samples contained approximately 250 μM peptide in 50 mM Sodium Phosphate pH 7.4 and 15% acetonitrile, with or without 50% 2,2,2-trifluoroethanol. CD experiments were performed on a Jasco-1500 CD spectropolarimeter with data recorded between 260 nm and 190 nm with 5 accumulations per experiment. CD data sets were graphed using GraphPad Prism software, and percent helicity of each peptide was calculated based on the molar ellipticity minimum at 222 nm as described by Shepherd et al.[49] Helicity was determined by molar ellipticity of each peptide at 222 nm using the equations below.[49]

Equation 1:

$$\%_H = (([\theta]_{obs222} - [\theta]_C)/([\theta]_{\infty 222} - [\theta]_C)) * 100$$

Equation 2:

$$[\theta]_C = 2220 - 53T$$

Equation 3:

$$[\theta]_{\infty 222} = (-44000 + 250T)(1 - \frac{k}{N_p})$$

Where,

$\%_H$ = percent α-helix content

$[\theta]_{obs222}$= observed molar ellipticity at 222 nm

$[\theta]_C$= Random coil molar ellipticity

$[\theta]_{\infty 222}$= Infinite molar α-helix molar ellipticity

T = temperature in degrees Celsius

k = finite length correction

N_p = Number of peptide units

Molecular Modeling

Modeling of 4E-BP phosphoforms were generated from phosphorylated 4E-BP2 NMR data (PDB: 2MX4) in PyMol software.[50] Generation of pSer and pCys were done in PyMol using the mutagenesis wizard, builder tool, and PyTMs[51] plug-in for PyMol.

3.7 References

1 Dyson, H. J. & Wright, P. E. Intrinsically unstructured proteins and their functions. *Nat Rev Mol Cell Biol* **6**, 197-208, doi:10.1038/nrm1589 (2005).

2 Wright, P. E. & Dyson, H. J. Intrinsically disordered proteins in cellular signalling and regulation. *Nat Rev Mol Cell Biol* **16**, 18-29, doi:10.1038/nrm3920 (2015).

3 Noren, C. J. A.-C., Spencer J.; Griffith, Michael C.; Schultz, Peter G. A General Method for Site-Specific Incorporation of Unnatural Amino Acids into Proteins. *Science* **244**, 182-188 (1989).

4 Norne, C. J. A.-C., Spencer J.; Suich, Daniel J.; Noren, Karen A.; Griffith, Michael C.; Schultz, Peter G. In vitro suppression of an amber mutation by a chemically aminoacylated transfer RNA prepared by runoff transcription. *Nucleic Acids Res* **18**, 83-88 (1990).

5 Martina Schnölzer, S. B. H. K. Constructing Protains br Dovetailing Unprotected Synthetic Peptides: Backbone-Engineeres HIV Protease. *Science* **256**, 221-225 (1992).

6 Philip E. Dawson, T. W. M., Ian Clark-Lewis, Stephen B. H. Kent. Synthesis of Proteins by Native Chemical Ligation. *Science* **266**, 776-779 (1994).

7 Reimann, O., Glanz, M. & Hackenberger, C. P. Native chemical ligation between asparagine and valine: application and limitations for the synthesis of tri-phosphorylated C-terminal tau. *Bioorg Med Chem* **23**, 2890-2894, doi:10.1016/j.bmc.2015.03.028 (2015).

8 Zhan, C., Varney, K., Yuan, W., Zhao, L. & Lu, W. Interrogation of MDM2 phosphorylation in p53 activation using native chemical ligation: the functional role of Ser17 phosphorylation in MDM2 reexamined. *J Am Chem Soc* **134**, 6855-6864, doi:10.1021/ja301255n (2012).

9 Muir, T. W. S., Dolan; Cole, Philip A. Expressed protein ligation: A general method for protein engineering. *Proc Natl Acad Sci U S A* **95**, 6705-6710 (1998).

10 Shogren-Knaak, M. A., Fry, C. J. & Peterson, C. L. A native peptide ligation strategy for deciphering nucleosomal histone modifications. *J Biol Chem* **278**, 15744-15748, doi:10.1074/jbc.M301445200 (2003).

11 Luo, X. F., Guangsen; Wang, Rongsheng E.; Zhu, Xueyong; Zambaldo, Claudio; Liu, Renhe; Liu, Tao; Lyu, Xiaoxuan; Du, Jintang; Xuan, Weimin; Anzhi, Yao; Reed, Sean A.; Kang, Mingchao; Zhang, Yuhan; Guo, Hui; Huang, Chunhui; Yang Penh-Yu; Wilson, Ian A.; Schultz, Peter G.; Wang, Feng. Genetically encoding phosphotyrosine and its nonhydrolyzable analog in bacteria. *Nat Chem Biol* **13**, 845-851 (2017).

12 Rogerson, D. T. *et al.* Efficient genetic encoding of phosphoserine and its nonhydrolyzable analog. *Nat Chem Biol* **11**, 496-503, doi:10.1038/nchembio.1823 (2015).

13 Dawson, P. E. Native Chemical Ligation Combined with Desulfurization and Deselenization: A General Strategy for Chemical Protein Synthesis. *Israel Journal of Chemistry* **51**, 862-867, doi:10.1002/ijch.201100128 (2011).

14 Okeley, N. M. Z., Yantao; van der Donk, Wilfren A. Facile Chemoselective Synthesis of Dehydroalanine-Containing Peptides. *Org Lett* **2**, 3603-3606 (2000).

15 You, Y. O. L., M.R.; Ihnken, L.A. Furgerson; Knowlton, A.K.; van der Donk, Wilfred, A. Lacticin 481 Synthetase a a General Serine/Threonine Kinase. *ACS Chem Biol* **4**, 379-385 (2009).

16 Hashimoto, K. S., Mitsura; Okuno, Toshikatsu; Shirahama, Haruhisa. B-Phenylselenoalanine as a dehydroalanin precursor-efficient synthesis of alternariolide (SM toxin I). *Chem Commun*, 1139-1140 (1996).

17 Clark Peter, G. L. Conversion of the Active-Site Cysteine Residue of Papain into a Dehydro-serine, a Serine and a Glycine Residue. *Eur. J. Biochem* **84**, 293-299 (1978).

18 Wang, J., Schiller, S. M. & Schultz, P. G. A biosynthetic route to dehydroalanine-containing proteins. *Angew Chem Int Ed Engl* **46**, 6849-6851, doi:10.1002/anie.200702305 (2007).

19 Chalker, J. M. *et al.* Methods for converting cysteine to dehydroalanine on peptides and proteins. *Chemical Science* **2**, 1666, doi:10.1039/c1sc00185j (2011).

20 Chalker, J. M., Lercher, L., Rose, N. R., Schofield, C. J. & Davis, B. G. Conversion of cysteine into dehydroalanine enables access to synthetic histones bearing diverse post-translational modifications. *Angew Chem Int Ed Engl* **51**, 1835-1839, doi:10.1002/anie.201106432 (2012).

21 Clark, P. I. L., Gordon. Chemical Muatiations of Papain. The preparation of Ser 25- and Gly 25-Papain. *J.C.S. Chem. Comm.*, 923-924 (1977).

22 Beugnet, A., Wang, X. & Proud, C. G. Target of rapamycin (TOR)-signaling and RAIP motifs play distinct roles in the mammalian TOR-dependent phosphorylation of initiation factor 4E-binding protein 1. *J Biol Chem* **278**, 40717-40722, doi:10.1074/jbc.M308573200 (2003).

23 von Manteuffel, S. R. G., Anne-Claude; Ming, Xiu-Feng; Sonenberg, Nahum; Thomas, George. 4E-BP1 phosphorylation is mediated by the FRAP-p70s6k pathway and is independent of mitogen-activated protein kinase. *PNAS* **93**, 4076-4080 (1996).

24 Pause, A. B., Graham J.; Gingras, Anne-Claude; Donzé, Olivier; Lin, Tai-An; Lawrence Jr., John C.; Sonenberg, Nahum. Insulin-dependent stimulation of protein syntheisis by phosphorylatin of a regulator of 5'-cap function. *Nature* **371**, 762-767 (1994).

25 Li, S. *et al.* Translational Control of Cell Fate: Availability of Phosphorylation Sites on Translational Repressor 4E-BP1 Governs Its Proapoptotic Potency. *Molecular and Cellular Biology* **22**, 2853-2861, doi:10.1128/mcb.22.8.2853-2861.2002 (2002).

26 Haghighat, A. M., Sylvie; Pause, Arnim; Sonenberg, Nahum. Repression of cap-dependent translation by 4E-binding protein 1: competition with p220 for binding to eukaryotic initiation factor 4E. *The EMBO Journal* **14**, 5701-5709 (1995).

27 Ayuso, M. I., Hernandez-Jimenez, M., Martin, M. E., Salinas, M. & Alcazar, A. New hierarchical phosphorylation pathway of the translational repressor eIF4E-binding protein 1 (4E-BP1) in ischemia-reperfusion stress. *J Biol Chem* **285**, 34355-34363, doi:10.1074/jbc.M110.135103 (2010).

28 Gingras, A. C. *et al.* Hierarchical phosphorylation of the translation inhibitor 4E-BP1. *Genes Dev* **15**, 2852-2864, doi:10.1101/gad.912401 (2001).

29 Bah, A. *et al.* Folding of an intrinsically disordered protein by phosphorylation as a regulatory switch. *Nature* **519**, 106-109, doi:10.1038/nature13999 (2015).

30 Gingras, A. C. G., Steven P.; Raught, Brian; Polakiewicz, Roberto D.; Abraham, Robert T.; Hoekstra, Merl F.; Aebersold, Ruedi; Sonenberg, Nahum. Regulation of 4E-BP1 phosphorylation: a novel two-step mechanism. *Genes Dev* **13**, 1422-1437 (1999).

31 Tait, S. *et al.* Local control of a disorder-order transition in 4E-BP1 underpins regulation of translation via eIF4E. *Proc Natl Acad Sci U S A* **107**, 17627-17632, doi:10.1073/pnas.1008242107 (2010).

32 Chooi, K. P. *et al.* Synthetic phosphorylation of p38alpha recapitulates protein kinase activity. *J Am Chem Soc* **136**, 1698-1701, doi:10.1021/ja4095318 (2014).

33 Andrew, D. C. W., J.; Jones, G.R.; Doig, A.J. Effect of phosphorylation on alpha-helix stability as a function of position. *Biochemistry* **41**, 1897-1905 (2002).

34 Elbaum, M. B. & Zondlo, N. J. OGlcNAcylation and phosphorylation have similar structural effects in alpha-helices: post-translational modifications as inducible start and stop signals in alpha-helices, with greater structural effects on threonine modification. *Biochemistry* **53**, 2242-2260, doi:10.1021/bi500117c (2014).

35 Luo, P. B., Robert L. Mechanism of Helix Induction by Trifluoroethanol: A Framework for Extrapolating the Helix-Forming Properties from Trifluoroethanol/Water Mixtures Back to Water. *Biochemistry* **36**, 8413-8421 (1997).

36 Hackl, E. V. Limited proteolysis of natively unfolded protein 4E-BP1 in the presence of trifluoroethanol. *Biopolymers* **101**, 591-602, doi:10.1002/bip.22422 (2014).

37 Fauman, E. B. e. a. The X-Ray Crystal Structures of Yersinia Tyrosine Phosphatase with Bound Tungstate and Nitrate. *Journal of Biological Chemistry* **271**, 18780-18788 (1996).

38 Doig, A. J. B., R.L. N- and C-capping preferences for all 20 amino acids in alpha-helical peptides. *Protein Science* **4**, 1325-1336 (1995).

39 Pace, C. N. S., J.M. A Helix Propensity Scale Based on Experimental Studies of Peptides and Proteins. *Biophysical Journal* **75**, 422-427 (1998).

40 Creamer, T. P. R., G.D. alpha-Helix-Forming Propensities in Peptides and Proteins. *Proteins: Structure, Function, and Genetics* **19**, 85-97 (1994).

41 Lyu, P. C., Marky, L. A. & Kallenbach, N. R. The role of ion pairs in .alpha. helix stability: two new designed helical peptides. *Journal of the American Chemical Society* **111**, 2733-2734, doi:10.1021/ja00189a067 (1989).

42 O'Neil, K. T. D., W.F. A Thermodynamic Scale for the Helix-Forming Tendencies of the Commonly Occuring Amino Acids. *Science* **250**, 646-651 (1990).

43 Padmanabham, S. M., S.; Ridgeway, T.; Laue, T.M.; Baldwin, R.L. Relative helix-forming tendencies of nonpolar amino acids. *Nature* **344**, 268-270 (1990).

44 Wright, T. H. *et al.* Posttranslational mutagenesis: A chemical strategy for exploring protein side-chain diversity. *Science* **354**, doi:10.1126/science.aag1465 (2016).

45 Bertran-Vicente, J. *et al.* Chemoselective synthesis and analysis of naturally occurring phosphorylated cysteine peptides. *Nat Commun* **7**, 12703, doi:10.1038/ncomms12703 (2016).

46 Stols, L. *et al.* A new vector for high-throughput, ligation-independent cloning encoding a tobacco etch virus protease cleavage site. *Protein Expr Purif* **25**, 8-15, doi:10.1006/prep.2001.1603 (2002).

47 Delaglio, F. G., Stephan; Vuister, Geerten W.; Zhu, Guang; Pfiefer, John; Bax, Ad. NMRPipe: A multidimensional spectral processing system based on UNIX pipes. *Journal of Biomolecular NMR* **6**, 277-293 (1995).

48 Lee, W., Tonelli, M. & Markley, J. L. NMRFAM-SPARKY: enhanced software for biomolecular NMR spectroscopy. *Bioinformatics* **31**, 1325-1327, doi:10.1093/bioinformatics/btu830 (2015).

49 Shepherd, N. E. H., H.N; Abbenante, G.; Fairlie, D.P. Single Turn Peptide Alpha Helices with Exceptional Stability in Water. *J Am Chem Soc* **127**, 2974-2983 (2005).

50 The PyMOL Molecular Graphics System, 2.0.7, Schrödinger, LLC.

51 Warnecke, A. S., T.; Achour, A.; Harris, R.A. PyTMs: a useful PyMOL plugin for modifications. *BMC Bioinformatics* **15**, 370 (2014).

Chapter 4 – Conclusions and Future Directions

4.1. Conclusions

IDPs and their conformational transitions are intricately tied to function, allowing disordered proteins to play a number of critical roles in normal cell growth and turnover.[1-3] The work described here reveals the enormity of potential for chemical approaches to study, dissect, and modulate such transitions. The hypothesis that targeting protein conformation and dynamics will directly affect function is supported through examples that include studies on the stabilization of regulatory loops in kinases,[4] as well as small molecule helix stabilization in the case of mitochondrial aldehyde dehydrogenase (ALDH2).[5] When considering 4E-BPs as a case study, work on stapled peptides carried out by my colleagues in the Garner laboratory lay preliminary groundwork for the positive impacts of structural stabilization of this protein family.[6] Development and discovery of small molecules and biologics through *in vitro* approaches, such as those being conducted in our lab, demonstrate the vast opportunity for development of a chemically diverse collection of compounds that can be tested *in vivo* for a deeper understanding of how protein disorder functions in cell signaling.

4.1.1 On the Use of Conditionally Fluorescent Reporters of Structural Polymorphism in IDPs/IDRs

An exciting outcome of my dissertation research is the development of a fluorescent 4E-BP1-based peptide reporter of disorder in the hotspot binding region.[7] Its amenability to high-throughput screening will undoubtedly lead to the specific discovery of secondary structure modulating compounds. While, this approach to high-throughput compound discovery has yet to be applied, targeting of the 4E-BP amphipathic helix makes an interesting case study on the power of such a method. In addition to the insights that will be provided on how chemical perturbation at this axis of cap-dependent translation affects cellular metabolism in disease states, 4E-BP based peptides can be used to gather *in vitro* information on ways to infer specificity for peptides with similar sequences and modes of action. Of interest, the probing of the thiol-aromatic interaction between Phe58 and Cys62 with our peptide reporter has revealed its importance to 4E-BP1 helix stability. With this knowledge, the unique reactivity of Cys can be utilized to confer ligand specificity over both eIF4G and 4E-BP2. The potential for 4E-BP1 specific targeting is particularly exciting, as literature suggests that this would be a means of inducing tissue specific targeting of cap-dependent translation.[8-13]

The information gained through studies of the 4E-BP binding-induced helix will provide insights for application of conditionally fluorescent peptide reporter to systems beyond induction of α-helicity. Native chemical ligation can be used for the incorporation of a fluorophore and quenching thioamide via protein semi-synthesis to probe the dynamics of larger protein folds and protein domains.[14,15] A relevant example of such a fold is the phosphorylation induced 4E-BP β-fold.[16]

4.1.2 On Chemical Mutagenesis as a Route to PTM Mimicry in IDPs/IDRs

As discussed in Chapter 3, the potential of chemical mutagenesis methodology[17-25] to study post-translational regulation of IDPs is heavily dependent on biological, structural, and local environmental contexts of a specific PTM. While pCys appears to be a clever, yet simplistically obtained pSer and pThr mimic in over systems, this is not this case for 4E-BPs. First, the large radius of the sulfur atom appears to hinder pCys from adopting the optimal conformation for β-hairpin induction. In addition, Cys itself is extremely disruptive of α-helix.[26] In fact that only amino acids with lower helical propensity are Pro and deprotonated Glu.[26] This significantly complicates the interpretation of data suggesting pCys destabilizes the 4E-BP helix, as the sulfur atom itself makes some measurable contribution to this observation. Challenges in chemical conversion reactions to obtain pCys must also be noted. Even if pCys exhibited the hypothesized structural outcomes, difficulty of chemical conversions limit the use of the "tag-and-modify" technique by biologists who are best poised to make impactful discoveries through its use. Further studies of protein length, sequence, and structure on the efficiency of the conversion reactions used to obtain both Dha and pCys will not only yield information on what systems made be favorable or unfavorable for "tag-and-modify" methodology, but will also provide inspiration for development of new bioorthogonal chemistry for contexts deemed unfavorable.

4.2. Future Directions

Through my dissertation research, I have taken an interdisciplinary approach to explore the structure—function dynamic of IDPs in cellular signaling with two foci: conformational regulation of protein disorder and its effect on the PPI of 4E-BPs with

eIF4E and PTM mediated regulation of IDP structure and function. While this work certainly has implications for chemotherapeutic development in our system and other pathways that similarly rely on IDP-mediated regulation, there is still a great deal of work to be done on PPI targeting its long-term effects on signaling networks. Specific to targeting of cap-dependent translation, many mRNAs that are well-documented to be translated in a cap-dependent manner have been found to overcome inhibition of cap-dependent translation initiation via Internal Ribosomal Entry Site (IRES) units in the mRNA transcript.[27,28] While the molecular details of how this happen are not yet understood, this must be a consideration when targeting the 4E-BP—eIF4E interaction in disease states. Additionally, targeting IDPs is an arduous undertaking, and future studies must justify the advantages of targeting an IDP over its more ordered binding partners or other well-folded proteins in its signaling pathway.

4.2.1 On Targeting Structural Polymorphism in 4E-BP and Other IDPs

It will be interesting to see the results of future high-throughput screening efforts with the fluorescent peptide reporter that was developed in Chapter 2. A potential advantage of structure stabilization as a focus for IDP ligand discovery in cell signaling is that it does not explicitly rely on competition with endogenous binding partners. Instead, our technique can be viewed as a means of chemically reprogramming a cell and its signal transducing components, using a chemical probe to redirect the cell back to a more standard mode of functioning. As implied above, obtaining 4E-BP isoform specificity will be a major challenge in structural manipulation in this system, considering the high sequence homology between the eIF4E-binding sequences of eIF4G and the 4E-BPs. There is also the broader question of what chemical libraries for structure inducing ligand

discovery will look like. While the dearth of studies on chemical helix stabilization, make this question difficult to answer, it does reveal an important research area that medicinal chemists and chemical biologists are perfectly primed to elucidate.

As mentioned above, the combination of native chemical ligation with distance dependent thioamide fluorescence quenching is a promising approach to chemical probing phosphorylation induced 4E-BP β-fold.[14,29,30] There is both biochemical[31-35] and biophysical[16,36] evidence that this fold is critical for inhibition of 4E-BP function and stimulation of cap-dependent translation initiation. When considered along with the abundance of studies showing the correlation between hyperphosphorylated 4E-BP and disease, it can be hypothesized that disruption of the phosphorylation induced fold would present a mode of stabilizing the 4E-BP—eIF4E interaction in a way that is resistant to the aberrant upstream signaling that drives the increased cap-dependent translation observed in cancer and neurological disease models. Finally, it must be stated that while ligands discovered in this by this route may modulate structure, the possibility of such ligands being biologically inactive cannot be precluded. Thus, functional validation of discovered compounds in *in vitro* binding assays, cell-based assays, and eventually in *in vivo* models will be absolutely necessary for informing structure modulation as a biologically relevant method of targeting 4E-BP and other disordered signaling proteins.

4.2.2 On Chemical and Biological Considerations for the "Tag-and-Modify" Route to PTM Mimicry

Stereospecific phosphomimicry will be a critical consideration for future work on chemical mutagenesis for PTM generation. It is possible that this could be achieved, at least in part, by templating by the local structural environment, or a conformational

restraint at the peptide backbone, as is the case if the target of modification is adjacent to a Pro residue. Carbon-carbon bond formation through radical addition to Dha,[24] may also be able to address this issue if a stereospecific mode of hydrogen introduction at the α-carbon is developed. Conditional upon the aforementioned points being holistically addressed, chemically accessible PTMs yield immense potential for understanding PTMs in the context of protein disorder in a way that does not presently exist. It would certainly allow for controlled and intentional dissection of hierarchal PTMs in protein structure, protein function, and cell signaling. It could also be adapted for the identification of novel PTM mediated IDP binding partners. Finally, identification of novel conformational transitions by a chemical phosphomimetic, could be targeted for chemical invention via an adaptation of the methodology described in Chapter 2.

4.3 References

1 Dyson, H. J. & Wright, P. E. Intrinsically unstructured proteins and their functions. *Nat Rev Mol Cell Biol* **6**, 197-208, doi:10.1038/nrm1589 (2005).

2 Wright, P. E. & Dyson, H. J. Intrinsically disordered proteins in cellular signalling and regulation. *Nat Rev Mol Cell Biol* **16**, 18-29, doi:10.1038/nrm3920 (2015).

3 Wright, P. E. D., H.J. Intrinsicall Unstrctured Proteins: Re-assesing the Protein Structure-Function Paradigm. *J. Mol. Biol.* **293**, 321-331 (1999).

4 Nolen, B., Taylor, S. & Ghosh, G. Regulation of Protein Kinases: Controlling Activity through Activation Segment Conformation. *Molecular Cell* **15**, 661-675, doi:10.1016/j.molcel.2004.08.024 (2004).

5 Perez-Miller, S. *et al.* Alda-1 is an agonist and chemical chaperone for the common human aldehyde dehydrogenase 2 variant. *Nature Structural & Molecular Biology* **17**, 159-164, doi:10.1038/nsmb.1737 (2010).

6 Gallagher, E. E. S., J. M.; Menon, A.; Mishra, L. D.; Chmiel, A. F.; Garner, A. L. Probing the Importance of Folding Dynamics in the Design of Stapled Peptide Mimics of the Disordered Proteins 4E-BP1 and eIF4G. *in revision* (2018).

7 Petersson, E. J., Goldberg, J. M. & Wissner, R. F. On the use of thioamides as fluorescence quenching probes for tracking protein folding and stability. *Phys Chem Chem Phys* **16**, 6827-6837, doi:10.1039/c3cp55525a (2014).

8 Rojo, F. *et al.* 4E-binding protein 1, a cell signaling hallmark in breast cancer that correlates with pathologic grade and prognosis. *Clin Cancer Res* **13**, 81-89, doi:10.1158/1078-0432.CCR-06-1560 (2007).

9 Castellvi, J. *et al.* Phosphorylated 4E binding protein 1: a hallmark of cell signaling that correlates with survival in ovarian cancer. *Cancer* **107**, 1801-1811, doi:10.1002/cncr.22195 (2006).

10 Chakravarthy, R. *et al.* Role of the eIF4E binding protein 4E-BP1 in regulation of the sensitivity of human pancreatic cancer cells to TRAIL and celastrol-induced apoptosis. *Biol Cell* **105**, 414-429, doi:10.1111/boc.201300021 (2013).

11 Hsu, H. S. *et al.* The 4E-BP1/eIF4E ratio is a determinant for rapamycin response in esophageal cancer cells. *J Thorac Cardiovasc Surg* **149**, 378-385, doi:10.1016/j.jtcvs.2014.09.047 (2015).

12 Gkogkas, C. G. *et al.* Autism-related deficits via dysregulated eIF4E-dependent translational control. *Nature* **493**, 371-377, doi:10.1038/nature11628 (2013).

13 Santini, E. *et al.* Exaggerated translation causes synaptic and behavioural aberrations associated with autism. *Nature* **493**, 411-415, doi:10.1038/nature11782 (2013).

14 Batjargal, S., Huang, Y., Wang, Y. J. & Petersson, E. J. Synthesis of thioester peptides for the incorporation of thioamides into proteins by native chemical ligation. *J Pept Sci* **20**, 87-91, doi:10.1002/psc.2589 (2014).

15 Wang, Y. J., Szantai-Kis, D. M. & Petersson, E. J. Semi-synthesis of thioamide containing proteins. *Org Biomol Chem* **13**, 5074-5081, doi:10.1039/c5ob00224a (2015).

16 Bah, A. *et al.* Folding of an intrinsically disordered protein by phosphorylation as a regulatory switch. *Nature* **519**, 106-109, doi:10.1038/nature13999 (2015).

17 Chalker, J. M., Bernardes, G. J., Lin, Y. A. & Davis, B. G. Chemical modification of proteins at cysteine: opportunities in chemistry and biology. *Chem Asian J* **4**, 630-640, doi:10.1002/asia.200800427 (2009).

18 Chalker, J. M. & Davis, B. G. Chemical mutagenesis: selective post-expression interconversion of protein amino acid residues. *Curr Opin Chem Biol* **14**, 781-789, doi:10.1016/j.cbpa.2010.10.007 (2010).

19 Chalker, J. M. *et al.* Methods for converting cysteine to dehydroalanine on peptides and proteins. *Chemical Science* **2**, 1666, doi:10.1039/c1sc00185j (2011).

20 Chalker, J. M., Lercher, L., Rose, N. R., Schofield, C. J. & Davis, B. G. Conversion of cysteine into dehydroalanine enables access to synthetic histones bearing diverse post-translational modifications. *Angew Chem Int Ed Engl* **51**, 1835-1839, doi:10.1002/anie.201106432 (2012).

21 Chooi, K. P. *et al.* Synthetic phosphorylation of p38alpha recapitulates protein kinase activity. *J Am Chem Soc* **136**, 1698-1701, doi:10.1021/ja4095318 (2014).

22 Davis, B. G. Biochemistry. Mimicking posttranslational modifications of proteins. *Science* **303**, 480-482, doi:10.1126/science.1093449 (2004).

23 van Kasteren, S. I. *et al.* Expanding the diversity of chemical protein modification allows post-translational mimicry. *Nature* **446**, 1105-1109, doi:10.1038/nature05757 (2007).

24 Wright, T. H. *et al.* Posttranslational mutagenesis: A chemical strategy for exploring protein side-chain diversity. *Science* **354**, doi:10.1126/science.aag1465 (2016).

25 Wright, T. H., Vallee, M. R. & Davis, B. G. From Chemical Mutagenesis to Post-Expression Mutagenesis: A 50 Year Odyssey. *Angew Chem Int Ed Engl* **55**, 5896-5903, doi:10.1002/anie.201509310 (2016).

26 Pace, C. N. S., J.M. A Helix Propensity Scale Based on Experimental Studies of Peptides and Proteins. *Biophysical Journal* **75**, 422-427 (1998).

27 Averous, J. & Proud, C. G. When translation meets transformation: the mTOR story. *Oncogene* **25**, 6423-6435, doi:10.1038/sj.onc.1209887 (2006).

28 Braunstein, S. *et al.* A hypoxia-controlled cap-dependent to cap-independent translation switch in breast cancer. *Mol Cell* **28**, 501-512, doi:10.1016/j.molcel.2007.10.019 (2007).

29 Dawson, P. E. Native Chemical Ligation Combined with Desulfurization and Deselenization: A General Strategy for Chemical Protein Synthesis. *Israel Journal of Chemistry* **51**, 862-867, doi:10.1002/ijch.201100128 (2011).

30 Philip E. Dawson, T. W. M., Ian Clark-Lewis, Stephen B. H. Kent. Synthesis of Proteins by Native Chemical Ligation. *Science* **266**, 776-779 (1994).

31 Ayuso, M. I., Hernandez-Jimenez, M., Martin, M. E., Salinas, M. & Alcazar, A. New hierarchical phosphorylation pathway of the translational repressor eIF4E-binding protein 1 (4E-BP1) in ischemia-reperfusion stress. *J Biol Chem* **285**, 34355-34363, doi:10.1074/jbc.M110.135103 (2010).

32 Gingras, A. C. *et al.* Hierarchical phosphorylation of the translation inhibitor 4E-BP1. *Genes Dev* **15**, 2852-2864, doi:10.1101/gad.912401 (2001).

33 Gingras, A. C. G., Steven P.; Raught, Brian; Polakiewicz, Roberto D.; Abraham, Robert T.; Hoekstra, Merl F.; Aebersold, Ruedi; Sonenberg, Nahum. Regulation of 4E-BP1 phosphorylation: a novel two-step mechanism. *Genes Dev* **13**, 1422-1437 (1999).

34 Karim, M. M. *et al.* A quantitative molecular model for modulation of mammalian translation by the eIF4E-binding protein 1. *J Biol Chem* **276**, 20750-20757, doi:10.1074/jbc.M011068200 (2001).

35 Showkat, M., Beigh, M. A., Bhat, B. B., Batool, A. & Andrabi, K. I. Phosphorylation dynamics of eukaryotic initiation factor 4E binding protein 1 (4E-BP1) is discordant with its potential to interact with eukaryotic initiation factor 4E (eIF4E). *Cell Signal* **26**, 2117-2121, doi:10.1016/j.cellsig.2014.06.008 (2014).

36 Tait, S. *et al.* Local control of a disorder-order transition in 4E-BP1 underpins regulation of translation via eIF4E. *Proc Natl Acad Sci U S A* **107**, 17627-17632, doi:10.1073/pnas.1008242107 (2010).